

**EXPERIMENTAL STUDY OF THE ELECTROHYDRAULIC REMOTE
SYSTEM OF AGRICULTURAL TRACTORS FOR IMPROVED ENERGY
EFFICIENCY AND CONTROLLABILITY**

by

Josias Magdiel Cruz Gomez

A Thesis

Submitted to the Faculty of Purdue University

In Partial Fulfillment of the Requirements for the degree of

Master of Science in Mechanical Engineering



School of Mechanical Engineering

West Lafayette, Indiana

December 2020

THE PURDUE UNIVERSITY GRADUATE SCHOOL
STATEMENT OF COMMITTEE APPROVAL

Dr. Andrea Vacca, Chair

Department of Mechanical Engineering

Dr. Gregory Shaver

Department of Mechanical Engineering

Dr. John Lumkes

Department of Agricultural and Biological Engineering

Approved by:

Prof. Nicole Key

TABLE OF CONTENTS

LIST OF TABLES.....	5
LIST OF FIGURES	6
ABSTRACT	9
1. INTRODUCTION.....	10
1.1 Energy Consumption in Agricultural Tractors	10
1.2 Goals & Research Approach	13
2. BACKGROUND AND STATE OF THE ART	16
2.1 State of the Art Load Sensing Systems.....	17
2.1.1 Flow Saturation in Pre-Compensated Load Sense Systems.....	22
2.2 EHR Valve Circuit Simulation Model	25
2.3 Standards for Ag. Tractors.....	26
2.3.1 Nebraska Test Standard.....	26
2.3.2 DLG Power Mix Test	32
3. REFERENCE MACHINE SPECIFICATIONS.....	36
3.1 High pressure Load Sense Systems in Reference Machine	46
3.2 EHR Valve Description	49
3.3 Energy Efficiency in EHR Valve Circuits	51
4. EHR INSTRUMENTATION AND EXPERIMENTAL TEST PLAN	56
4.1 EHR Experimental Test Plan.....	56
4.1.1 Single Remote Tests	58
4.1.2 Multiple EHR Tests	62
4.2 Reference Machine Instrumentation	64
4.2.1 Sensor Location	68
4.2.2 EHR Lever Signal Modification	71
4.3 Data Acquisition (DAQ) system	72
4.3.1 NI DAQ Hardware.....	72
4.3.2 NI DAQ Custom Built Software.....	75
5. EHR TEST PLAN RESULTS.....	78
5.1 Post Processing with Matlab script.	78

5.2	EHR Single Remote Tests Results	81
5.2.1	PFC Single EHR Tests Results	82
5.2.1.1	LS line and actual load Discrepancy	98
5.3	Multiple EHR Test Results	99
5.4	Model Validation Through Experimental Characterization	105
6.	EHR VALVE IMPROVEMENTS	109
6.1	Flow saturation in PFC and TF pumps	109
6.2	EHR Flow Sharing as a Solution to Flow Saturation.....	111
6.2.1	Approach 1: Pump Based Feedback	112
6.2.1.1	Machine Implementation and Validation.....	120
6.2.2	Approach 2: EHR Spool Pressures Feedback	125
7.	CONCLUSION AND FUTURE WORK	132
7.1	Future Work.....	133
	APPENDIX A: TESTING PROCEDURE.....	134
	APPENDIX B: SINGLE EHR TEST TABLES	136
	APPENDIX C: MULTIPLE EHR TEST TABLES	143
	REFERENCES	145
	PUBLICATION.....	147

LIST OF TABLES

Table 1-1 Primary Tractor Farming Applications	11
Table 1-2 Tractor Size Categories	12
Table 4-1 Testing Conditions for EHR Valves	60
Table 4-2 Flow Commands for EHR Testing	61
Table 4-3 Preview of Test Table for EHR valves	62
Table 4-4 Multiple EHR Tests Conditions	63
Table 4-5 EHR Valves Test Summary	63
Table 4-6 Pressure Transducer Specs	66
Table 4-7 Flow Meter Specs	68
Table 4-8 EHR Lever Output Breakdown	71
Table 5-1 EHR Efficiency Values- Low Oil Temp	95
Table 5-2 EHR Efficiency Values- High Oil Temp	98
Table 5-3 Testing Conditions for Multiple EHR valve Tests	99
Table 5-4 Load Combination Tested in Multiple EHR Valves	99
Table 5-5 Efficiency % Values of Multiple EHR Tests	105
Table 6-1 Flow Saturation Data	109
Table 6-2 Simulation Parameters	114
Table 6-3 Simulation Test Results	115
Table 6-4 Flow Sharing Command Results- Simulation	128

LIST OF FIGURES

Figure 2.1 load Sense System- Basic	17
Figure 2.2 LS System Multiple Actuators.....	20
Figure 2.3 LS System in Flow Saturation with Multiple Actuators	23
Figure 2.4 LS System Representation when in Flow Saturation	24
Figure 2.5 TF Circuit Validated Model	26
Figure 2.6 MAO of OECD Standard Acceptance	27
Figure 2.7 DLG Testing Instrumentation at Certified Test Centers	33
Figure 2.8 Reference Unscaled Data for DLG Testing	34
Figure 3.1 New Holland T8 390 Agricultural Tractor	37
Figure 3.2 Pump Location on Reference Machine	39
Figure 3.3 Simplified High Pressure Hydraulic Circuit Layout	40
Figure 3.4 Medium Pressure Circuit [orange highlights].....	43
Figure 3.5 LS Variable Displacement Pump	45
Figure 3.6 Complete PFC Pump High Pressure Circuit	47
Figure 3.7 Complete TF High Pressure Circuit	49
Figure 3.8 EHR Valve Main Components	50
Figure 3.9 Active Components in PFC Pump High Pressure Circuit when 1 EHR is used	52
Figure 3.10 Pressure Distribution Plot Example	54
Figure 3.11 Power Distribution Example.....	55
Figure 4.1 PFC EHR Valves (red) TF EHR Valves (purple).....	56
Figure 4.2 TF Pump Circuit Sensor Location	59
Figure 4.3 Pressure Transducer Types	65
Figure 4.4 Types of Flow Meters	66
Figure 4.5 Magnetic Pickup Example	67
Figure 4.6 PFC Hydraulic Circuit Instrumentation Location	69
Figure 4.7 TF Hydraulic Circuit Instrumentation Location	70
Figure 4.8 EHR Command Signal Flow	71
Figure 4.9 DAQ System Layout	73
Figure 4.10 Data Aliasing Example	74

Figure 4.11 Main Panel of DAQ System Host Code.....	75
Figure 4.12 Full Custom Built LabVIEW Vi.....	77
Figure 5.1 Example of Desired Test Data	79
Figure 5.2 Data Flow and Conversion.....	79
Figure 5.3 Output Text File Example	80
Figure 5.4 Processed Data Compilation Example	82
Figure 5.5 Pressure Distribution of EHR 1	83
Figure 5.6 Power Distribution of EHR 1	84
Figure 5.7 Pressure Distribution of EHR 4	85
Figure 5.8 Power Distribution of EHR 4.....	85
Figure 5.9 Average Efficiency of PFC & TF EHR Valves	86
Figure 5.10 Pressure Distribution of EHR 1 (A) & EHR 2 (B)	87
Figure 5.11 Power Distribution of EHR 1	88
Figure 5.12 Pressure Distribution of EHR 4 (A) & EHR 5 (B)	89
Figure 5.13 Power Distribution of EHR 4 (A) & EHR 5 (B)	89
Figure 5.14 Average Efficiency of PFC & TF EHR Valves.....	90
Figure 5.15 Pressure Distribution of EHR 1	91
Figure 5.16 Power Distribution of EHR 1	92
Figure 5.17 Pressure Distribution of EHR 4	93
Figure 5.18 Power Distribution of EHR 4 (A) & EHR 5 (B)	93
Figure 5.19 Average Efficiency of PFC & TF EHR Valves.....	94
Figure 5.20 Pressure Distribution of EHR 1	95
Figure 5.21 Power Distribution of EHR 1	96
Figure 5.22 Pressure Distribution of EHR 4	96
Figure 5.23 Power Distribution of EHR 4	97
Figure 5.24 Average Efficiency of PFC & TF EHR Valves.....	97
Figure 5.25 Pressure Distribution EHR 4 & 5 Forward	100
Figure 5.26 Power Distribution EHR 4 & 5 Forward	100
Figure 5.27 Pressure Distribution EHR 4 & 5 Forward	101
Figure 5.28 Power Distribution EHR 4 & 5 Forward	102
Figure 5.29 Pressure Distribution EHR 4 & 5 Forward	102

Figure 5.30 Power Distribution EHR 4 & 5 Forward	103
Figure 5.31 Pressure Distribution EHR 4 & 5 Forward	104
Figure 5.32 Power Distribution EHR 4 & 5 Forward	104
Figure 5.33 Single TF EHR Model Layout.....	106
Figure 5.34 EHR Valve Model Layout	107
Figure 5.35 Single EHR Valve Test Results Comparison	108
Figure 6.1 Flow Saturation vs No Saturation Model Simulation	113
Figure 6.2 Validation of $s > px$	114
Figure 6.3 Testing Parameters for Flow Saturation Simulation	115
Figure 6.4 Flow Sharing Algorithm Flow Chart.....	116
Figure 6.5 Cascade Structure for PID Controllers	117
Figure 6.6 PID Control Structure.....	118
Figure 6.7 Simulation Model with PID Control Implementation	118
Figure 6.8 Controller Simulation Results with 100% (A) & 75% (B) Command.....	119
Figure 6.9 Host Code Front Panel Update	120
Figure 6.10 PID Vi Implementation	121
Figure 6.11 RAW Data Flow Sharing Control Test Results.....	122
Figure 6.12 Flow Sharing with Final Gains Test Results	123
Figure 6.13 Flow Sharing Controllers Simulation vs Experimental Results	124
Figure 6.14 Location for Pressure Transducer Placement for px Measurement	126
Figure 6.15 Validation of $sc > px$ when in Flow Saturation	127
Figure 6.16 Simulation Flow Sharing Test Conditions Approach 2	127
Figure 6.17 Flow Results of Flow Sharing Tests Approach 2	129
Figure 6.18 Final Updated Front Panel of Host Code	129
Figure 6.19 Flow Sharing Controller LabVIEW Implementation- Approach 2.....	130
Figure 6.20 Experimental Test Results Flow Sharing Approach 2	130

ABSTRACT

Massive energy consumption is known to occur in agricultural tractors. Tractors are state of the art machines engineered to output high power quantities, resulting in high fuel consumption. Fuel consumption is a great concern on these complex machines. The quantification of energy loss within the hydraulic systems of tractor working cycles is an important step that will lead the development of current technologies with performance and cost effective solutions.

In this work, the state of the art load sense technology implemented in an agricultural tractor will be studied with the goal of understanding key points where excessive energy loss may occur. The reference machine, a New Holland T8 390 category 4 tractor has been fully instrumented to make measurements of power within its high pressure hydraulic systems. A custom built DAQ system with National Instruments hardware and software acquired data. The machine has a pre-compensated load sense hydraulic system architecture. This work details specifics of load sense systems in general and also those to the reference machine. The particular focus of this work is to test energy efficiency and behavior of the Electro-Hydraulic Remote valves [EHR valves] located in two different high pressure circuits. This work will detail the rationale for developing an experimental test plan that was based on input from performance standards in tractors and knowledge from expert operators and farmers. The experimental characterization of the EHR valves demonstrated internal system behaviors that the EHR valves have. It helped identify the most favorable working conditions at which EHR could achieve at least 80% efficiency. Furthermore, scenarios where EHR valves may have low performance or unwanted behavior were also tested. These conditions yielded values as low as 53% efficiency. Solutions to flow saturation scenarios were implemented to assure functionality at lower speeds in the implements of the tractor if a saturation scenario was met. With the study of this work, potential technologies may be implemented in the EHR valve circuits to further increase efficiency.

1. INTRODUCTION

Agricultural industry has greatly increased over the course of the years. With it, also has the increase of crop and product demand. Therefore, agricultural companies that supply farmers with farming equipment such as agricultural tractors have set a goal to develop and deliver state of the art equipment for the industry. The development of well-designed tractor systems always has in mind these important goals: safety, productivity, and cost. These three objectives can sometimes stand in the way of each other since a solution that may improve a specific objective, may end up penalizing the others. The challenge in innovation within agricultural tractors is to develop systems that can simultaneously benefit all three of these objectives.

A path that tractor developers have taken to approach this challenge in the best manner possible is the utilization of state-of-the-art technologies in the design of these machines. This work focused on the hydraulic technology used within these very complex farming machines. Hydraulics allow for great power transmission while maintaining a balance between safety, productivity and cost. The high-pressure hydraulic subsystem studied within the extension of this work are the Electrohydraulic Remote valves (EHR). Top technologies, strategies and methodologies have been utilized for the design of such valves. EHR valves are particularly important within agricultural tractors since their main function is to deliver hydraulic power to any farming implement connected to the valve. Therefore, a correct design will allow for high reliability and low costs. The following pages will state problems within this high-pressure hydraulic circuits.

1.1 Energy Consumption in Agricultural Tractors

Agricultural tractors are state of the machines used in farming and forestry applications. A tractor is a vehicle specifically engineered to deliver a high tractive effort (or torque) at slow speeds, for the purposes of hauling a trailer or machinery used. Most commonly, the machine is utilized as a farm vehicle that provides the power and traction to mechanize agricultural tasks, especially (and originally) tillage, one of the most difficult agricultural tasks previously done by large animals. Nowadays, there has been an expansion of great variety of tasks for which a tractor may be used

(Table 1.1). Agricultural implements may be towed behind or mounted on the tractor, and the tractor may also provide a source of power if the implement is mechanized through the Power Take Off or PTO as it is commonly known

Table 1-1 Primary Tractor Farming Applications

Primary Tractor Farming Applications
Soil cultivation
Planting
Produce sorter
Harvesting / post-harvest
Hay making
Loading

Size of agricultural tractors can vary widely. Therefore, in order to have a better understanding of the capabilities of the machine and size, tractors are categorized by the hitch pin size and drawbar power range. The hitch is a 3-point type hitch (Fig.) widely used type of hitch for attaching ploughs and other implements to an agricultural or industrial tractor. The three-point hitch attaches the implement to the tractor so that the orientation of the implement is fixed with respect to the tractor and the arm position of the hitch. The tractor carries some or all the weight of the implement.

Therefore, the primary benefit of the three-point hitch system is to transfer the weight and resistance of an implement to the drive wheels of the tractor. This gives the tractor more usable traction than it would otherwise have, given the same power, weight, and fuel consumption. Another main mechanism for attaching a load is through a drawbar, a single point, pivoting attachment where the implement or trailer is not in a fixed position with respect to the tractor.

The size of the hitch has 5 category levels starting from the smallest category size 0 to the largest category size 4. The differences in dimensions and tractor power can be seen in Table 1.2.

Table 1-2 Tractor Size Categories

Category	Hitch pin size		Lower hitch spacing	Tractor drawbar power
	upper link	lower links		
0	17 mm ($\frac{5}{8}$ ")	17 mm ($\frac{5}{8}$ ")	500 mm (20")	<15 kW (<20 hp)
1	19 mm ($\frac{3}{4}$ ")	22.4 mm ($\frac{7}{8}$ ")	718 mm (26")	15-35 kW (20-45 hp)
2	25.5 mm (1")	28.7 mm (1 $\frac{1}{8}$ ")	870 mm (32")	30-75 kW (40-100 hp)
3	31.75 mm (1 $\frac{1}{4}$ ")	37.4 mm (1 $\frac{7}{16}$ ")	1010 mm (38")	60-168 kW (80-225 hp)
4	45mm (1 $\frac{3}{4}$ ")	51 mm (2")	1220 mm (46")	135-300 kW (180-400 hp)

The category specific to the reference machine is category 4. The largest category size in agricultural machines. In order to drive implements large enough to fit this category size, the engine must be able to yield enough power to the drawbar and auxiliary remote valves. Agricultural tractors and its implements are high energy consumers. This makes energy efficiency a major point.

From the large energy consumption already seen in these machines, the majority of it comes from the hydraulic system. The hydraulic system itself is made up of many subsystems that all consume different amounts of energy given a specific working cycle. The subsystems that are most commonly used are the hydrostatic steering system and the auxiliary remote valves. Tractors can be heavy and the steering system must output large quantities of energy so that the steering effort for the operator is minimized. The auxiliary remote valves output power to the agricultural attachment connected to the tractor. Some of these attachments may even be as large or even larger than the tractor itself.

Since the tractor may realize many types of working cycles, to measure and quantify the cost or advantages of hydraulic systems different architectures proves to be a challenge. The compilation of many systems like suspension, steering, auxiliary valves and braking that all draw power from the same source causes many sources of possible power loss.

Simultaneous use of the different high pressure systems can cause saturation conditions, where not enough flow or power is available to satisfy demand. Asymmetric pressure losses natural to hydraulic architectures like load sense systems may also be encountered. Temperature effects on efficiency and even operator command habits affect the way energy is spent in the high consuming tractor machines. With today's technology and advances in modeling systems, it is still difficult to develop a high fidelity model that will state all the major energy dissipation points.

Modeling such complex systems without experimental data to account and validate these points is difficult. This work will focus on developing the necessary experimental data so that these high fidelity models may be developed and also a full knowledge and expertise of the machine in normal working conditions may be achieved.

The main hydraulic system that this work will focus on and cover in is the auxiliary remote valve. The auxiliary remote valves within our reference machine are electro hydraulic. The origin of this technology comes from the evolution of the necessity for better controllability and efficiency in tractor hydraulics and as a consequence of the ever-developing farming implements that can be connected to such valves. The general purpose and use of the EHR valves remain the same as auxiliary valves: Supply hydraulic power to an external implement to allow realization of farming maneuvers.

The first designs of agricultural tractors that contained hydraulics and that pioneered in using hydraulic power to drive farming implements contained the first generation of AR valves. The simplest type of AR valves are spring center valves shown in Fig. 1.1. This type of AR valve has a simple spool type design that can be actioned mechanically to allow flow to the implements through one of its outlet ports, while the other port becomes a return port to close the hydraulic circuit. As stated before, the valve contains a simple lever that when you pressed forward or back and subsequently released, it pops right back to the center position. These valves are the most mechanically simplistic, and they're the least expensive. The development of these valves all leads to the current and most technological advanced type of AR valve: The EHR Valve that now a day is the most common type of AR valve present in state-of-the-art agricultural tractors.

1.2 Goals & Research Approach

The challenge stated in the previous section is to understand where the energy losses, our main problem in hydraulics in tractors, exist. The goal of this work is to develop and describe a sound methodology for the analysis of performance and energy consumption of the current EHR valves in the reference agricultural tractor. To achieve this, the following objectives were determined:

- Comprehend current state of the art hydraulics utilized by the reference machine.

- Develop a method or strategy to characterize the efficiency behavior of the hydraulic sub circuit from which the EHR valves are part of.
- Provide meaningful metrics for performance analysis.
- Develop guidelines for experimental testing of agricultural tractors.
- Create a working model of hydraulic systems of the machine

These goals will aid in the achievement of the main purpose of this work, to fully dissect all key point of energy loss, improve these points and make the high energy consumption agricultural tractors, an instrument with high performance and energy efficiency.

No objective may be reached without a proper methodology. The approach to reach the goal is as important as the goal itself. The reference machine has to be studied and understood as much as possible. The first step is to get as much data of the behavior of the hydraulic system that the EHR valve may be part of. To accomplish that the following steps were taken:

- Fully instrument machine in specific points that allow for experimental energy efficiency analysis.
- Create a suitable test plan to characterize EHR valve hydraulic circuit in terms of energy efficiency.
- Use experimental data to develop and validate a lumped parameter model of the EHR valve and other components within its circuit such as the hydraulic pump, lines and fittings.
- Utilize the pre-defined suitable metrics for assessing the performance of such hydraulic system.
- Analyze suitable graphical methods for expressing the metrics assessing performance.
- If needed, develop solution for problems that may be discovered.
- Implement these solutions into the machine.

This work will help in developing guidelines for future experimental testing of not only agricultural tractors, but also any type of high energy consuming machine that utilizes hydraulics. Energy efficiency will be improved with this work since the usual aspects of a machine that are in

general, unseen due to the different working cycles and architectures that a machine will have will now be able to be studied and improved.

2. BACKGROUND AND STATE OF THE ART

This chapter examines the past work and contributions into the design and engineering of agricultural tractors and hydraulic sub systems like EHR valves. Though the present investigation has some novel aspects; it is built on and expands a foundation laid by several previous works in different areas of the machine. Hydraulic circuits have many state of the art architectures that can be implemented in mobile machinery. One architecture in particular has gained ground over others, this is Load Sense (LS) technology. This architecture has been implemented and studied in other mobile machinery like excavators. Casoli, P. et al. [1] propose a traditional Post Compensated LS system. The objective of this research was to develop a complete simulation model of an excavator with the capability of reproducing the actual characteristics of the system. Section 2.2 will introduce similar work done in the reference machine of this work. A model was validated with the experimental results obtained from this work.

Zimmerman et al. [2] proposes a nonlinear mathematical model of the excavators LS system, that can be utilized to facilitate study of alternate control strategies other than LS. It is analyzed in an energy efficiency perspective and discusses possible energy savings by elimination directional control valves. As stated before, load sense systems are also present in agricultural tractors and work has been done by Wu [3] in modeling such system by an experimental evaluation approach.

Other approaches have been considered that propose other architectures than LS. In [4] an independent metering with an electronic LS pump is proposed as an alternative to both LS systems and current state of the art technology of EHR valves, this work also discusses the energy efficiency analysis current implementation of EHR valve technology and its embedded energy loss natural to this EHR valve technology when utilizing pressure compensators. With single spool valve and pressure compensation technology, Borghi et al. [5] present a 59% efficiency. When compared to other technologies like independent metering, while still utilizing LS, the efficiency can be increased to 68%. As it will be presented in the results section, this work lead to the discovery of the most efficient working conditions for LS systems and EHR valves. Efficiency in a single EHR valve was measured to be at around 80% efficient.

2.1 State of the Art Load Sensing Systems

Load sensing makes the flow to an actuator to be a function of only the area being commanded to the valve that drives such actuator. Load sensing has many advantages; the main advantage is that the operator has complete control of the speed of the actuator. Another major advantage is energy efficiency, by only providing the required flow to build only the pressure requested by the load and the user, unnecessary energy consumption is minimized. Load sensing works with fixed or variable displacement pumps. Since our system has a variable displacement pump, we will focus on load sense with pumps of this technology. The most basic load sense system can be seen in Figure 6.1.

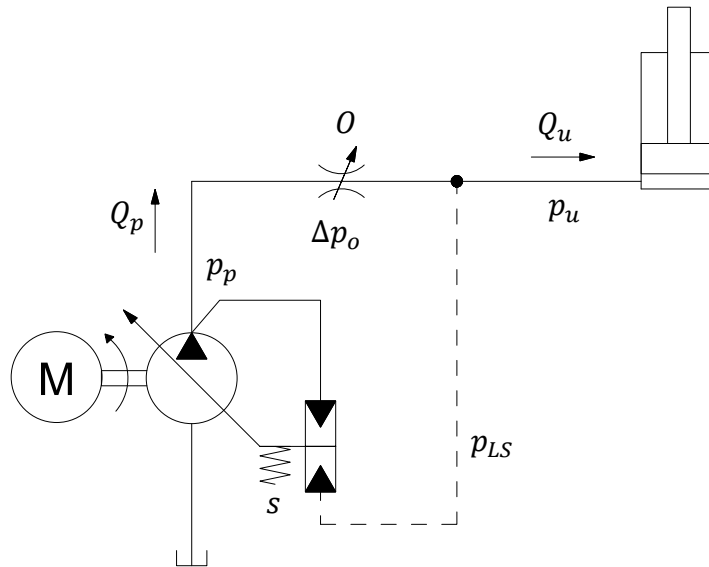


Figure 2.1 load Sense System- Basic

The figure above incorporates a variable displacement pump. This pump will supply flow to the control orifice O , and this orifice will command only a single actuator. A system without load sense will supply flow based on the command to valve O and also the pressure induced in the system by the actuator. A load sense system will supply flow only on the command given by the valve O . The feedback of the load p_u through the load sense pilot line eliminates the dependency of the user pressure in our system.

So that we can explain how the feedback of the load makes load sensing work, equations 3.1-3.3 are established based on the layout of the system. Equation 3.1 comes from the pressure p_u being transmitted through the pressure line into the LS line. 3.2 comes from the hydrostatic pressure balance in the control element of the pump. On one side we have the feedback of the pump outlet pressure. On the other we have the LS line feedback plus a spring. The last equation 3.3 examines the pressure drop across orifice O .

$$p_u = p_{LS} \quad 3.1$$

$$p_p = p_{LS} + s \quad 3.2$$

$$\Delta p_O = p_p - p_u \quad 3.3$$

By taking equation 6.1 and substituting it into equation 3.2, we now have equation 3.4

$$p_p = p_u + s \quad 3.4$$

Given that there exists a pressure drop at orifice O , there is also flow through the area of that orifice. Therefore, by utilizing the orifice equation and analyzing the flow passing through the orifice O to determine the value of Q_u , we obtain equation 3.5.

$$Q_u = c_d A_o \sqrt{\frac{2 * \Delta p_O}{\rho}} \quad 3.5$$

Where: c_d = coefficient of discharge and ρ = fluid density.

We will focus for an instant on the numerator of the radical inside the square root. We will give a different interpretation of the value Δp_O . By taking equation 3.3 & 3.4 and solving for Δp_O we obtain:

$$\Delta p_O = p_u + s - p_u \quad 3.6$$

$$\Delta p_o = s \quad 3.7$$

The pressure value of the spring s , is a known constant. Therefore once we substitute the new redefined value of Δp_o into the orifice equation 3.5, we can see that the dependency of flow Q_u is only a function of the area commanded since all other parameters are constants, and the pressure drop across the orifice Δp_o is the setting of the spring s .

$$Q_u = c_d A_o \sqrt{\frac{2 * s}{\rho}} \quad 3.8$$

$$Q_u = K A_o \quad 3.9$$

The flow to the user is now directly proportional only to the command given to the valve. This theory as it is presented, only applies to a single actuator in the system and also takes into consideration the different values of s that may be seen in the pump. Different values of s may be encountered in the same pump at different rpm levels. The change in s values is called a variable margin. As a load sense pump experiences more rpms at its input and deals with more flow and flow forces generated in its internal components, the value of s will be affected. The value of s is constant given the rpms of the pump are not altered. This variable margin does not jeopardize LS theory.

The LS system in our reference machine has multiple actuators. In order to make load sensing possible in multiple actuators, extra components are introduced, a pressure compensator per actuator and a shuttle valve. The first component, is designed to be able to deal with a behavior natural to multiple actuators in LS systems, load interference. In a multiple actuator LS system, when multiple user work at the same time, one will be of higher load with than the other. The challenge of multiple actuators is that most of the time if not all; the loads at multiple users will not be the same.

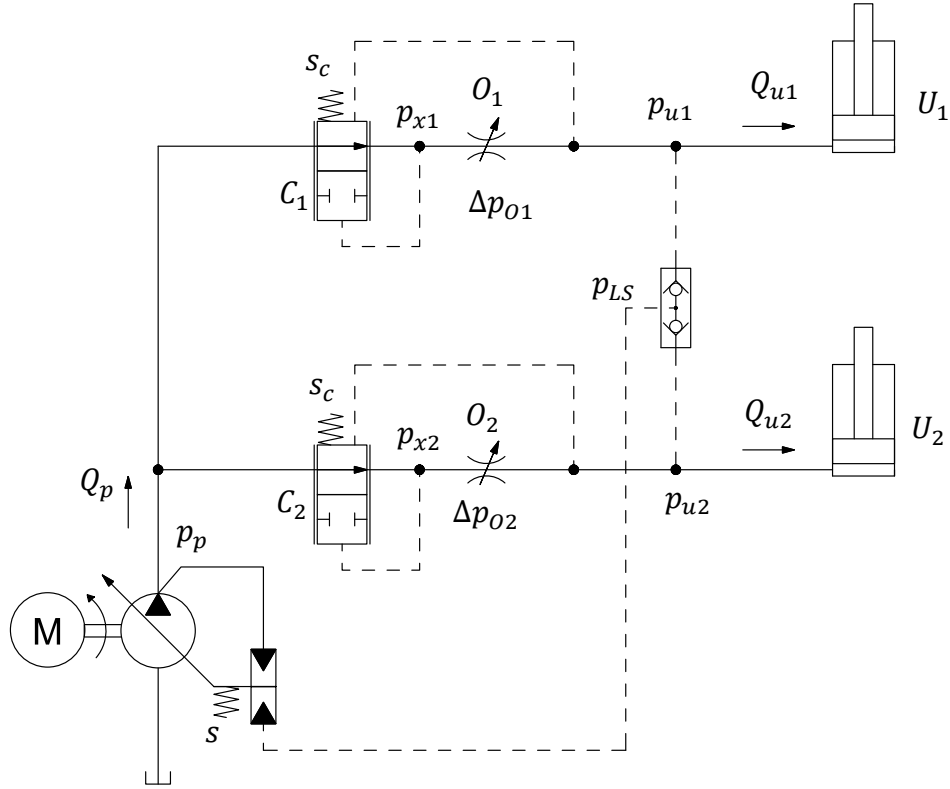


Figure 2.2 LS System Multiple Actuators

In figure 3.2, we have expanded to multiple actuators, the most basic load sense systems with multiple actuators is shown in the figure above. One load will be the highest, for the explanation of load sensing in multiple actuators, we will assume that the load at $U_1 > U_2$. Therefore the pressures in the system will also follow this assumption, $p_1 > p_2$.

We know that the value of the load sense line p_{LS} will be the highest of the two user pressures. In this case p_1 . From this we define the outlet pump pressure to be expected as:

$$p_p = p_{u1} + s \quad 3.10$$

As before, we will establish certain equations based on the layout of the system.

$$p_{x1} = p_{u1} + s_c \quad 3.11$$

$$p_{x2} = p_{u2} + s_c \quad 3.12$$

$$\Delta p_{O1} = p_{x1} - p_{u1} \quad 3.13$$

$$\Delta p_{O2} = p_{x2} - p_{u2} \quad 3.14$$

The values of p_x represent the pressure balance of the compensator in order to supply the user with the required pressure. As we stated before, $p_1 > p_2$, therefore the pressure at the pump will be set by user 1. Since the pressure requested by user 2 is lower, the compensator C2 will act as a pressure reducing valve in order to supply only the required pressure that the load is demanding. When the scenario reversed, and pressure at user 2 is higher, the compensator C1 would then act as a pressure reducing valve to the user U_1 . Up to this point, only the difference in load pressures has been solved, the load sense part of the system is yet to be explained.

The corresponding orifice equations on O_1 and O_2 can be seen below.

$$Q_{u1} = c_d A_{o1} \sqrt{\frac{2 * (p_{x1} - p_{u1})}{\rho}} \quad 3.15$$

$$Q_{u2} = c_d A_{o2} \sqrt{\frac{2 * (p_{x2} - p_{u2})}{\rho}} \quad 3.16$$

If we substitute the value of p_{x1} & p_{x2} into equations 3.15 & 3.16 respectively we can obtain the orifice equations 3.17 & 3.18.

$$Q_{u1} = c_d A_{o1} \sqrt{\frac{2 * (s_c)}{\rho}} = K A_{o1} \quad 3.17$$

$$Q_{u2} = c_d A_{o2} \sqrt{\frac{2 * (s_c)}{\rho}} = K A_{o2} \quad 3.18$$

Equations 3.17 and 3.18 once more prove that the flow across is function of the area of the orifice since the pressure drop across both of the orifices is the set value of s_c . This theory of pre compensated load sense system is required to fully understand the phenomena to be discussed in this chapter about flow saturation problems.

2.1.1 Flow Saturation in Pre-Compensated Load Sense Systems

As we learned in section 3.2 of this chapter, flow to an actuator is based only on operator command when using LS systems. In load sense systems, there can be scenarios that an operator can unknowingly command a value of flow and place the system in flow saturation. Since the pump is asked to deliver more flow than what it can yield, the actual flow available has to be distributed in all the users requesting flow. Flow saturation is reached when:

$$Q_{u1} + Q_{u2} > Q_{p_{max}} \quad 3.19$$

Flow saturation in pre compensated load sense systems has a particular behavior. The system behavior can be described by knowing how the available flow splits between the multiple actuators. The example set up in the previous section will be used to explain flow saturation in pre compensated LS systems. With this example, the assumptions below are made:

$$\begin{aligned} Q_{u1} &< Q_{p_{max}} \\ Q_{u2} &< Q_{p_{max}} \\ p_{u1} &> p_{u2} \end{aligned} \quad 3.20$$

With the scenario above we can see that the pump is sized to be able to handle a single actuator at a time. When multiple actuators are used, then the flow saturation condition of 3.19 is reached. Once again the pressure at the LS line is the one of p_{u1} . Since the pump is in flow saturation, the condition $p_p = p_{LS} + s$ cannot be met. In reality, that expression becomes:

$$p_p = p_{LS} + \Delta p_x \quad 3.21$$

Where $s > \Delta p_x$. This value of p_p is sufficient to allow LS theory to still work at user U2, which has a lower pressure. To better explain this example from Fig. 3.2 will be taken and modified to represent the system when it is in flow saturation scenario when $Q_{u1} + Q_{u2} > Q_p$, we get fig. 3.3.

The pressure at the pump outlet will still be driven by the highest load p_1 . The flow at U1 will be:

$$Q_{u1} = Q_{p_{max}} - Q_{u2} \quad 3.22$$

This will cause C1 to be fully opened, however there is not enough flow to keep a constant pressure drop of s_c across O1. The compensator will tend to open as much as possible so enough flow arrives to be able to achieve a constant pressure drop of s_c . This makes the pressure drop across O1 be:

$$\Delta p_{o1} = p_p - p_{u1} = \Delta p_x \quad 3.22$$

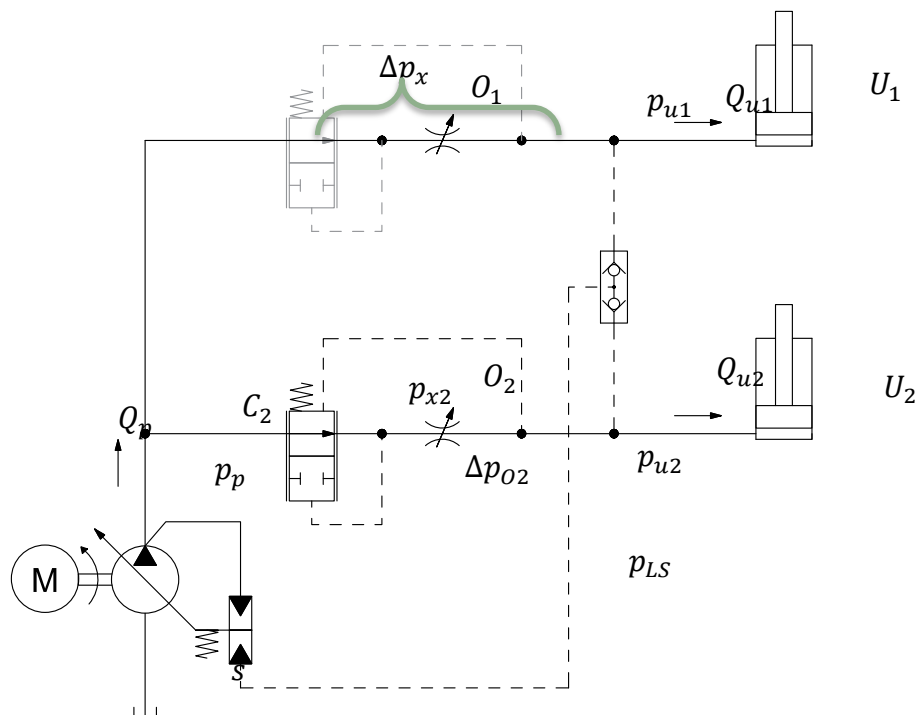


Figure 2.3 LS System in Flow Saturation with Multiple Actuators

Since the compensator is now open as much as possible it becomes a fixed orifice in series with a variable orifice O1. We can then alter figure 3.3 and temporarily remove C1 since it is not causing major pressure drops and O1 as the orifice Ox seen in figure 3.4. By taking the pressure drop across this simulated orifice we obtain equation 3.23.

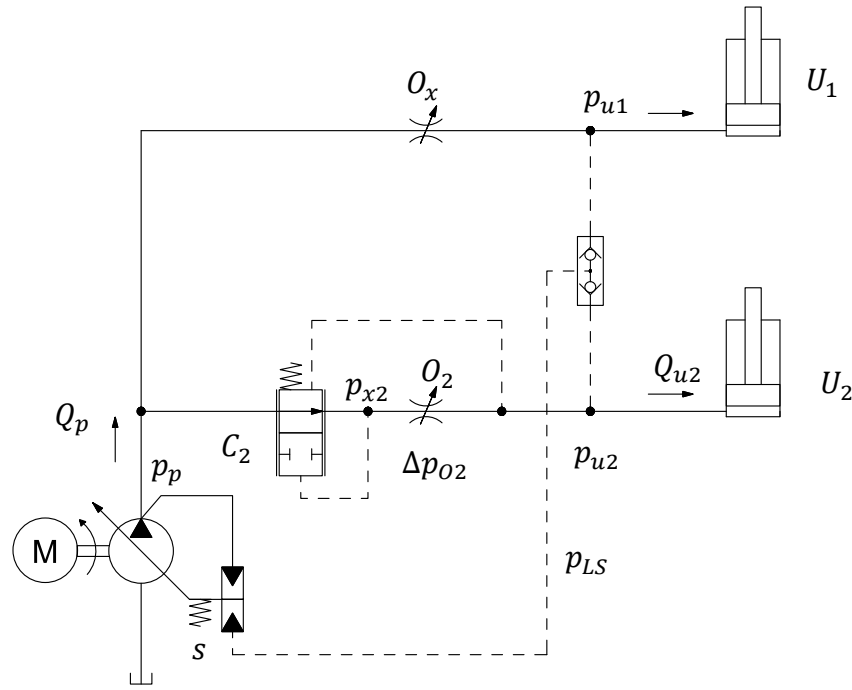


Figure 2.4 LS System Representation when in Flow Saturation

$$\Delta p_{Ox} = p_p - p_{u1} = \Delta p_x \quad 3.23$$

$$\Delta p_x = \frac{\rho}{2} \left(\frac{Q_p - Q_{u2}}{c_d A_{O1}} \right)^2 \quad 3.24$$

Equation 3.24 comes from the orifice equation. The value of p_x can be calculated by knowing the available flow left from the pump and solving the orifice equation across our simulated orifice Ox.

Re arranging equation 3.23. We notice that pump pressure under flow saturation conditions will be:

$$p_p = p_{u1} + \Delta p_x \quad 3.25$$

This expression is the exact same as our initial equation 3.21. In the end, when in flow saturation a pre compensated system will penalize the highest load, priority is given to the user that has the lowest load. The demand of this low load actuator will be met assuming the pump has enough flow to satisfy it. From there the rest of the flow will be distributed in a hierarchy of lower loads to higher loads, until all the pump flow is utilized.

2.2 EHR Valve Circuit Simulation Model

Experimental methodologies also have been developed for tractor performance, Diaz Lankenau [6] mentions an experimental characterization of a machine by utilizing agricultural standards and utilizing these results to validate a model of the reference machine interacting with soil. This work utilized a similar approach, to validate a model of the machine hydraulic systems based on experimental data.

A direct result from this work, in terms of experimental characterization was the development of a working and validated simulation model of all of the high pressure sub-systems present in the reference machine. The model specific to the EHR valves was a great tool in the implementation of the two approaches for implementing a flow sharing algorithm discussed in chapter 6. Tian [7] proposes a methodology for model development and Cruz [7] an experimental characterization for model validation. A research paper was co-written [See Publication section] and data from this work allowed for the model to be created. The model was used to simulate flow saturation conditions and implement the control structure to correct this flow saturation problem.

A separate working model was made for both PFC and TF pump circuits. The methodology used a lumped parameter approach and done in the commercial software Simcenter Amesim. In particular, the model to be introduced in this work is the one of the TF pump. This model was used for the flow share algorithm implemented. It includes the TF LS pump, manifold, hitch valve and two working EHR valves. The in depth considerations, steps and methodology for creating this model can be seen in the publication section.

trade. The OECD Standard Codes for the official testing of agricultural and forestry tractors represent a set of rules and procedures. They were first established in 1959.

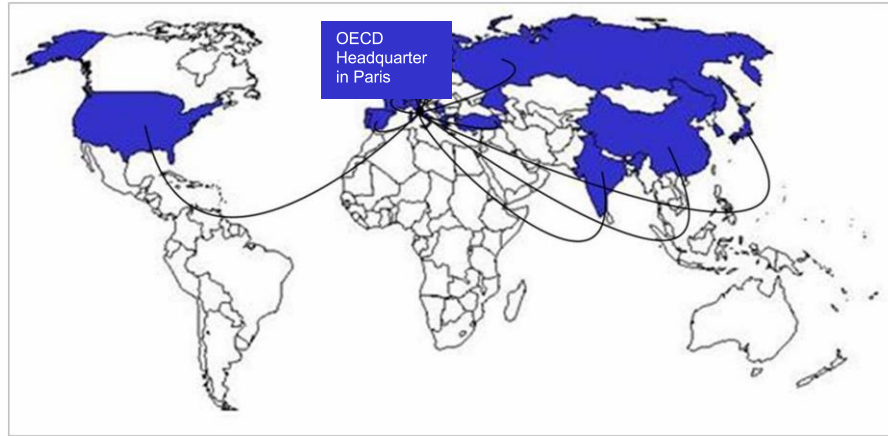


Figure 2.6 MAO of OECD Standard Acceptance

To this date there are 9 Codes:

Code 2: OECD Standard Code for the Official Testing of Agricultural and

Code 3: OECD Standard Code for the Official Testing of Protective Structures on Agricultural and Forestry Tractors (Dynamic Test).

Code 4: OECD Standard Code for the Official Testing of Protective Structures on Agricultural and Forestry Tractors (Static Test).

Code 5: OECD Standard Code for the Official Measurement of Noise at the Driving Position(s) of Agricultural and Forestry Tractors.

Code 6: OECD Standard Code for the Official Testing of Front-mounted Protective Structures on Narrow-track Wheeled Agricultural and Forestry Tractors.

Code 7: OECD Standard Code for the Official Testing of Rear-mounted Protective Structures on Narrow-track Agricultural and Forestry Tractors.

Code 8: OECD Standard Code for the Official Testing of Protective Structures on Agricultural and Forestry Tracklaying Tractors.

Code 9: OECD Standard Code for the Official Testing of Protective Structures for Telehandlers (Testing of Falling-Object and Roll-Over Protective Structures fitted to self-propelled variable reach all-terrain trucks for agricultural use).

Code 10: OECD Standard Code for the Official Testing of Falling Object Protective Structures on Agricultural and Forestry Tractors.

For the purpose of this test plan, Code 2 is the most adequate. That code focuses on all the working systems of the tractor, among those the hydraulic systems. In Chapter 4 of the Code 2 OECD Standard, section 4.2 within the July 2012 edition one can find the Hydraulic Power test requirements. Within this sections these important factors were learned:

For all tests:

- The hydraulic fluid shall be as recommended by the manufacturer and identified by type and viscosity in accordance with ISO 3448:1992. [8]
- At the start of each test, the temperature of the hydraulic fluid in the tractor hydraulic case shall be at $65\text{ }^{\circ}\text{C} \pm 5\text{ }^{\circ}\text{C}$ and be recorded. If this cannot be achieved, due to the presence of an oil cooler or other system component, the temperature measured during the test shall be stated in the test report. [8]
- Tractor-mounted flow controls shall be adjusted to obtain maximum flow. [8]

These variables help set repeatable testing conditions within our test plan. Like stated before, we want to evaluate the efficiency with methodical well elaborate tests that will yield significant data, in order for us to obtain more data and different performance percentages, the points before were taken into consideration and a new set of tests was designed.

The standard has two sets of tests, compulsory and supplementary tests. Each type of tests aims to test a different aspect of the machine. Both compulsory and supplementary test help in our case study.

Compulsory Tests:

For the compulsory tests, the following conditions must be set when running the test:

- They shall be conducted with the throttle or governor control lever adjusted to the maximum engine speed condition. The engine speed is recorded during the tests. [8]
- For tests conducted at maximum engine speed, the engine speed is continuously recorded during the tests. [8]

Engine speed must be kept constant and at maximum engine speed. The purpose of the compulsory test is to test in a steady state condition the following characteristics: Hydraulic pressure, flow and power (maximum available power).

In section 4.2.2 of the OECD Code 2 standard, the results that need to be reported so that the performance specs of the machine are known are:

- The maximum hydraulic pressure sustained by the open relief valve, with the pump stalled in the case of closed-center system with pressure-compensated variable delivery pump; (ISO 789/OECD-10:2006 section 6.1);
- Hydraulic power available at the auxiliary service coupling, at the flow rate corresponding to a hydraulic pressure equivalent to 90 % of the actual relief valve pressure setting in the circuit;
- Maximum available hydraulic power test with flow through a single coupler pair, and corresponding flow and available coupler outlet pressure (pressure near coupler where oil is exiting from tractor);
- Maximum available hydraulic power test with coupler pairs operating simultaneously (flow through two or more coupler pairs if required), and corresponding flow and available coupler outlet pressure (pressure near coupler where oil is exiting from tractor). If the maximum hydraulic power is obtained with one coupler pair, this test is not required.

The second to last bullet points aided in the design of the test plan. The maximum operating pressure was to be 90% of the pressure compensator setting of the pump that supplies flow. Given that there are no relief valves in our circuits, the value of the pressure compensator of the LS pumps was taken as the relief valve.

Supplementary Tests:

These tests are available in order to provide extra information that is relative to the hydraulic system performance. They are not mandatory and any one of them can be selected to be tested and reported. This is true for the standard. For this work, the information of these tests was useful so that correct testing condition were chosen. As mentioned before, EHR valves can be placed into infinitely many working conditions, by analyzing these supplementary tests, these infinitely many conditions were brought down to a minimum number of conditions, so that the experimental test plan was capable of capturing the LS system different behaviors in the best manner possible. These behaviors may be saturation conditions, load interference, variable load sense margins due to

difference in pump flows. Capturing all these behaviors in an in a well elaborated test plan is the goal.

Supplementary tests have the goal to study steady state hydraulic pressure and flow tests - maximum usable power, maximum available differential pressure, peak pressure, and sump return pressure. [8]

In section 4.2.3 of the OECD Code 2 standard, the results that need to be reported so that the spec of the machine may be known are:

- Maximum usable (continuous) hydraulic power test with flow through a single coupler pair, and corresponding flow and available differential pressure (pressure near coupler where oil is exiting from tractor - pressure near coupler where oil is re-entering the tractor, ISO/OECD 789-10:2006, section 7.2.1);
- Maximum usable (continuous) hydraulic power test with flow through two (or more if required) coupler pairs operating simultaneously, and corresponding flow and available differential pressure (pressure near coupler where oil is exiting from tractor - pressure near coupler where oil is re-entering the tractor, ISO/OECD 789-10:2006, section 7.2.2);
- Maximum available differential pressure with flow through a single coupler pair (30 l/min - category 1, ISO/OECD 789-10:2006, section 6.1.2.2);
- Maximum available differential pressure with flow through a single coupler pair (50 l/min - category 2 & 3, ISO/OECD 789-10:2006, section 6.1.2.2);

With these recommended tests, the experimental test plan was developed so that not only maximum usable energy be tested of efficiency but also other conditions. Conditions like minimum output power from the EHR. In both single and multipole EHR valves. The standard aims to yield performance information on the maximum performance output from the machine. The experimental test plan developed for this machine, expand beyond that maximum performance point. Flow and pressure saturation conditions could also be conditions tested. All of the considered conditions and test will be explained in chapter 4, under the experimental test plan section.

2.3.2 DLG Power Mix Test

The DLG acronym stands for the German Agricultural Society (Deutsche Landwirtschafts-Gesellschaft). The Power mix test aims to simulate real life working conditions in a repeatable indoor environment. It consists of 14 test cycles that simulate various loads on the tractor and measure its fuel and AdBlue consumption, its output and efficiency as the machine goes through the test cycle. The individual test cycles replicate typical field and transport applications at half load and full load.

These applications include pure draught work (e.g. ploughing or cultivating) but also mixed work that applies load on the transmission, the PTO and the hydraulic system. This is a typical scenario when operating a power harrow, a mower, a manure spreader or a baler. In addition, the test simulates heavy and light transport work, testing the tractor as on the road to obtain a general efficiency profile under reproducible field conditions.

The standard aims to have a repeatable testing environment that allows for a correct simulation of real farming working cycles without actually being in the field where testing variables are much more difficult to control and replicate. Alike the Nebraska test, the testing methods are based on static operating states but based on the trajectory on a real life working cycle. Certified DLG Power mix test centers have the ability to conduct all of the test with the set up seen in figure 4.2. In our case, we used the testing instructions as reference to generate our own test plan.

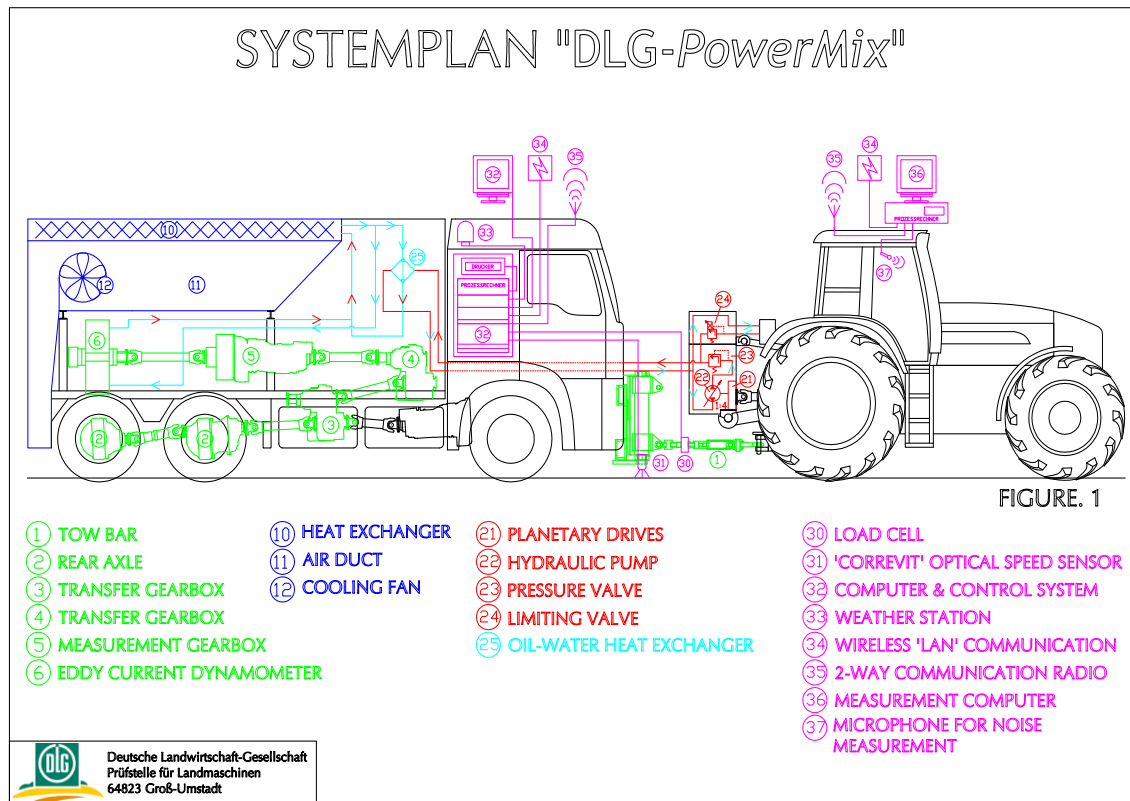
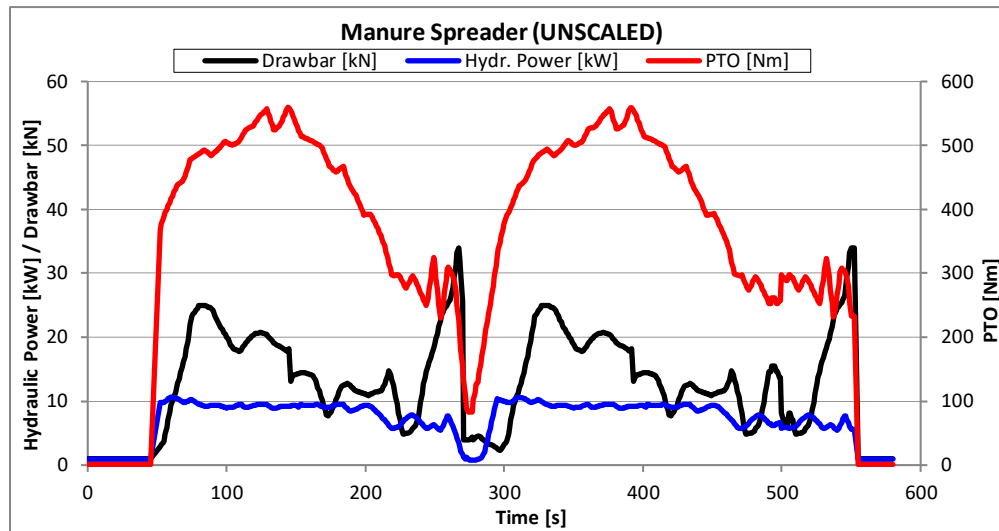
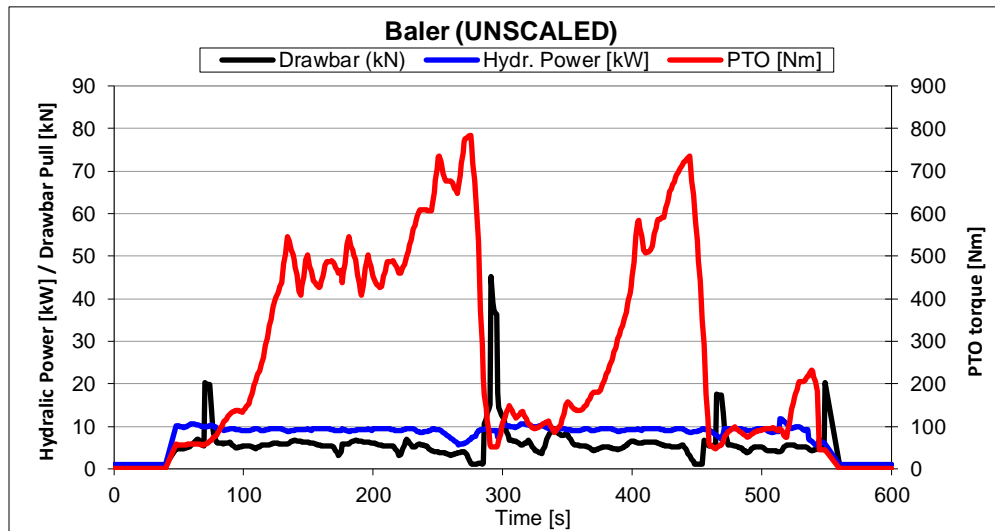


Figure 2.7 DLG Testing Instrumentation at Certified Test Centers

The instructions within the test is to command the tractor to follow the working cycle previously recorded by the DLG. The DLG takes instrumented tractors like the one in figure 3.17 and records their behavior during a particular working cycle. In this manner, the DLG has a set of data for all 14 working cycles. Looking specifically at those cycles that actuate hydraulics and within those, the ones that actuate hydraulic EHR valves, we acquired the DLG working cycle and studied it.



A



B

Figure 2.8 Reference Unscaled Data for DLG Testing

Looking at two particular working cycles like the ones on Fig. 3.18 parts A & B, we can notice in blue, the hydraulic power being consumed during both baling and manure spreading cycles. During almost all operation the hydraulic power being consumed, is in steady state, even if the machine is moving. With this we can conclude that a steady state oriented test plan will be the best option. Since it replicates the behavior of the machine on a normal working cycle. The data has an unscaled label due to the fact that, the tractor utilized to acquire this data for the DLG

was a certain tractor Category. Given the actual machine that the cycle will be performed on may be of a smaller category, scaling of the data must be done to fit the category size of the tractor being tested. Having established all necessary test procedures and test data points from both testing standards. A local test plan was developed and designed. The next chapter will go more in depth into the conditions selected for testing and machine instrumentation rationale

3. REFERENCE MACHINE SPECIFICATIONS

Having discussed in general the background behind the work under consideration, the next step towards the goal for this work is to build more specific knowledge and theory that makes up our reference machine. This is crucial to all the subsequent activities of this work, as the understanding of the machine will aid to foster new ideas about proposing new strategies to better improve the current design within the machine.

This chapter aims to describe the reference machine in concrete terms and will allow for the better understanding of subsequent chapters. As a starting point, understanding of the general specs of the machine is necessary. From there, the different types of hydraulic circuits it possesses and its functionality. Once we understand these hydraulic circuits, and focusing mainly on the high-pressure circuits, a detail description of the instrumentation will be addressed. This leading up to how the data acquisition system was developed in order for the necessary data that the test plan, proposed in the next chapter aims to obtain.

The reference machine is a category 4 agricultural tractor. A New Holland T8.390 tractor [Fig. 3.1] was provided to the research team to be used as the development prototype. It is equipped with a standard rear hitch [category 4]. This model has 6 EHR valves available within the high-pressure hydraulic circuit. In order to have enough flow for the demand of 6 EHR valves, the machine comes equipped with 2 load sensing pumps. The details about this circuit will be addressed further in this chapter.



Figure 3.1 New Holland T8 390 Agricultural Tractor

Built in 2015, the reference machine for this work consists of state-of-the-art technologies within its engine, transmission and hydraulic circuits. That makes it the ideal candidate to develop this work on. The maximum speed that may be reached by this T8 is 35 mph [56 km/h]. With its AWD system and gross power of 340 HP [353.5 kW] it is important to understand and address that the available energy is being used adequately.

The heart of many off-road machine's types ranging from construction equipment to farming and forestry will most likely be a diesel engine, particularly tractors. This is due to the fact that as we stated before, tractors are designed to deliver a high tractive effort (or torque) at slow speeds. Therefore, the most adequate source of energy to be able to meet this design criterion is a diesel engine.

The engine within the NH T8 390 is a four-stroke 8.7 L diesel engine. The diesel engine can deliver high torque at low engine speeds with the best efficiency when compared to other internal combustion engine types. The torque yielded by the crankshaft is set solely by the mass of injected fuel, which is always mixed with as much air as possible. It is not uncommon in diesel engines to be turbocharged or supercharged as we know that intake air mass does not have to precisely match the injected fuel mass. The engine within the reference machine is indeed also turbocharged.

With the current technological advancements, the diesel engine has become a very complex system of its own. Capable of yielding high power density through the crankshaft the diesel engine mounted on the T8 390 is top of the line. However, studying the concepts of diesel engines and the state of the art advancements is not within the scope of this work. Understanding the necessity of a diesel engine within this type of machine is more important. The high power that the engine give is utilized by the hydraulic systems that will be studied in this work.

Hydraulic Circuits

Hydraulics have been the state-of-the-art technology for energy transmission within heavy duty machinery in all sorts of fields, particularly in agricultural tractors for several decades. This is due to the ease and accuracy of control for hydraulic systems. In purely hydraulic control joysticks, the operator can have a feedback of the behavior of the system. Another major advantage of hydraulics within agricultural tractors is the power to weight ratio. Hydraulics allow for compact high-power density components which is a big aspect when designing a mobile machine. The less components and the smaller these components are the better it is in general for the final design. Likewise, having smaller components means also flexible arrangements of such components. Maintenance of hydraulic components also plays a big role. Hydraulic components tend to lubricate themselves with the hydraulic fluid which also acts as a temperature dissipater. These are some advantages of using hydraulics as a means for energy transmission. However, hydraulics tends to have some disadvantages that reflect mostly into power loss. Phenomena like leakages within hydraulic components along with frictions generated between the fluid and moving mechanical components inside valves, motors and pumps. Fluid contamination can also affect the performance and fatigue of hydraulic components. It is that specific phenomena that drive the efficiency of such systems down that we wish to study and improve for this work.

The hydraulic components and circuits in the T8 390 tractor have 3 pressure range levels. The tractor uses three hydraulic pumps to supply the circuits mentioned. The pumps are driven through a drive housing on the right side of the transmission. The pump drive housing gears are driven by the Power Take-Off (PTO) drive line and all the pumps turn at approximately 1:33 times engine speed. A Pressure and Flow Compensating (PFC) piston pump is attached to the front of the pump drive housing, while the tandem gear pump is attached to the rear of the pump drive

housing. Within our model of machine, a fourth pump is added to supply flow at high pressure called the Twin Flow Pump (TF).

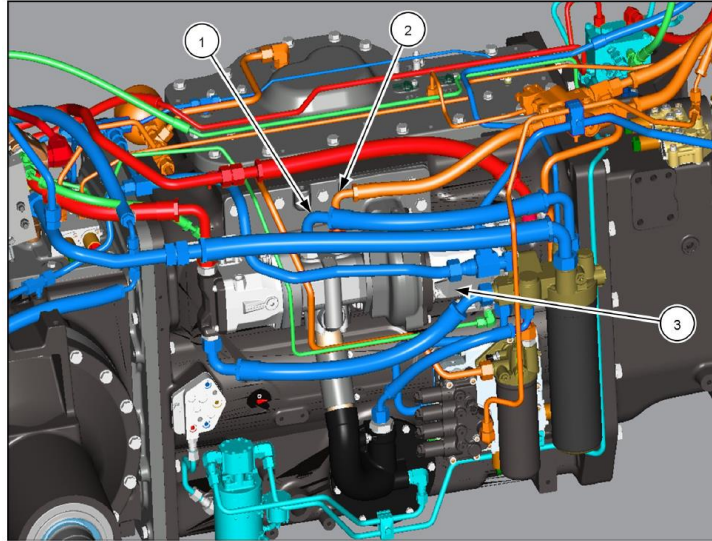


Figure 3.2 Pump Location on Reference Machine

- | | |
|-----------------------------------|----------------------|
| 1. Charge/lubrication pump outlet | 3. Standard PFC pump |
| 2. Regulated circuit pump outlet | |

The 2 load sensing pumps, PFC and TF supply all the high-pressure circuits. The tandem pump is made up of two gear pumps. The charge/lubrication pump is the rear section of the tandem gear pump and it is used to supply the main PFC pump with a charged inlet condition to prevent cavitation. The pump also supplies lubrication requirements for the transmission. The pump draws oil from the transmission housing through a mesh suction screen. The pump flow is directed across the main filter assembly to provide clean charge and lubrication oil. The regulated circuit pump is the front section of the tandem gear pump. The pump draws oil from the system reservoir through another mesh suction screen. The pump flow passes into the cooler bypass valve; the cooler bypass valve will send flow onto the oil cooler at temperatures above 82 °C (180 °F). The cooler bypass valve will bypass the cooler at temperatures below 82 °C (180 °F). Whether the regulated circuit pump flow bypasses oil cooler, or not all the flow passes through the regulated circuit filter.

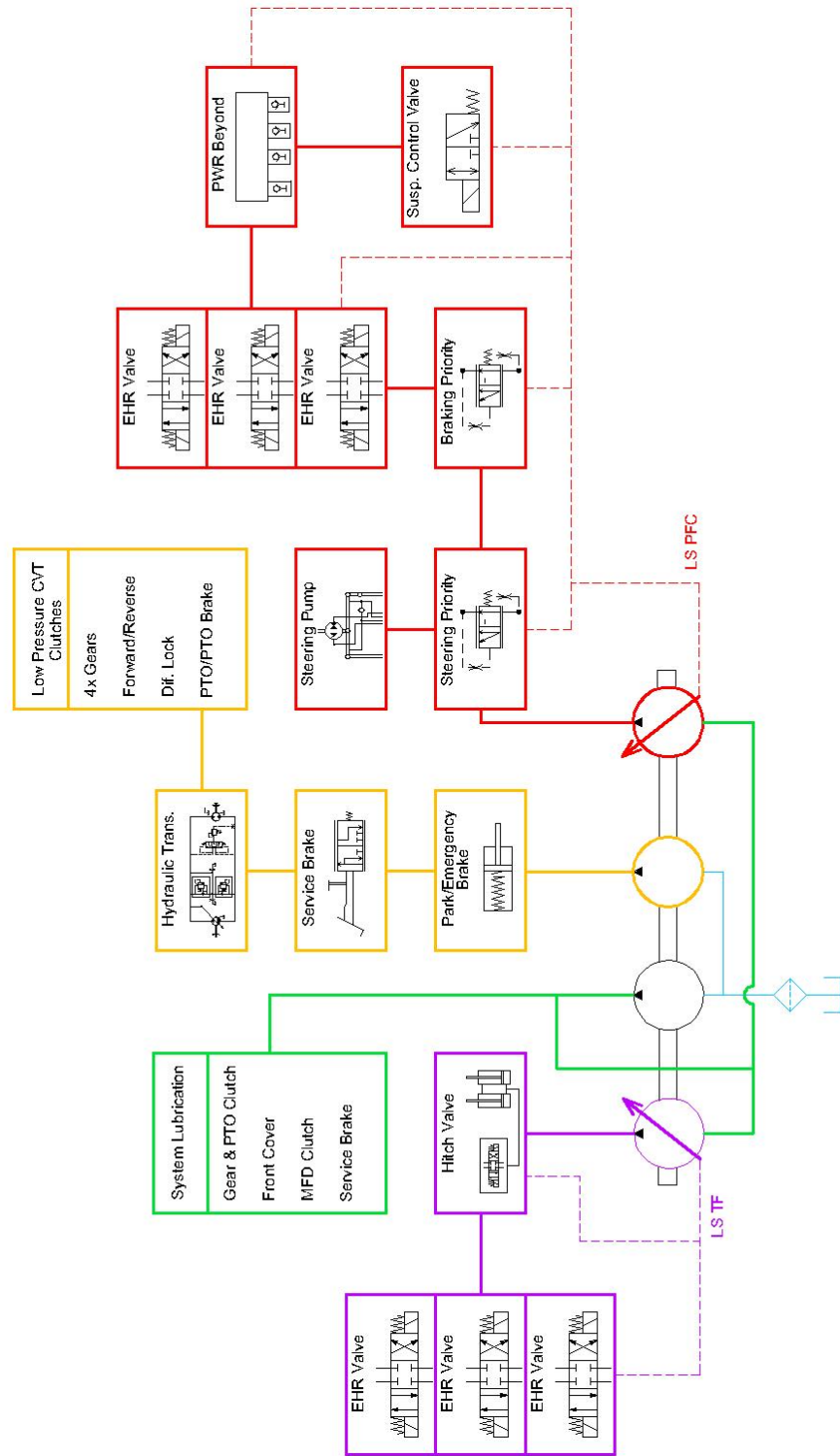


Figure 3.3 Simplified High Pressure Hydraulic Circuit Layout

A general schematic with all the pressure levels and component hierarchy can be seen in figure 3.4. Here from left to right, we have the load sensing Twin Flow Pump represented in purple color. The TF pump supplies high pressure fluid to the hitch and 3 of the EHR valves present in the machine. From there comes the first pump that composes the tandem gear pump called the charge & lubrication pump. This pump represented in green, supplies low pressure flow to all the lubrication systems along with flow to the inlets of the load sensing pumps. Then comes the regulated circuit pump in yellow. This section of the hydraulic systems of the tractor comes in a mid-range pressure. This pump serves as a charge pump for the hydrostatic section of the CVT, supplies the gear clutches and service brakes and the park brake. Finally, there is the Pressure and Flow Compensating pump in red that is the main pump of the tractor. This pump supplies the steering priority valve then another braking priority valve for a trailer if available and finally the rest of the high-pressure functions, including another 3 of the EHR valves we seek to study with this work.

In order to achieve full familiarity of the machine, all the hydraulic circuits were analyzed and studied. Within each section calculations of its respective ideal corner power were made. This study showed the power difference in terms of consumption that is present in the machine. Validating that the high pressure circuits consume much of the power in tractors.

Low Pressure/Lubrication System

As stated before, the tractor contains three pressure levels of hydraulic architectures. All independent of each other. The first section of the hydraulic circuits to be described in detail the low-pressure lubrication system. This low-pressure hydraulic circuit is supplied by the charge/lubrication pump. As the name of the pump that supplies this circuit suggests, the main purpose for the low-pressure lubrication circuits is to lubricate necessary components. In order to avoid cavitation, the pump also pre-charges the inlet of the two load sensing pumps

The charge pump is capable of supplying when it spins at its rated speed a total of 178 l/min (47.0 US gpm). This flow that is supplied from an idle speed to a nominal speed of the pump will always have a maximum pressure of 4.5 bar. With this in mind, the corner ideal hydraulic power ($\eta_v = 1$) yielded in kW by the pump can now be calculated in the following way:

$$P_{hyd}[kW] = \frac{Q_{pump}p_{pump}}{600}\eta_v$$

$$P_{hyd}[kW] = \frac{178 \left[\frac{L}{min} \right] * 4.5[bar]}{600} \quad 3.1$$

$$P_{hyd} = 1.3 kW$$

It will be seen that the corner power of the lubrication system, given the high flow rate, is still quite low compared to the high pressure hydraulic systems power consumption analysis. This is due to the fact that it's fluid at low pressure.

Medium Pressure Regulated Circuit

The second level of pressure within the 3 levels in the hydraulics of the tractor is supplied by the second pump of the gear tandem pump. This circuit is regulated at 38 bar and it is utilized to supply flow in order to activate the transmission clutches, service brake and emergency/park brake. This pump is also a charge pump for the hydraulic transmission used in the CVT. In particular, this circuit has another feature that is not listed in figure 3.5 due to the fact that it's not a user. This feature allows for the oil to be directed into and out of the oil cooler. It is done by an electrically activated valve. All regulated circuit pump flow is directed to the cooler bypass valve inlet. The tractor control unit (TCU) controls the cooler bypass valve function based on transmission oil temperature.

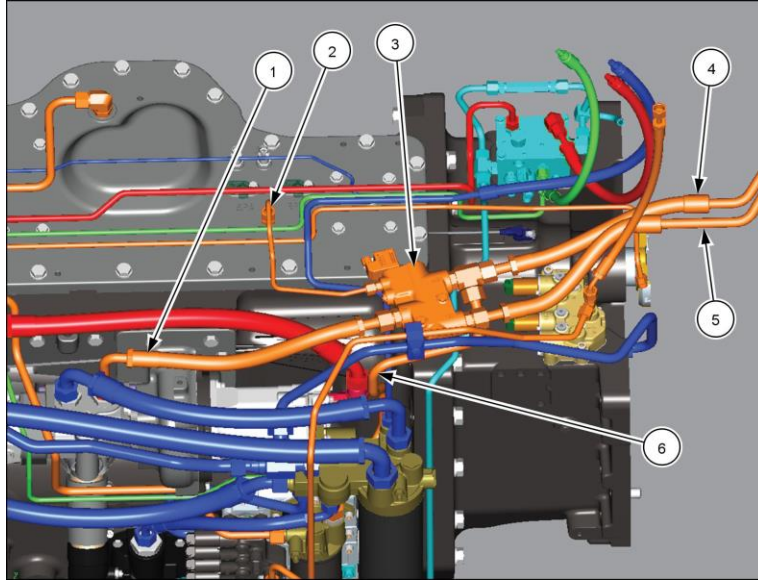


Figure 3.4 Medium Pressure Circuit [orange highlights]

- | | |
|--|---|
| 1. Regulated supply to cooler bypass valve | 4. Cooler return line |
| 2. Cooler bypass drain | 5. Cooler supply line |
| 3. Cooler bypass valve | 6. Cooler bypass to regulated filter assembly |

The regulated hydraulic circuit can be seen in figure 3.5 in orange lines. The cooler bypass valve is highlighted by the pointer with the number 3. This valve is very important for the correct cooling of the oil. This will ensure the temperature is always at a level that will not damage the integrity of the oil itself and the integrity of seals within all of the hydraulic components, lines and fitting of all the hydraulic circuits.

The flow at the rated speed of this gear pump is 102 L/min. the pressure regulator portion of the valve maintains the regulated pressure circuits at 22.4 - 24.5 bar (325-355 psi). All excess regulated circuit flow joins the charge/lube flow circuit. With this data we can observe the ideal hydraulic corner power ($\eta_v = 1$) expected to be yielded from the pump of this circuit:

$$P_{hyd}[kW] = \frac{Q_{pump} p_{pump}}{600} \eta_v \quad 3.4$$

$$P_{hyd} = 4.165 \text{ kW}$$

One thing to consider is that this is the maximum amount of power that may be consumed when the machine is at high rpm. Since the regulated pump is fixed displacement, when the machine is still, and no power is required by the clutches and transmission, the power yielded by the regulated pump is mostly dissipated by the cooler. This with the current configuration of the machine, is unavoidable.

High Pressure LS Circuit

The final level of pressure in the hydraulics of the machine is the two high-pressure circuits. As stated, these two circuits are independently supplied by the PFC LS pump and the TF LS pump. Both of these pumps are variable displacement. The pressure range in this circuit is from 25-210 bar for the PFC pump circuit and 20-210 for the TF pump circuit. The low end of the range on both circuits is dictated by the respective spring margin from the load sensing pumps. The high end will be dictated by the pressure compensator within the LS pumps, both of which are set at 210 bar. Load sense principles will be explained in the next section.

The PFC and TF pumps are designed to operate in two different modes according to the demand for flow and pressure. The modes are:

- Low pressure standby: When there is no demand for flow or pressure, the pump provides just enough flow to make up for internal leakage in the hydraulic system at low pressure. In this mode the pump requires very little power to drive it.
- Pressure/flow delivery and compensation: When there is a demand for flow and pressure from the hydraulic system, the pump responds to provide only the flow required. This limits the power consumption of the system.

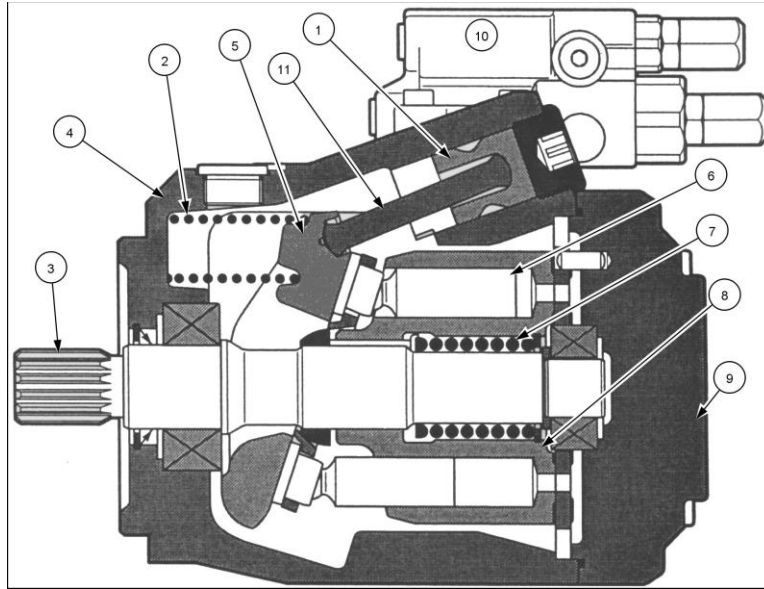


Figure 3.5 LS Variable Displacement Pump

- | | |
|-------------------|--------------------------------|
| 1. Control piston | 7. Piston block loading spring |
| 2. Control spring | 8. Piston block |
| 3. Drive set | 9. Back plate |
| 4. Pump housing | 10. Compensator assembly |
| 5. Swash plate | 11. Control piston rod |
| 6. Piston | |

Figure 3.6 gives an idea of what a LS pump looks like. For high pressure applications variable displacement axial piston pumps are generally used. The PFC pump is the biggest of the two with a flow of 166 L/min at rated speed. Taking into consideration the fact that the pump can reach up to 210 bar in pressure, and it is pre-charged by the lubrication pump at 4.5 bar, the ideal hydraulic corner power ($\eta_v = 1$) of the system can be calculated:

$$P_{hydraulic}[kW] = \frac{Q_{pump} \Delta p_{pump}}{600} \eta_v$$

$$P_{hydraulic}[kW] = \frac{166 \frac{L}{min} (210 - 4.5) bar}{600} \quad 3.3$$

$$P_{hydraulic}[kW] = 56.9 kW$$

The same analysis can be completed for the TF pump, knowing that at rated speed the flow of this pump is 118 L/min. With a maximum allowed pressure of 210 bar and a pre-charge of 4.5 bar, the ideal hydraulic corner power ($\eta_v = 1$) of this pump is:

$$P_{hydraulic}[kW] = \frac{Q_{pump}\Delta p_{pump}}{600}\eta_v$$

$$P_{hydraulic}[kW] = \frac{118 \frac{L}{min} (210 - 4.5) bar}{600} \quad 3.4$$

$$P_{hydraulic}[kW] = 40.5 kW$$

This particular section of the tractor hydraulics is the one that uses the most hydraulic energy, and within the section the individual high-pressure circuits supplied by the PFC and TF pump both utilize the EHR valve the most frequently. Therefore, by positively impacting the energy efficiency of this valve we can affect the overall efficiency of the hydraulic system in a positive way. In order to have a better perspective on how to approach the improvements to the EHR valves, it is important to understand the load sensing architecture that is implemented in the tractor.

3.1 High pressure Load Sense Systems in Reference Machine

Up to this point of this work, we have understood that high energy consumption may come from both of the high pressure load sensing systems. This section will focus on load sensing theory applied to the reference machine. This will later be key to understanding aspects such as instrumentation rationale, efficiency calculations and saturation. The load sense architecture to be described and studied will be Pre-Compensated Load Sense systems since the architecture of our reference machine utilizes this technology.

As we can see in the schematic of the PFC circuit [Fig. 3.6], the system has many sub systems or users that are supplied by one pump.

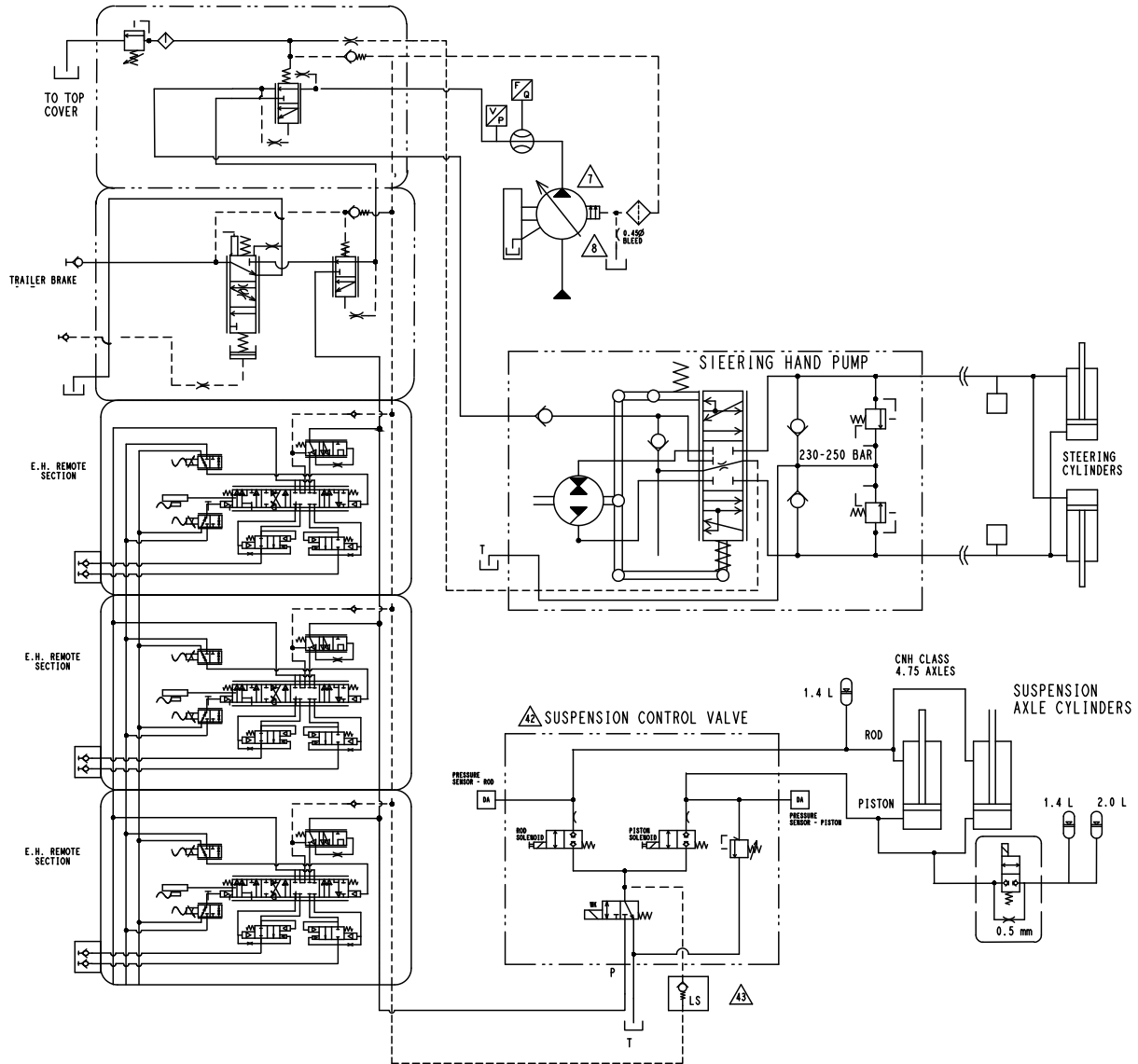


Figure 3.6 Complete PFC Pump High Pressure Circuit

The pump supplies a steering priority valve first. This valve will decide which user between steering pump and the rest of the sub systems will get priority of flow. Of course in an emergency situation, maneuvering the machine takes priority over all other users. From the steering priority, another priority is in series, this is the trailer brake priority. If a trailer is connected to the tractor, the trailer has its own braking system that needs to be supplied hydraulic power to work. Since our machine has no trailer, if flow is not taken by the steering priority, then all available flow from the pump may go to the 3 EHR valves or the suspension. The internal working of the EHR valve will be explained later in this chapter.

The suspension technology in the machine is a passive suspension technology. There is no consumption from the pump whenever the machine is in a working cycle. Energy that is inputted by the road when the tractor is in motion is dissipated by the accumulators and small orifice that can be seen in the schematic. The suspension valve is there to monitor the pressure in the rod and piston side of the machine. A feature that the suspension carries, is that the stiffness can be adjusted. The stiffness has to be adjusted before the machine is used in a working cycle.

The hydraulic schematic from the TF pump has much less users. This high pressure circuit is also pre compensated. From the outlet of the pump the first user met is the hitch valve. This valve only consumes power from the pump whenever it is actuated. We can see that the valve R in the hydraulic schematic is normally closed, so no energy is consumed other than small leakages. From there the 3 EHR valves of the TF circuit can be seen. Unlike the priority valves in the PFC circuit that always consume some small quantity of power, the TF circuit will only supply power to the users that request it. Another point worth mentioning, the restrictions and distance between the TF pump and the inlet of each EHR valve are less than those EHR of the PFC pump. The layout of these components can be observed in Fig. 3.11.

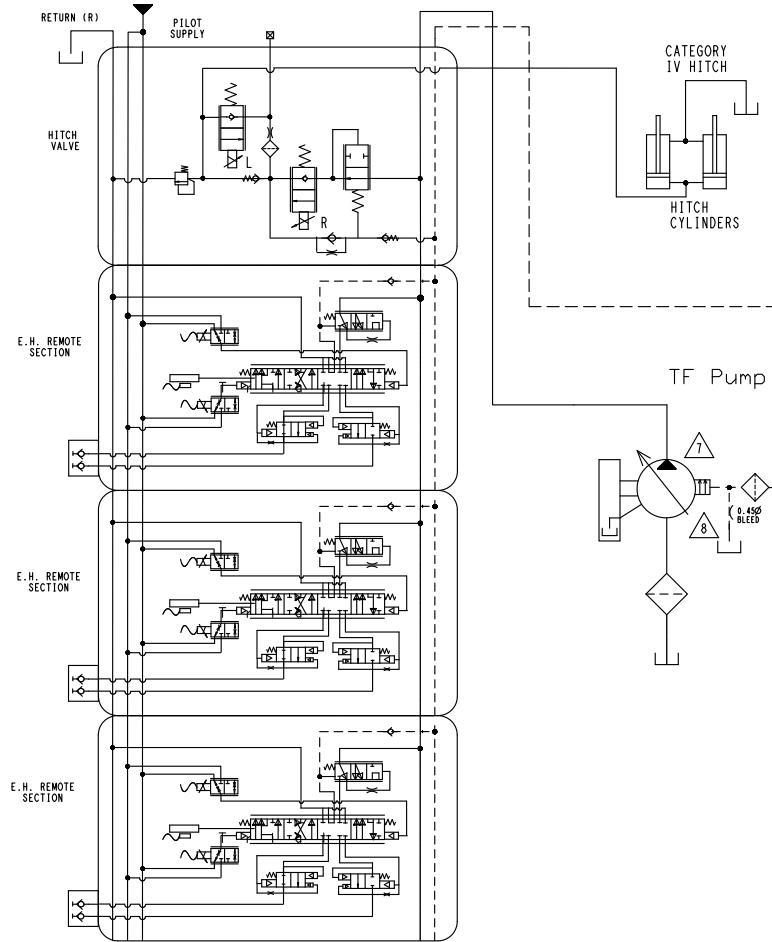


Figure 3.7 Complete TF High Pressure Circuit

3.2 EHR Valve Description

As stated before, this work focused on generating an experimental characterization of the EHR valves. Before any in depth test plan and actual test be taken, it is important to understand the internal workings of the EHR valve. The EHR valve is a pre-compensated proportional spool valve. It has 4 main components; such are listed in the figure below.

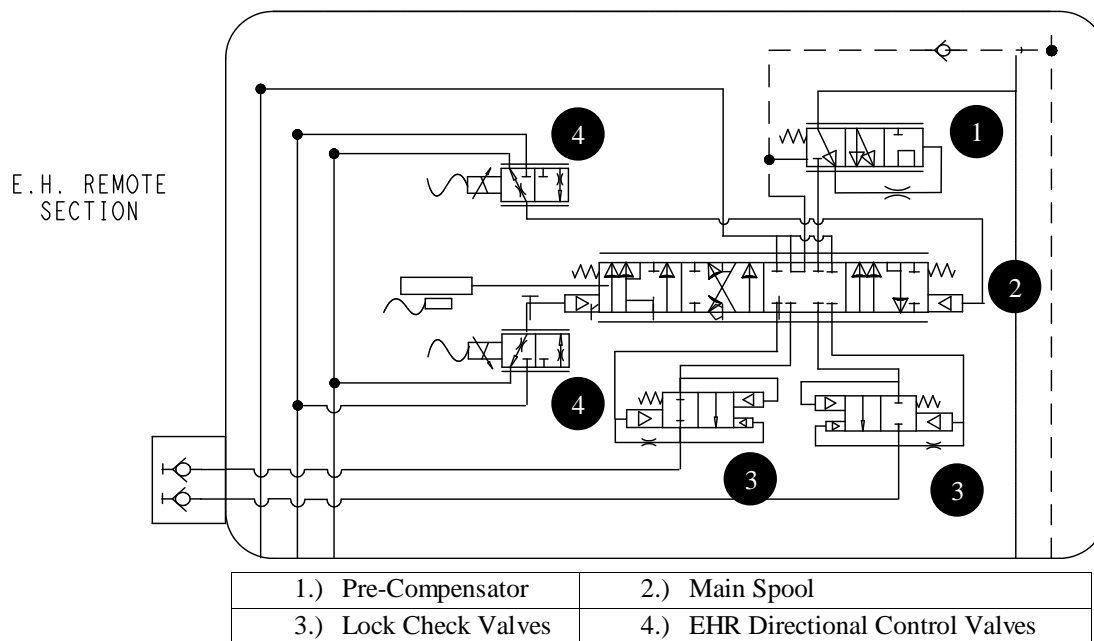


Figure 3.8 EHR Valve Main Components

With the call out of all the major components that are inside the EHR valve, the internal workings can now be explained. Flow comes into the compensator which will adjust itself to burn off excess pressure if needed. Downstream the compensator we have the main spool valve. This valve is commended by two EH proportional valves that determine how much pilot pressure reaches the main spool so that it may be actuated. Downstream the main spool we have two lock check valves. These valves will remain closed when the EHR is not in use. They function as an over center valve, to be more precise, like a counter balance valve in order to be able to hold loads in place hydrostatically.

The main spool can be commanded into 3 positions other than the closed center position that it normally sits in. The positions are: forward flow, reverse flow and float position. In forward direction flow the valve will go into the position to the right of the closed center position. In reverse, the position of the spool will be the one directly left of the closed center position. In float mode, the position furthest left, the two outlet ports of the remote are short circuited and they both connect to tank. Up to this point the hydraulic system in the tractor has been described and shown. It is possible now to discuss about energy efficiency in the EHR valves.

3.3 Energy Efficiency in EHR Valve Circuits

This section explains the reasoning, motivation and purpose of the instrumentation of the machine to acquire hydraulic power. It will also explain the types of sensors and strategies used to place the instrumentation without affecting the current behavior of the machine so that its true behavior can be captured.

The first step towards the instrumentation of the machine is to better understand the hydraulic circuit and component layout in the actual machine all of this was explained in the previous section. The hydraulic circuits in the machine all contain a pump, since most if not all the hydraulic power will be generated by such. The way the pump will generate the hydraulic power will be by converting mechanical power being inputted into its shaft by an external source of energy and displace fluid with a given pressure. This prime mover is the diesel engine. If we go back to the basic definition of energy efficiency, one can state that the energy efficiency of any system is the ratio between the useful energy over the energy input.

By applying this definition to our case, a hydraulic system, focusing only on the EHR valves. The input is the mechanical power yielded by the diesel engine to the LS pumps. With this in mind, the two most important experimental measurement needed are the power input, and the hydraulic output seen at the EHR valves.

Taking these measurements is a challenge due to the complexity of the hydraulic circuit and the machine itself. The first challenge encountered was geometrical restrictions. In order to have the full characteristic of the system, let take into reference the PFC pump circuit in figure 3.13 when only using one EHR valve. The flow of power comes from the input shaft, P_{in} , that drives the PFC pump converting the input mechanical power into hydraulic power. This hydraulic power expressed in flow and pressure travels through the steering priority valve, and into the inlet of the EHR valve. The power at the outlet of the EHR valve is the resulting useful power that the user will have available for external applications.

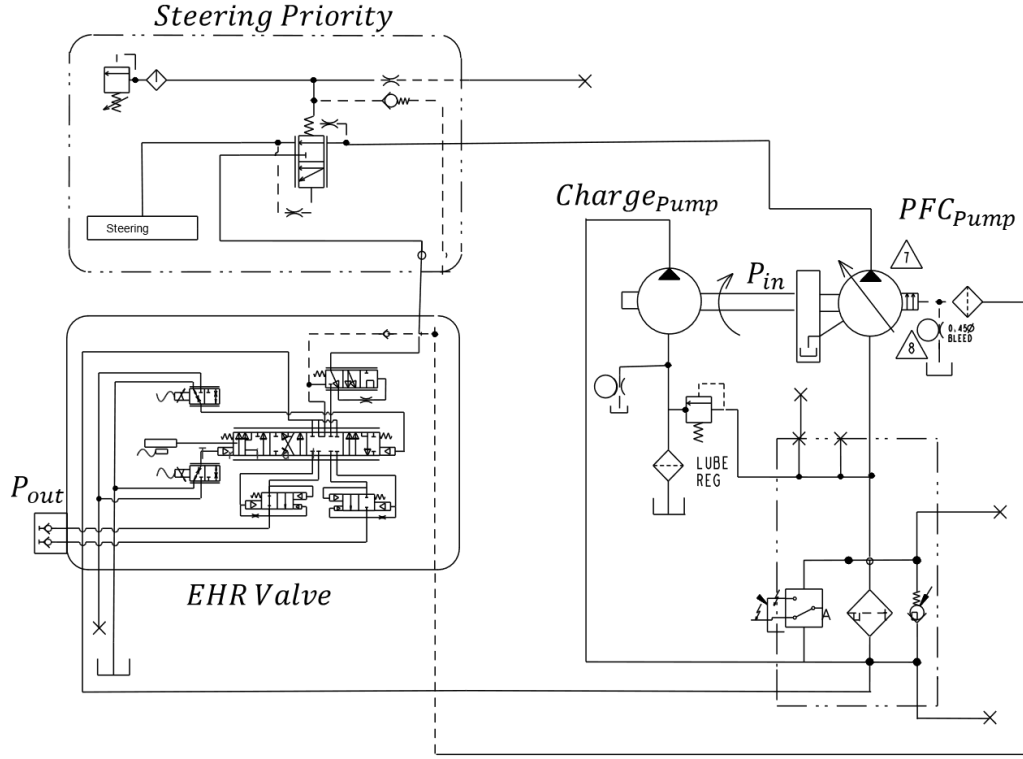


Figure 3.9 Active Components in PFC Pump High Pressure Circuit when 1 EHR is used

The efficiency of the full hydraulic system is then:

$$\eta_{system} = \frac{P_{out}}{P_{in}} \quad 3.26$$

Where:

$$P_{in} = P_{mech} = T_{shaft} \omega_{shaft} \quad 3.27$$

$$P_{out} = P_{hydr} = Q_{EHR} \Delta p_{EHR_{ports}} \quad 3.28$$

This takes into account the efficiency of the pump itself, and all the losses due to pressure drops and heat dissipation when flow travels through the different paths of the hydraulic circuit. However, measuring P_{in} is a challenge due to geometrical constraints at the shaft of the pump. In order to assess the mechanical power input two sensors are needed, one for angular velocity of the input shaft and another for the torque applied to the shaft. A method for instrumenting the machine in order to acquire the measurements addressed before was not possible.

The next strategy was to obtain the hydraulic power at the outlet of the pump. This power is purely hydraulic, and it disregards the efficiency of the pump. However, since the purpose is to test the hydraulic efficiency of the EHR valve circuit, calculating the efficiency of the EHR valve is still possible since it is downstream of the pump. In simpler words, we want to understand how the EHR handles/distributes the available power from the pump. The definition of the efficiency of the system was modified in order to avoid confusion of the power input and output. The power input P_{in} from equation 3.13 was re defined as the power at the outlet of the pump and can be seen in equation 3.29.

$$P_{in} = P_{hydr_{in}} = Q_{Pump_{outlet}} \Delta p_{pump} \quad 3.29$$

Where:

$$\Delta p_{pump} = p_{pump_{outlet}} - p_{pump_{inlet}} \quad 3.30$$

The expression for the system remains the same as before. Only the re-definition of the power input was changed. With this new approach, the sensors needed to acquire the necessary data to achieve our energy efficiency analysis are pressure transducers and flow meters. The specific location of the sensors, the amount and type will be addressed experimental characterization chapter.

The type of data that the motivation of this work seeks to find is power distribution points. Pressure and flow yield these calculations. As stated before, the EHR valve has two working positions, forward or reverse. Since it is a proportional valve, these two general discrete positions may be broken down into infinitely many positions whenever actuated in either forward or reverse direction. To these infinitely many positions, the combination of load and flow command that the EHR valves may encounter is also as vast. A methodology to be able to represent the behavior of the EHR valves in terms of power distribution points without having to take infinitely many tests was proposed. The method is to compile a select variety data points into a single scatter plot based

on certain criterion so that more than one operating condition may be seen and also visual data trends may be observed. Without the need of exponential quantities of tests.

The criterion for data sorting is already given by the definition of energy efficiency in the reference machine. Input values of pressure and flows will be plotted along with output values of the same data, pressure and flow. By selecting an adequate range of load and flow points we can populate scatter plots like the ones seen below:

Load vs Pressure

The purpose of this plot is to give a visual the behavior of the pressure within all EHR. Fig. 3.14 is a general example of the way the actual scatter plots of the results look like. Each dot represents a data point of pressure taken during a test. Each different color in the points indicates a certain test number. In this manner, we can plot multiple tests in one plot making it easier to compare in a qualitative manner while also showing quantitative measurements.

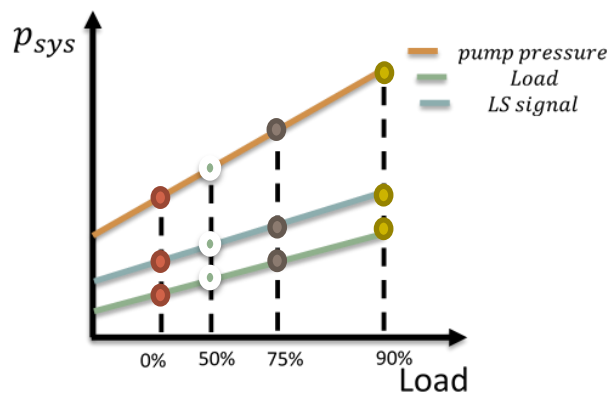


Figure 3.10 Pressure Distribution Plot Example

Load vs Power

The second type of chart created was that of load vs power. This plot is to better visualize the power distribution inside the system per each test. It allows us to understand more in detail where the power is going, where the efficiency decreases and how that loss of power happens.

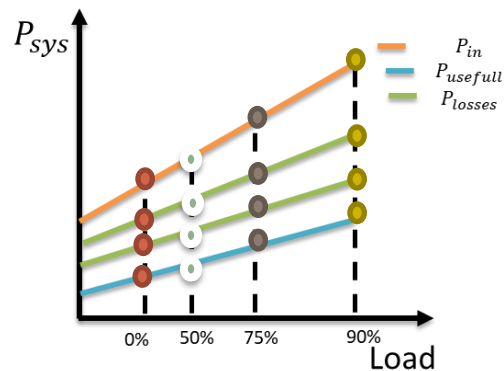


Figure 3.11 Power Distribution Example

In this manner we can identify components within the EHR valve circuits that may be a possible cause for energy loss. As with the previous plot type, there are points that represent a power calculated within the EHR tests. Each color represents a different test number. These scatterplots became a great tool for minimizing test numbers and conditions. In order to minimize tests and conditions, key working conditions of the tractor must be known. Section 3.7 will explain performance standards in agriculture. These standards will aid in understanding possible working conditions and settings so that tests may be minimized but the impact of the data maximized.

4. EHR INSTRUMENTATION AND EXPERIMENTAL TEST PLAN

There are a lot of working cycles that the EHR valves can eventually encounter [section 3.6]. In order to be able to quantify the energy efficiency of the EHR valves in the most common and most important working conditions, a test plan was developed based on input from expert farmers and also standards in agricultural tractor performance.

4.1 EHR Experimental Test Plan

The following test plan will consist of the testing conditions rationale and procedure details to running an experimental testing of the energy consumption study of the reference machine focused on the EHR valves. The reference machine has a total of 6 EHR valves, 3 per high pressure circuit. These with the purpose of supplying hydraulic flow generated in the tractor so that implements (agricultural, forestall, construction) may be used by the operator. In this chapter section the tests conducted along with all the instructions to perform such tests is covered.

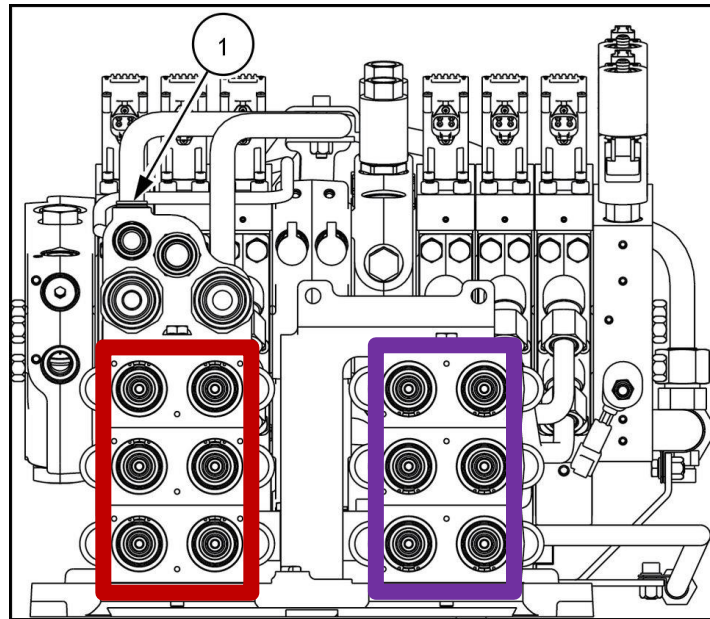


Figure 4.1 PFC EHR Valves (red) TF EHR Valves (purple)

The section highlighted in red in figure 4.4, describes the remotes supplied by the main Pressure and Flow Compensated Pump. The purple section are remotes powered by the Twin Flow Pump. As previously mentioned both pumps are load sensing and can have 60 cc and 45 cc displacement respectively. Both circuits are pressure compensated at 210 Bar.

The testing performed on the remotes will consider several specific aspects. The aspects that have to be the same and consistent throughout all the testing are:

- Engine will be at 2 speeds, high idle and low idle.
- When addressed, remotes with number 1-3 are from the PFC main circuit and remotes 4-6 are from the twin flow pump.
- Forward and reverse movements on the remotes will be tested.

The reason why the engine will be at two speeds is so that the full flow bandwidth of the pumps can be tested. Low rpms will have a different maximum performance than high rpms. Capturing the difference of this behavior is important. These two performance levels may later be compared and analyzed. As seen before, the EHR valve has two directions of command that can use energy. The EHR valve spool and case are not symmetrical, therefore testing both directions of command are important to be able to capture all of the behavior of the EHR.

Tests are divided into 2 categories, single remotes and multiple remotes. By testing only one EHR at a time, we can learn the behavior of the actual valve itself. By having no other load interference in the system, we can better measure the EHR valve efficiency. By including two maximum flow levels that the pump can each, behavior under low and large quantities of flow may be measured and studied. To have reliable data, two separate EHR valves per circuit were chosen and tested. All the EHR valves are identical, testing, more than one per time will show important data. If as an example. the data from one EHR to another within the same circuit were to be drastically different, this information will bring to light unexpected behaviors and considerations.

Multiple EHR tests will yield different sets of behavior that cannot be captured by testing a single EHR. Load interference and possible flow and pressure saturations may be expected when commanding multiple EHR. Certain behavioral aspects may be discovered. Multiple EHR valves

may or may not affect the efficiency value of each individual EHR, this can be known only until it has been tested. By testing multiple EHR valves at different maximum flow levels, low and high pump rpms, behavior of multiple EHR valves can expand knowledge of the system. This testing condition will show if flow saturation condition be achieved. If it is achieved, it will show under what conditions if any will this saturation be possible.

Whether it's a single or multiple EHR valves being tested, they will all be tested under the same 2 sub categories. The first category is: full flow with different loads. This condition will help understand the behavior of the machine when the maximum speed of an implement may be needed, and the load induced by the implement may vary. Since there can exists infinitely many load levels from 0 to 210 bar which is the highest pressure the system may work with, it was decided to first take both end of the spectrum. From the Nebraska test it was learned that the maximum performance of a tractor is at full flow command and 90% of the pressure capacity of the system. This work expanded that and stated that the medium performance level would be at full flow and 50% of the maximum pressure capacity of the system. This allowed for enough data points to be taken in order to be compiled in scatterplots and behavior may be observed.

The second condition is at full load (90% RV pressure) with different flows. This condition is to test whenever the implement connected to the machine requires max pressure at all times but working speeds may vary. This condition will give much information about the possible flow restrictions in the EHR valve circuits. Test tables have been generated to better keep track of test numbers and configuration of the test. Both circuits, PFC and TF pumps will be tested according to the test tables

4.1.1 Single Remote Tests

The ISO schematic for the test for the TF Pump can be seen in figure 4.5 below. The test circuit for the PFC pump was presented in figure 3.11. Since the circuits are independent, the same external instrumentation was used for both circuits. This was possible since the EHR valves from the two different circuits would not be tested simultaneously, only EHR from the same pump were tested simultaneously.

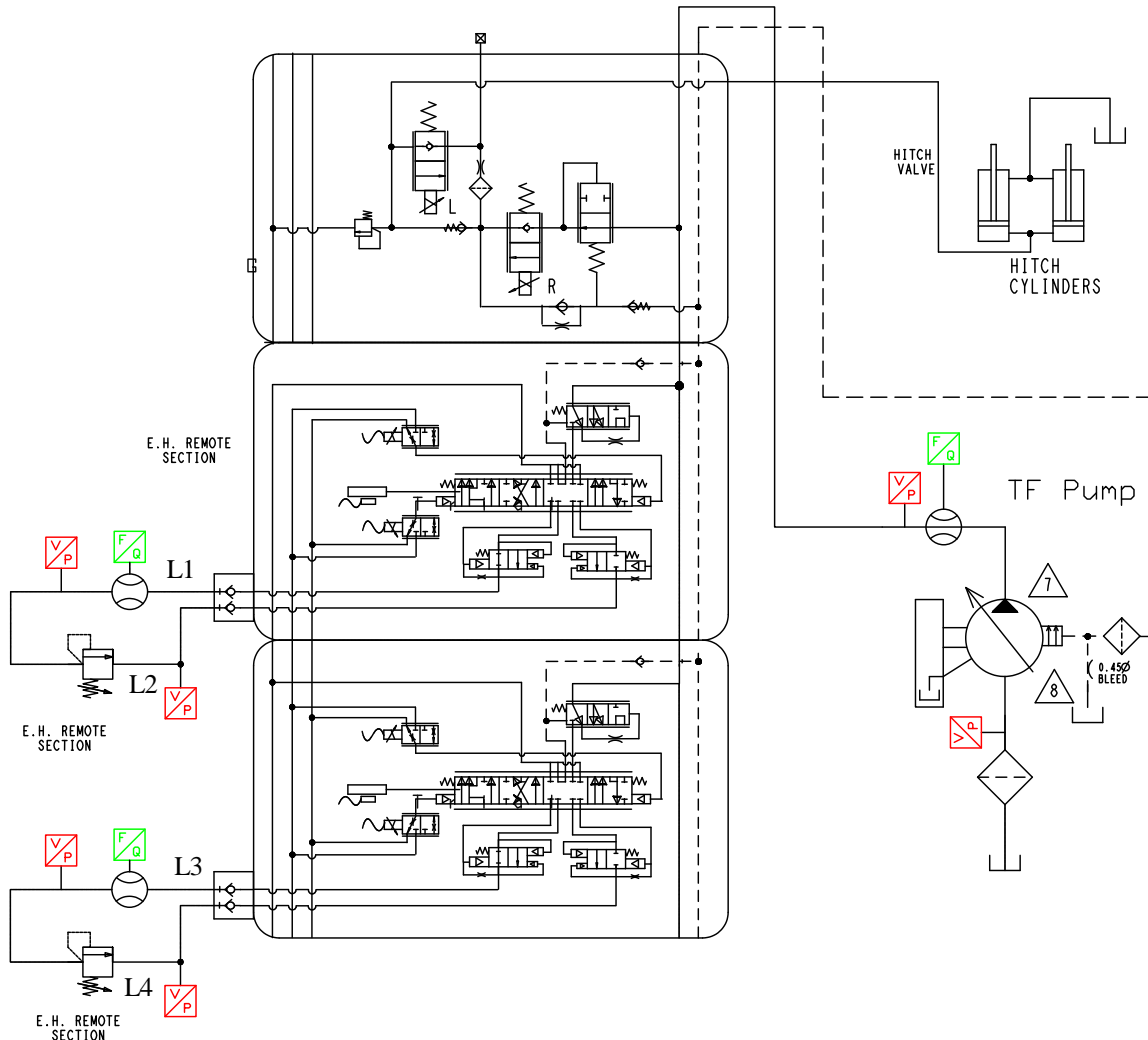


Figure 4.2 TF Pump Circuit Sensor Location

The schematic shows the set up for a multiple EHR valves on the twin flow circuit. This set up will be the same throughout all the remotes on the reference machine. When testing single EHR valves, only one valve was actuated at a time.

The dimensions of lines L1 - L4 were handwritten at the time of the first test and then kept the same for the remaining tests. Lines L1 & L3 are the connections from the quick connects to the flow meter. The connection from the flow meter to the loading relief valve is direct through fittings. Lines L2 & L4 were connected from the outlet of the loading relief valve to the quick

connect. Keeping the length of lines L1-L4 constant for all the tests ensures similar testing conditions and also aided in correct modeling strategies when the experimental test data was used to develop a working model of the tractor circuits. More on the model will be explained in the results section.

The simulation of the load will be given by the relief valve. A relief valve was chosen due to its characteristic behavior. It is easier to control the pressure induced in the system than a variable orifice. Load pressures are more controllable and also repetitive.

Within this section, we will look into the tables from which the test charts in the appendix were generated.

Table 4-1 Testing Conditions for EHR Valves

Single Remote [100% Flow]				
	Load			
Remote 1	0%	50%	75%	90%
Remote 2	0%	50%	75%	90%
Remote 4	0%	50%	75%	90%
Remote 5	0%	50%	75%	90%

The table above describes the tests conditions to be combined in order to run tests in each EHR valve. This is to characterize each sections efficiency focusing on different pressure levels with high flow. It takes into account a full flow (max command to the EHR) with different load levels. EHR's to be tested were chosen randomly. The ones randomly selected were remotes 1,2,4 & 5. Only two remotes per section were tested since remote valve are basically identical.

Table 4-2 Flow Commands for EHR Testing

Single Remote [90% Load]			
	Flow Command		
Remote 1	25%	50%	75%
Remote 2	25%	50%	75%
Remote 4	25%	50%	75%
Remote 5	25%	50%	75%

For this test table, the load is set to a constant value while the flow command is changed. No steering, braking, or other hydraulic consumption is done in any of the test that were made. Only parking brake is engaged. It is important to mention that these test tables also had other constant variables that were maintained the same during testing. All tests were run at low & high rpm, 900 and 2200 rpm respectively. Besides that, the oil temperature was tested at low and high temperatures. $30\text{ }^{\circ}\text{C} \pm 5\text{ }^{\circ}\text{C}$ and $65^{\circ}\text{C} \pm 5\text{ }^{\circ}\text{C}$. The tolerance of the temperature comes from the Nebraska Standard. If it is found that data between each test is consistent in an individual EHR, it is not necessary to run all tests for both tests tables.

The tables above generalize the testing configurations to be made on the remotes. The test tables developed can be seen in the appendix. Similar test plans were developed for the rest of the high pressure hydraulic systems like steering, hitch valve and suspension. These plans are not included in this work since this work is dedicated only to EHR valves.

A preview of the test tables in the appendix is shown below. This is so that the explanation of the test identifiers may be made and the test tables may be understood. The identifiers make it easy to read all the variables that were controlled during each individual test. An example is test 1, S-F-A-L-L-FC-0. For test 1, the nomenclature represents a test with a single remote, forward direction, 1 represents an EHR from PFC pump, low temperature and low rpm, full command at 0% load. All variables that are contained within this test chart and tables were all recorded.

Identifiers by column

- Single or multiple [S or M]- Indicates number of remotes used in the test
- Direction [F or R]- Indicates the orientation of the command given to the remote.
- Remote Number- Specifies what remote is being tested
- Oil Temperature- Gives the temperature of oil used for testing can be high or low
- RPM- indicates the idle speed of the engine adjusted for the test can be high or low
- Command- The value of flow command given to the remote can be expressed in percentages or FC [Full Command]
- Load- Indicates the load simulated at the remote. Can be expressed in percentages or FL [Full Load- 90% of RV setting]

Table 4-3 Preview of Test Table for EHR valves.

Test	Single\ multiple	Direction [F/R]	Remote Number	Oil Temperature [Hi/Lo]	RPM [Hi/Lo]	Command	Load
1	S	F	1	L	L	FC	0
2	S	F	1	L	L	FC	50
3	S	F	1	L	L	FC	75
4	S	F	1	L	L	FC	90
5	S	R	1	L	L	FC	0
6	S	R	1	L	L	FC	50
7	S	R	1	L	L	FC	75
8	S	R	1	L	L	FC	90

4.1.2 Multiple EHR Tests

Based on information on test procedures read in literature and knowledge from experienced farmers, most of the time, at least two remotes are being used at a time. For this reason, maximum EHR valves to be tested simultaneously is two per test. The ISO schematic is the same one as presented in the single EHR test section. As with the single remotes, two test tables have been designed. One table will keep a constant full flow command for every direction of the remote and only the load between will vary each test. While the other table keeps a constant loads and varies the flow.

Table 4-4 Multiple EHR Tests Conditions

Multiple Remotes [25% Flow]				Multiple Remotes [90% Load]			
Load				Flow Command			
Remote 1&2	50%	75%	90%	Remote 1&2	25%	50%	75%
Remote 4&5	50%	75%	90%	Remote 4&5	25%	50%	75%

One thing to mention at this point is that the original command to multiple EHR valves in the left table seen above originally was supposed only to be ran at 100% remote command. With a 100% command flow saturation condition was reached. Data under flow saturation was taken and analyzed. In order to fully understand how multiple EHR valve work under correct load sensing theory, tests were also taken at 25% command. For the right table, test under 50% flow and 75% flow to both of the EHR valves were not taken. This is due that it was validated that the flow saturation condition was the same behavior whenever more than 25% command was given to multiple EHR valves.

Table 4-5 EHR Valves Test Summary

Test Number Summary	
	Number of Tests
Single Remote	224
Multiple Remotes	48
TOTAL	272

The table above is a summary of all the remote tests. A total of 272 remote tests were conducted. All the corresponding data was analyzed. All tests proved to be of good quality with accurate data. The results of such test, the post processing and the efficiency analysis will be explained in the following chapter of this work.

4.2 Reference Machine Instrumentation

As stated before, the measurement of the available power to the hydraulic system and also the power that reaches the user at the EHR valve outlet are the two most important measurements for the purpose of this work. Therefore, choosing the correct instrumentation that will yield trustworthy data while keeping cost at a minimum is a difficult challenge.

The power that will be measured is hydraulic power. For the power input, there needs to be a measurement of the pressure at the inlet and outlet of the pump along with a measurement of the available flow at any given instant. By taking these measurements, we will have an idea of the energy that is being inputted into the system. The first measurement that we will consider is pump pressure. The sensors selected met a specific criterion in order to be able to take the most accurate measurements while also not overloading the DAC system with unnecessary data points. The second measurement is volumetric flow of the pump. Flow meters also need to meet specific criteria some of it is the same as with pressure sensors. An explanation of the specifics and how the sensor work is explained briefly.

Pressure Transducers

There are many points to consider when selecting the correct pressure sensor. The best compromise between quality, compactness and cost is desired. Since data is to be recorded in a digital DAQ system, pressure transducers with an analog read out were not considered. Pressure transducers work by converting and applied pressure into a measurable signal, usually an analog electrical signal which is linear and proportional to the pressure. There are 3 main types of pressure transducers as seen in figure 3.8.




Figure 4.3 Pressure Transducer Types

Absolute pressure is measured relative to a perfect vacuum. A common unit of measure is pounds per square inch absolute (PSIA). Differential pressure is the difference in pressure between two points of measurement (measured relative to a reference pressure). This is commonly measured in units of pounds per square inch differential (PSID). Gauge pressure is measured relative to current atmospheric pressure. Common measurement units are pounds per square inch gauge (PSIG).

The sensor type chosen to be utilized is the gauge type. It is the most common type for our application, since it will always take into account atmospheric pressure and give the true “gauge” pressure inside the system. The sensor must be able to measure up to 210 bar in order to fully span the working pressure at which the pump can be. The resolution of the sensor is not required to be extreme. Increments of 0.1 bar is more than enough to be able to acquire the data that we need. For our study, the pressure sensors selected are compact, precise and with low cost. The specs of the sensors can be seen in the table below.

Table 4-6 Pressure Transducer Specs

Pressure sensor Specs				
<i>Brand</i>	<i>Model Code</i>	<i>Quantity</i>	<i>Range (bar)</i>	<i>Signal output</i>
<i>Wika</i>	A10-6-P-G-534-NBZA-FC-AGZ-ZS	8	0-275	0-10 VCD
<i>Wika</i>	A10-6-P-G-411-NBZA-FC-AGZ-ZS	1	0-14	0-10 VCD
				

Flow Meters

Flow meters are devices utilized to measure the volumetric flow of any fluid inside and enclosed system. It detects and measures the volume being displaced over a value of time. In our case, it will detect the liter per minute that the hydraulic pump will yield. This is the second variable from equation 3.15 that needs to be measured in order to quantify the power being yielded by the pump. Flow meters need to be in-line to quantify the correct flow. Alike pressure transducers, flow meters have 3 main categories:

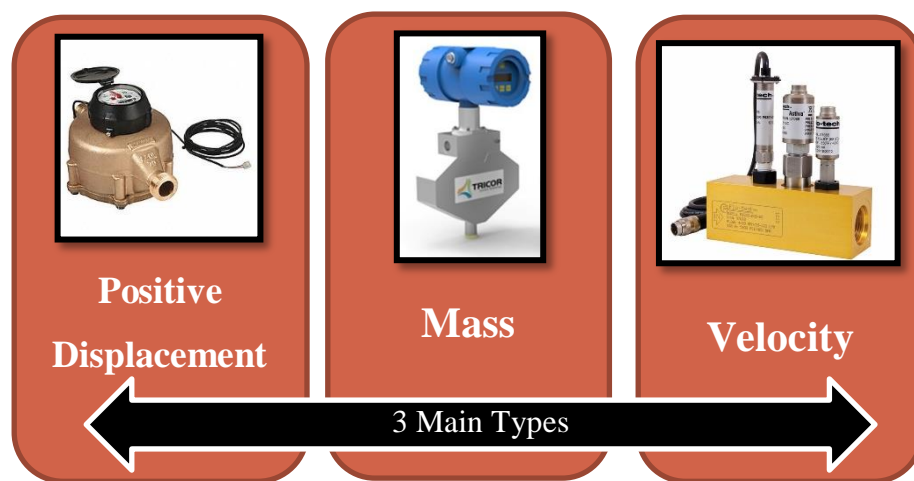


Figure 4.4 Types of Flow Meters

Positive displacement flow meters are unique as they are the only meter to directly measure the actual volume. All other types infer the flow rate by making some other type of measurement and equating it to the flow rate. With PD meters, the output signal is directly related to the volume passing through the meter. Includes bi-rotor types (gear, oval gear, helical gear), nutating disc, reciprocating piston, and oscillating or rotary piston. These types of flow meters are the most accurate, but also the most expensive. Since they can almost immediately identify the volume being displaced, they are more commonly used in high precision flow control applications.

Mass flow meters have an output signal is directly related to the mass passing through the meter. Thermal and Coriolis flow meters fall into this category. These are best when the flow comes in discrete intervals and to quantify actual mass being displaced.

The final category, and the category of the sensor that we utilized for this study, is the velocity flow meter, the output signal is directly related to the velocity passing through the meter. It is typical for these sensor to be propeller or turbine based. The technology utilized within velocity flow meters is frequency based. The propellers of the turbine will spin and a magnetic pick up sensor will detect this frequency. The flow rate change will proportionally affect the frequency and voltage.

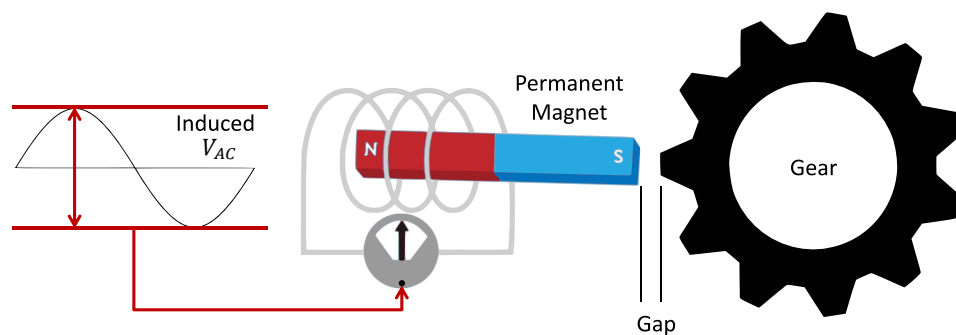



Figure 4.5 Magnetic Pickup Example

A magnetic pickup is essentially a coil wound around a permanently magnetized probe. When discrete ferromagnetic objects—such as gear teeth, turbine rotor blades, slotted discs, or shafts with keyways—are passed through the probe's magnetic field, the flux density is modulated. This induces AC voltages in the coil. One complete cycle of voltage is generated for each object

passed. The figure above is a basic representation of the measurement technology. As the gear spins, the gap between the magnetic pickup is discretely increased and decreased in equal intervals. The sine wave generated will alternate with different frequency that is based merely on the rpm of the gear. The voltage value will also increase in value when the gear spins faster since the magnetic field is stronger. The specs from the sensor utilized in this work are:

Table 4-7 Flow Meter Specs

Flow Meter Specs				
<i>Brand</i>	Model Code	Quantity	Range (LPM)	Signal output
<i>Flo Tech Ultima</i>	F6206-F	4	12-300	25-690 Hz
 <ul style="list-style-type: none"> • Four flow ranges • Turbine flow measurement 				

4.2.1 Sensor Location

The reference machine has a total of 6 EHR Valves. Are supplied by the PFC main pump and the other 3 by the TF pump. As stated before, both circuits are independent so the same study was conducted on both of the EHR circuits. They layout of the circuits is different, therefore the sensor location for each of the circuits is not the same.

For the purpose of the study, the outlet of both the PFC and TF pumps where instrumented along with their respective LS lines. Two EHR valve per circuit were instrumented with 2 pressure transducers and a flow meter each. It is important to mention that the pressure transducers and flow meter were externally mounted on an external circuit with quick connects. In this manner, the amount of sensors was kept low. That makes a total of 4 pressure transducers and 2 flow meters that were externally placed on the EHR valves and shared between PFC and TF circuits. For each pump a sensor was placed at the outlet and LS line of each pump. The inlet of both pumps were instrumented by only one pressure transducer. The reason for that is they both share the same

input line and the distance between the pumps is small enough to not introduce significant losses at the inlet of each pump.

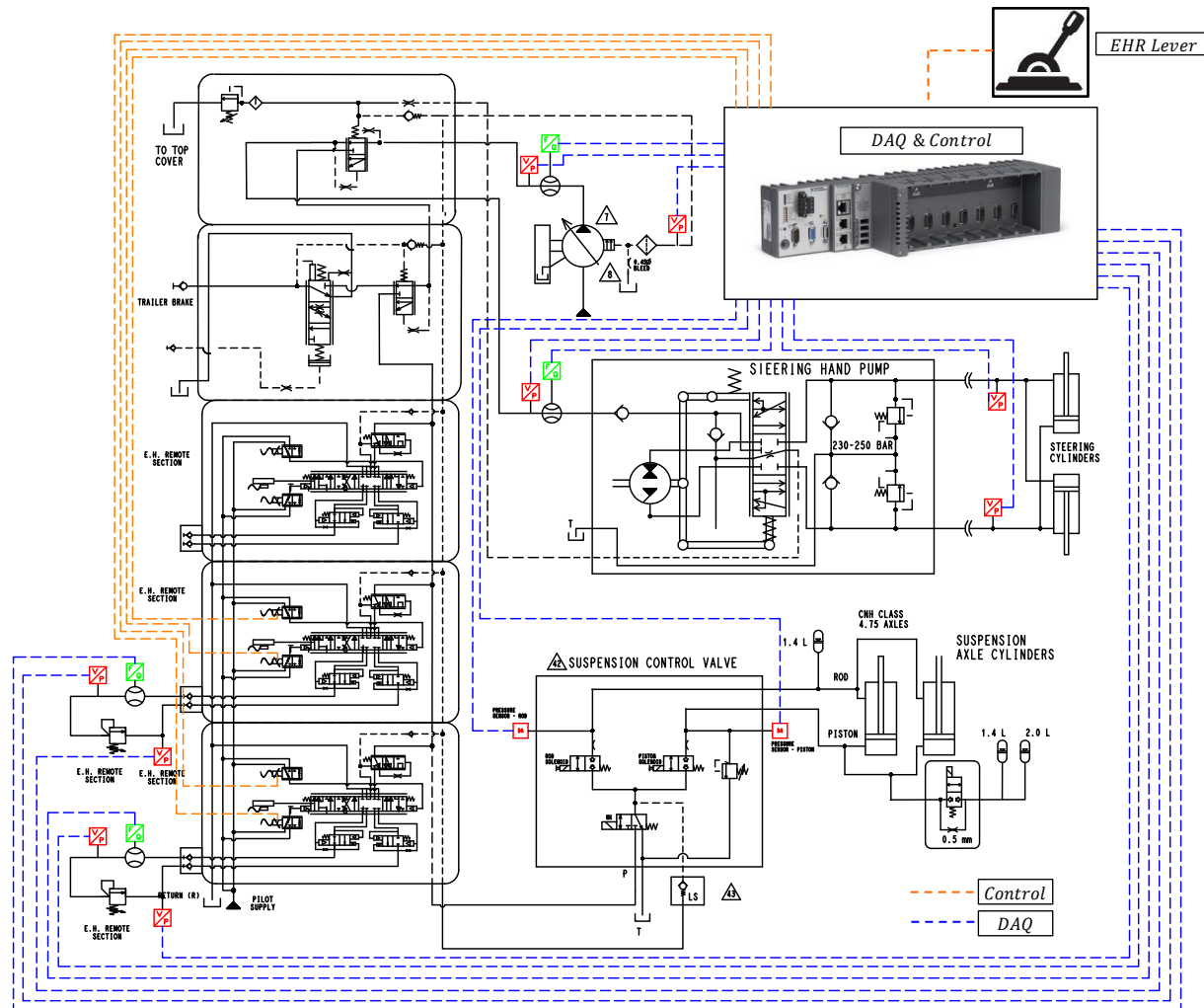


Figure 4.6 PFC Hydraulic Circuit Instrumentation Location

Fig. 4.7 displays of the location of all the sensors placed for the PFC pump circuit. A total of 7 dedicated pressure transducers, tagged in red and 2 dedicated flow meters tagged in green were placed. A couple external flow meters and 4 pressure transducers were also placed. All the control commands can also be seen in the figure. The signals for sensors and commands all go to the DAQ system also represented. The external sensors noted in this figure are the same sensor utilized for running tests with the TF pump circuit.

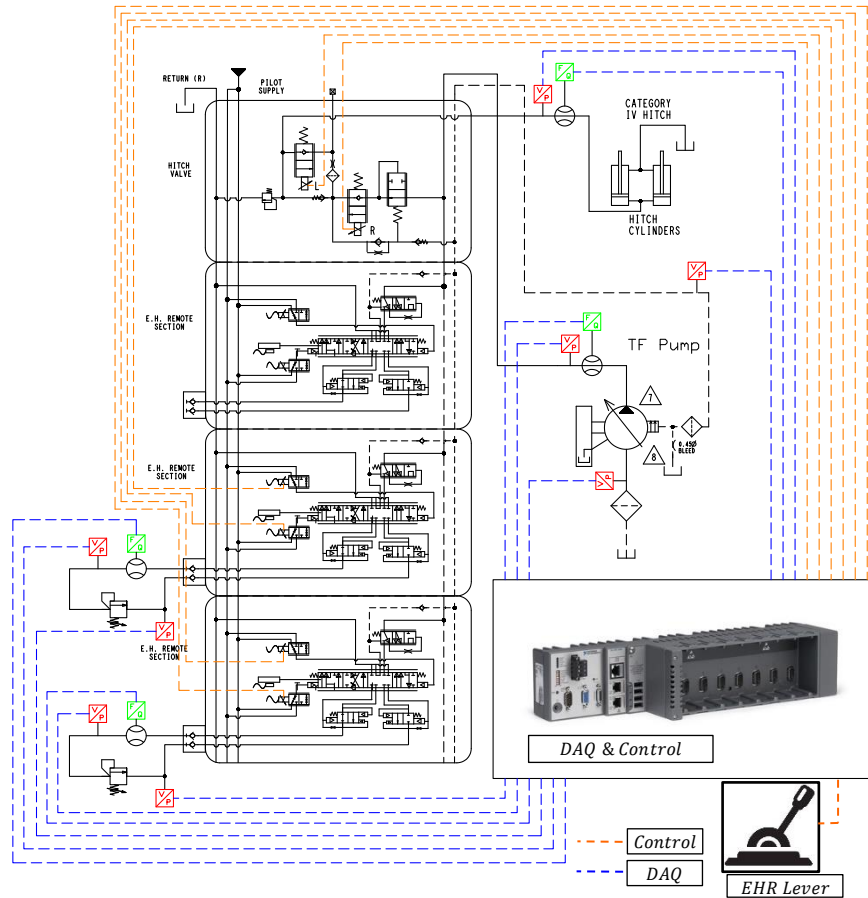


Figure 4.7 TF Hydraulic Circuit Instrumentation Location

A total of 4 dedicated pressure sensors also tagged in red and two dedicated flow meters in green were mounted in this circuit. The external sensors are a repetition of the ones previously seen in the PFC circuit. All pressure sensors are previously calibrated by the supplier with a 5-point linear calibration. The flow meters were calibrated based on a 3-point calibration. The correct measurement of the frequency at the flow meters is crucial, low frequencies can sometimes be contaminated by noise and high frequencies can cause an aliasing problem if the sampling rate is not fast enough. The hardware and software developed to acquire all signals to the sensors and machine signals [CAN bus] will be explained shortly in section 4.3.

4.2.2 EHR Lever Signal Modification

The EHR valves can be activated in the cabin through mechanical levers. By pushing the lever forward, the EHR goes into the forward position and when pushing the lever in reverse, the EHR goes into reverse position. These levers have potentiometers that output a signal based on the lever position. Each lever can output a signal from 0.5-4.5 V. Since there is no negative voltage, the way of detecting the direction of flow is by a voltage range.

Table 4-8 EHR Lever Output Breakdown

Direction	Voltage Range	Max Command
<i>Forward</i>	0.5-2.3	0.5
<i>Reverse</i>	2.7-4.5	4.5

The table above explains how the CAN controller detects the direction and command given by the lever. We can see that there is a dead zone of signal from 2.3 -2.7 V. This is the neutral position of the lever. Once it exits that zone it will give either a reverse command or forward command. Each EHR has a localized microcontroller that receives CAN signal from the main UCM of the EHRs. The command signal flow seen in figure 6.14.

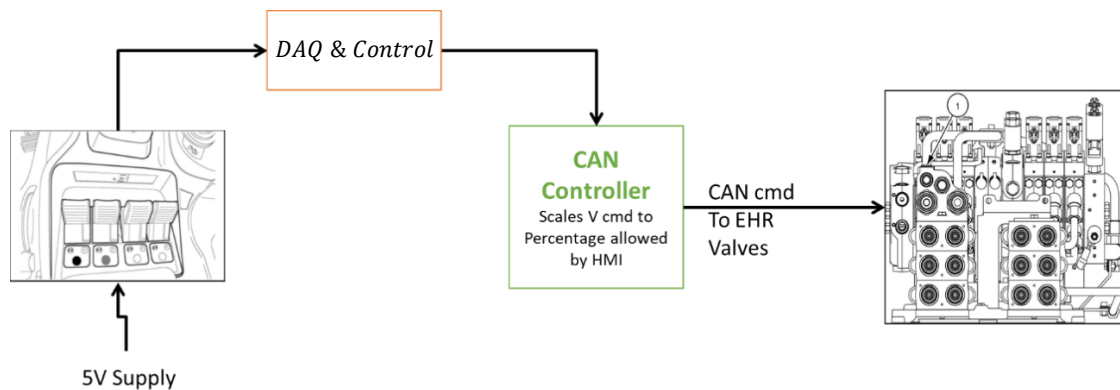


Figure 4.8 EHR Command Signal Flow

The CAN controller interfaces with the levers and the touch screen HMI in the cabin. With the touch screen HMI, the operator can set the maximum command given to the EHR. The command can be fixed from a 0-100% value. This is useful so that the operator can place the lever in a fully actuated position but only the maximum command signal allowed by the HMI is given.

Since there is no possible way to override the CAN command to the EHRs externally. The flow sharing control was implemented between the lever output and CAN controller input. The controller would receive the analog voltage from the levers, import them into LabVIEW and if the controller was active and the machine in flow saturation, the flow control would output a different command from the one requested at the lever.

There were modifications made in hardware areas in the operator cabin. For the hardware, the EHR levers output was rewired into the DAQ system and from the DAQ system wired into the input of the CAN controller. In this manner, it was capable to record the command voltage given by the levers. This allowed for correct command tracking in all the testing and for the incorporation of a flow sharing algorithm discussed in Chapter 6.

4.3 Data Acquisition (DAQ) system

Having acquired and placed the sensors in their respective key position for the best measurements, the following step is to design the DAQ system that will be able to record all the data we need. For this we look into National Instruments (NI) hardware and software.

4.3.1 NI DAQ Hardware

The hardware that makes up the data acquisition system is a design that integrates a cRIO chassis. A CompactRIO or cRIO for short is a real-time embedded industrial controller made by NI. The cRIO is a combination of a real-time controller, reconfigurable IO Modules, FPGA module and an Ethernet expansion chassis. Our system will have a signal flow chart like the one shown in figure 3.12.

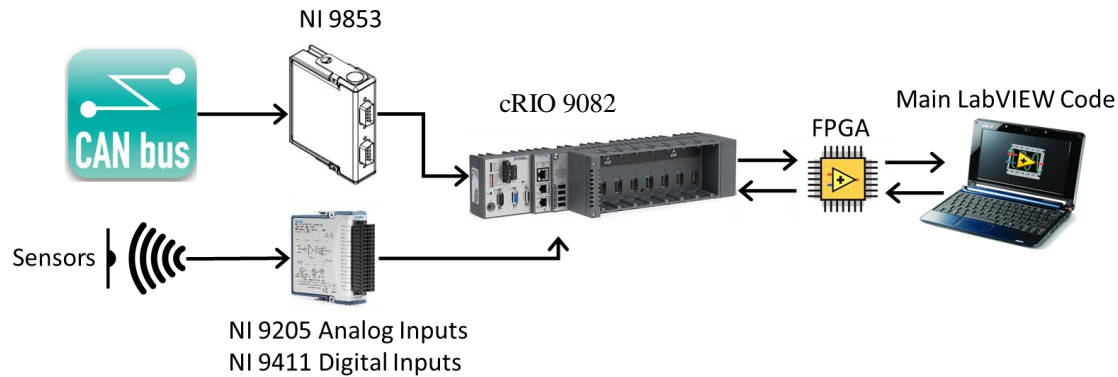


Figure 4.9 DAQ System Layout

All items in the previous figure will be explained one by one. The heart of the system like mentioned before is the cRIO 9082. This is the computer that is dedicated to run and administer resources for all the NI modules that are placed within the slots of the cRIO. The internal specs of the cRIO 9082 will not be discussed in detail, however all the pertinent details can be found in the service manual of this device.

Mounted into the cRIO, are NI modules that each can acquire a different set of data and/or command a different set of data. The modules such as the NI 9205 and NI 9411 are input modules. Analog and digital signals can be inputted into those modules respectively. The c-RIO was mounted on a custom electrical panel inside the tractor cabin. This panel included all power supplies required for all the instrumentation. Two 24 VCD power supplies were utilized. One to supply the cRIO and the other to supply all the pressure transducer of the system. The main power came from a 120 VAC power inverter that was connected to the 12 V battery of the tractor. All the power supplied drew power from the 120 VAC power inverter.

A factor that determined utilizing an NI 9205 card is that it has 32 input channels that each can sample up to 7.8 kS/s, in other words 7.8 kHz per channel. That speed is more than enough to be able to sample the highest frequency (690 Hz) that the flow meters can go up to. This is a very important factor in order to avoid aliasing. Aliasing is the phenomena that occurs whenever a signal being sampled, is sampled at a lower frequency at which the signal itself behaves, generating another signal that is not correct. Fig. ## illustrates this phenomenon in a simpler manner.

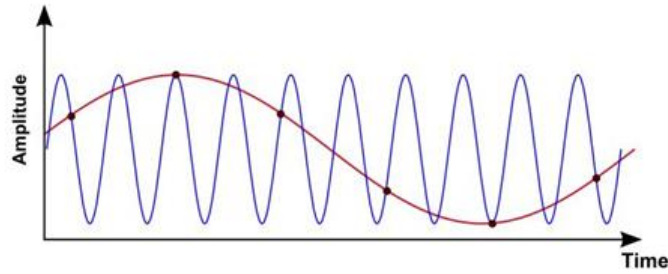


Figure 4.10 Data Aliasing Example

In the previous figure, the inadequately sampled signal appears to have a lower frequency than the actual signal. Increasing the sampling frequency increases the number of data points acquired in a given time period. For a given sampling frequency, the maximum frequency you can accurately represent without aliasing is the Nyquist frequency. The Nyquist frequency equals one-half the sampling frequency, as shown by the following equation.

$$f_N = \frac{f_s}{2} \quad 3.17$$

That formula allows for the correct minimum sampling frequency of the flow meters. Since we can expect up to 690 Hz from the flow meters, that makes the Nyquist frequency and sampling frequency be:

$$\begin{aligned} f_N &= 690 \text{ Hz} \\ f_s &= f_N * 2 \\ f_s &= 690 \text{ Hz} * 2 = 1380 \text{ Hz} \end{aligned} \quad 3.18$$

A minimum sampling frequency of around 1400 Hz is required. The NI 905 module can handle this sampling rate. The other module NI 9411 was utilized to aid in other research work unrelated to this work.

In order to monitor the CAN bus on the tractor, an NI 9853 module was also installed and utilized. The signals monitored and the purpose of these signals is detailed in chapter 4. All of this hardware was mounted in a custom made enclosure that was fitted into the cabin of the tractor. The final piece of the DAQ system is the PC laptop computer that was utilized. Within this computer and in the LabVIEW platform, a custom program was developed to acquire all the necessary data point, achieve data scaling, data recording and also achieve control strategies that will take part later in this work.

4.3.2 NI DAQ Custom Built Software

The laptop contained the FPGA computer code which was compiled to be run on the cRIO, as well as an acquisition host code which ran independently on the laptop (both developed in the LabVIEW programming environment). In order to implement the system, a LabVIEW program (called a VI) was created in a laptop computer. This laptop computer would interface with the DAQ system installed on the tractor. Through this communication data was acquired and also the controller command was given to the EHR valves. The front panel of this software can be seen below.

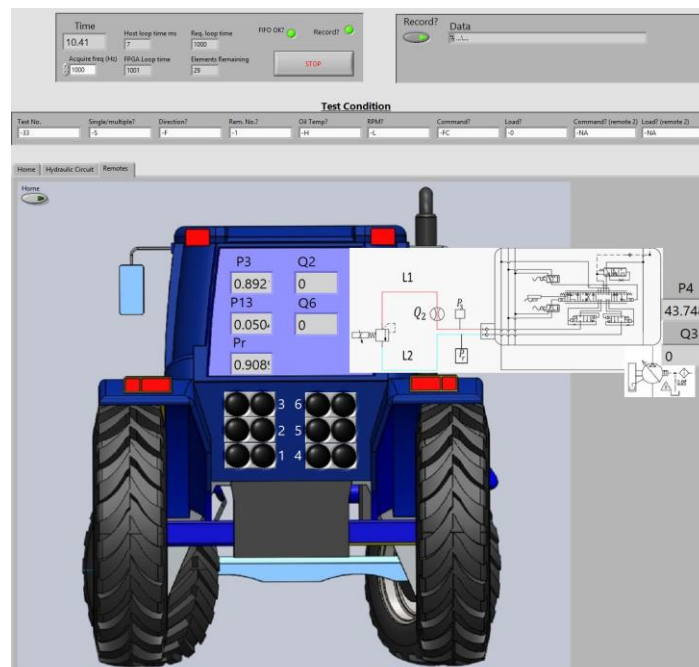


Figure 4.11 Main Panel of DAQ System Host Code

This was the front panel utilized for data acquisition control. As can be seen in the figure, the front panel had a stop button to stop the code. A record button whenever data wanted to be recorded. A read out of the elapsed time and also code loop speed, to verify correct sampling and data recording speed. The picture of the tractor represents the rear side where the remotes are located. An ISO schematic was placed for understanding of the data points being recorded. Real time read outs of the values of the data can also be observed. All sensor scaling was done real time in the background Vi.

Due to the background Vi being so vast, a high level description will be given while pointing out important sections of the code built for this work. There are 4 main sections inside a while loop. This while loop will execute as soon as the code is initiated and will continue until commanded to stop in the front panel. The order in which each section is presented is not the order in which the sections execute. That order is defined internally by LabVIEW.

The first section will read the data coming from a FIFO of data that is being transmitted by the cRIO. It will also scale the acquired data in real-time to turn analog voltages and frequencies into pressure and flow values. Section 2 is a live handshake to the cRIO in order to be able to command EHR valves in real time. This live handshake is important since signals are not sent through a FIFO back to the cRIO. This is to avoid delays. Section 3 places any: live command signal given, pressure and flow measurement taken and all available CAN messages and generates an array of data and column headers in TDMS file format to store all recorder data. This happened whenever the record button is pressed in the front panel. Finally, section 4 is the section where the flow share approaches 1 & 2 were implemented. This section will output original operator EHR command, manual in program EHR command or controller EHR command outputs.

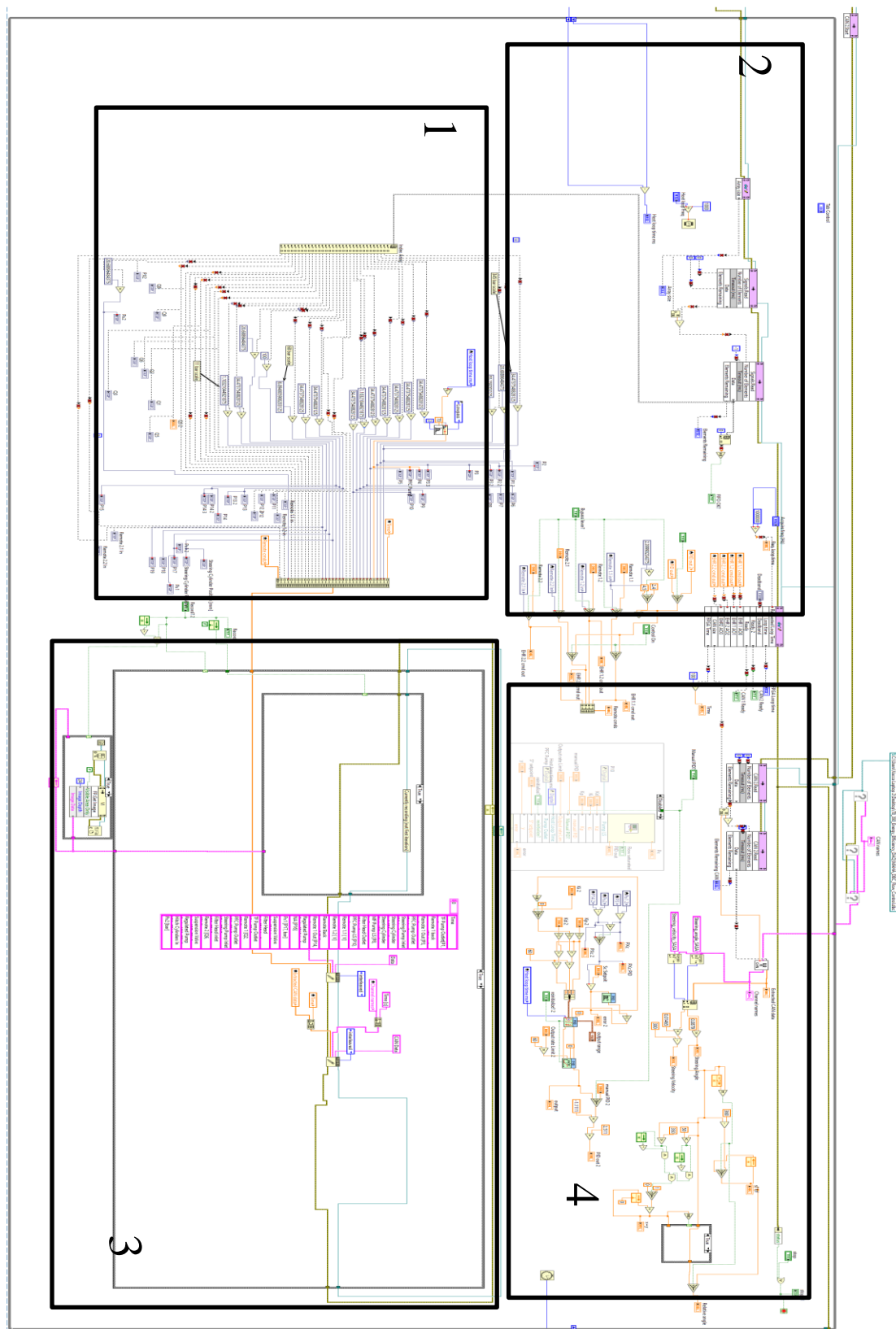


Figure 4.12 Full Custom Built LabVIEW Vi

5. EHR TEST PLAN RESULTS

Once all the testing was done, it was time to analyze all of the data that was recorded. The machine was instrumented on all of the hydraulic circuits. For the purpose of this work and study, only the sensors that are utilized during the EHR tests are going to be mentioned. Since there was a lot of tests taken and a lot of data, processing all tests one by one manually was going to be challenging. In order to be able to show the data in a better format, and since all of the tests were run at steady state, it was decided that the representation would be through a scatter plot. A point of the plot would represent the average values of a certain time interval of a single test. To facilitate the processing all the data was post processed in the Matlab environment.

5.1 Post Processing with Matlab script.

The Matlab script served to be able to open all the excel files generated through our DAQ system, and input them into Matlab where it would average the data based on the steady state time interval inputted by the user. Since not all tests began command at the exact moment, the input of the user was still needed so that the script could automatically average all the data at the time interval desired.

To grasp a better understanding, Test 3 raw signals can be seen in figure 5.1 below. In that graph one can notice that the command to the EHR valve began at around second 15.8. From there the flow to the EHR arrived and it built pressure in the load relief valve, once the set pressure of load was met, the relief valve opened limiting the pressure and setting the required simulated load. Test 3 calls for 75% load, which meant 150 bar based on a 200 bar max setting. We also notice at around second 16.5, the data starts its steady state condition. All measured pressure signals do not vary for the next 5 seconds, more than enough time to have an accurate measurement and correct test.

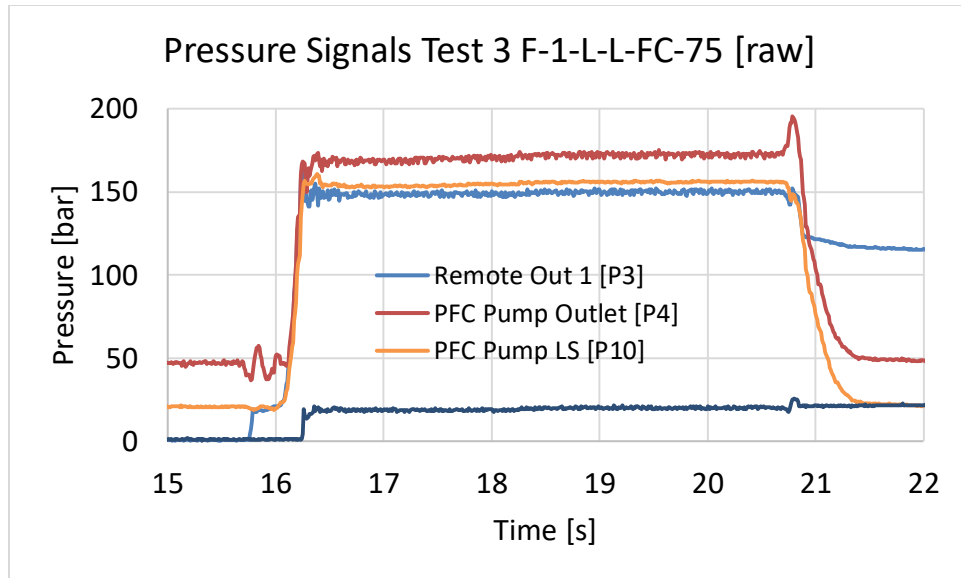


Figure 5.1 Example of Desired Test Data

Since there are more than 200 single EHR tests, manually looking and averaging the data would become an endless task. With the help of a Matlab script we were able to turn the recorded data into a text file output with all the averaged points we desired. The actual code may not be disclosed, however, the flow of data conversion may be shared and explained.

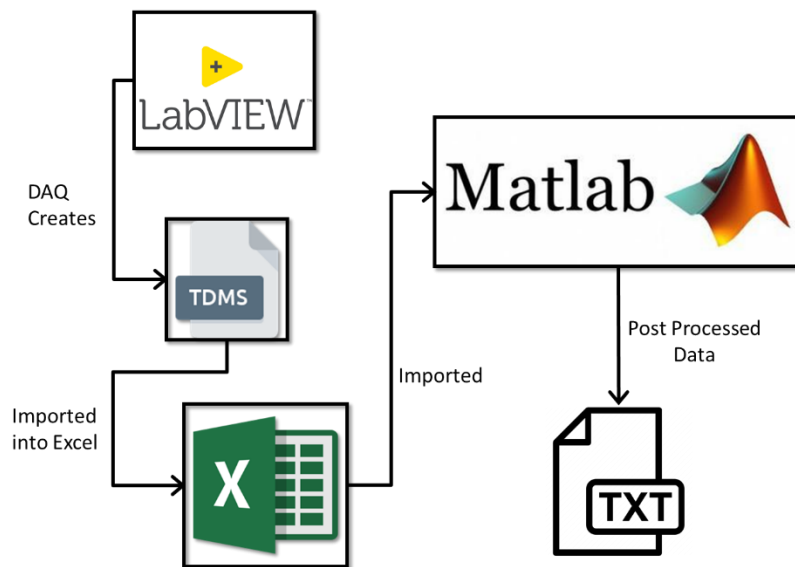
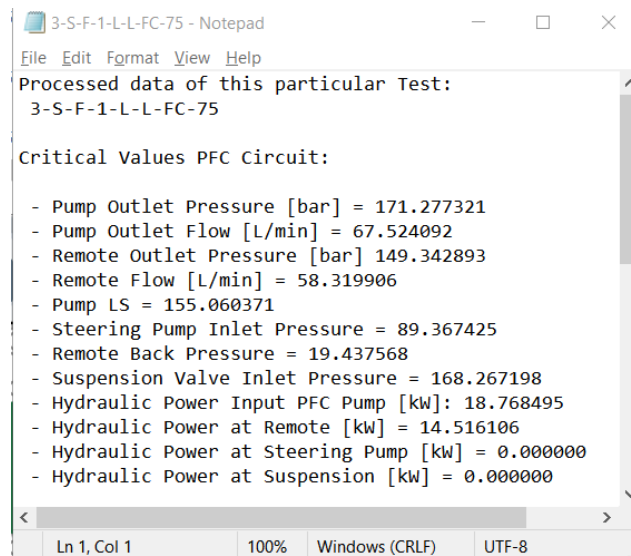


Figure 5.2 Data Flow and Conversion

LabVIEW generates a TDMS file, with a conversion plugin installed in Excel, the TDMS file may be converted into an Excel file, from there the files source address is placed in the Matlab script where it automatically imports it. Once imported, the user can state the time interval from which Matlab will perform the data post process. The final output is a text file with all the data required to be analyzed. The criteria for post processing the data was explained in chapter 3, where the definition of hydraulic power and efficiency was established.

Once all text files for each test are generated, the points go into another Excel spreadsheet where all the figures and plots can be made so the data can be analyzed visually. The inside of each text file looks like Fig 5.3.



```

3-S-F-1-L-L-FC-75 - Notepad
File Edit Format View Help
Processed data of this particular Test:
3-S-F-1-L-L-FC-75

Critical Values PFC Circuit:

- Pump Outlet Pressure [bar] = 171.277321
- Pump Outlet Flow [L/min] = 67.524092
- Remote Outlet Pressure [bar] 149.342893
- Remote Flow [L/min] = 58.319906
- Pump LS = 155.060371
- Steering Pump Inlet Pressure = 89.367425
- Remote Back Pressure = 19.437568
- Suspension Valve Inlet Pressure = 168.267198
- Hydraulic Power Input PFC Pump [kW]: 18.768495
- Hydraulic Power at Remote [kW] = 14.516106
- Hydraulic Power at Steering Pump [kW] = 0.000000
- Hydraulic Power at Suspension [kW] = 0.000000

Ln 1, Col 1    100%    Windows (CRLF)    UTF-8

```

Figure 5.3 Output Text File Example

From the text file of test 3, we can learn that the actual load at the remote was at around 149 bar. As long as the load pressure was 5 bar higher or lower than 150 bar (75% load) the test would be considered valid. The same criteria applied to all of the other tests. Pump Outlet pressure was at around 171 bar. Other pressure readings like steering pump were included since that data was useful for another work.

We also have a value of the flow commanded, with it, the hydraulic power input to the system was known, also the final available hydraulic power at the remote valve was known. With this, the energy efficiency for this test may be easily calculated.

$$\eta_{Test\ 3} = \frac{P_{At\ EHR\ valve\ Exit}}{P_{input\ by\ PFC\ Pump}} \times 100 \quad 5.1$$

$$\eta_{Test\ 3} = \frac{14.51}{18.76} \times 100 \quad 5.2$$

$$\eta_{Test\ 3} = 77.34\ \% \quad 5.3$$

This analysis was made with all of the remaining tests. In the next section, the most significant tests results will be presented. They will flow the same structure as the test plan, starting with single remotes from both PFC and TF pumps and ending with multiple remotes within the same two circuits.

5.2 EHR Single Remote Tests Results

Completing all the tests took a considerable amount of time, however once all the tests from HER were completed, all the data was post processed so that it may be analyzed. As we learned in the previous section the text file was generated from averaging 5 second of steady state data from all of the tests. Finally, all of these text files were imported into excel in order to be plotted.

Figure 5.4 shows a brief section of all the data compiled into the excel spreadsheet. All the variables recorded can be seen as column headers. Each row represents a single test. The difference in cell color represents a direction in which the EHR was tested, there are 4 colors due to the fact that there are two separate circuits and two direction of testing per circuit.

Test Number	Command	Pressure at pump [bar]	Flow at pump	Pressure at remote	Flow at Remote	Pump LS	Steering Pump Inlet Pressure	Remote Back Pressure	Suspension Valve Inlet Pressure	Power Input	Power at Remote	Power at Filter Assembly Inlet	Hydraulic Power at Steering Pump [kW]	Hydraulic Power at Suspension [kW]	Filter Assembly Inlet Flow	Filter Assembly Inlet Pressure	Filter Assembly Outlet Pressure	Load	Remote	Direction
1	100	53.730913	70.809028	30.289835	66.635012	40.975876	36.090102	19.83349	50.641187	5.82982	3.363939	0.88735	0	0	146.0408	3.645625	4.331962	0	1F	
2	100	124.78947	68.843349	102.865108	60.585117	109.824417	68.72857	19.24849	121.88487	13.82872	10.38682	0.892276	0	0	143.2557	3.737133	4.266152	50	1F	
3	100	171.277321	67.524092	149.342893	58.319906	155.060371	89.367425	19.43757	168.2672	18.7685	14.51611	0.943212	0	0	142.6862	3.966236	4.505774	75	1F	
4	100	214.493888	61.236717	195.843104	49.797735	198.551633	109.92698	17.00614	213.08742	21.47416	16.25424	0.85181	0	0	137.5558	3.715479	4.089181	90	1F	
5	100	56.337403	70.468553	30.174603	67.754511	43.269645	37.442479	19.25221	53.14979	6.076123	3.407442	0.894256	0	0	144.2737	3.719	4.602639	0	1R	
6	100	126.244368	68.744552	102.293741	63.496856	111.666696	69.678314	18.84064	123.8536	13.96224	10.82555	0.901746	0	0	142.6118	3.79385	4.382434	50	1R	
7	100	173.612339	67.228805	149.174676	61.643089	156.978593	90.687269	18.9866	170.56162	18.94081	15.32598	0.946431	0	0	141.2636	4.019849	4.57039	75	1R	
8	100	214.960735	55.885986	196.355137	48.712296	198.462883	110.209281	16.34837	213.31598	19.61433	15.94152	0.844387	0	0	130.007	3.896961	4.378466	90	1R	
9	100	54.613975	70.813016	30.377257	66.672627	41.191507	36.309145	20.00957	51.436905	5.93539	3.375553	0.88151	0	0	146.1223	3.619614	4.323308	0	2F	
10	100	88.907789	71.026942	66.745017									0	0				50	2F	
11	100	171.864347	68.029629	149.408995	58.902264	155.592928	89.928111	19.61557	169.39221	18.98565	14.66755	0.945908	0	0	144.6813	3.922721	4.416889	75	2F	
12	100	214.526379	58.893176	195.86044	47.798299	197.874291	110.014612	17.34666	213.19983	20.64103	15.60299	0.862252	0	0	135.5403	3.816952	4.236857	90	2F	
13	100	55.1652	70.684884	30.549233	67.931104	41.665333	36.895286	19.90587	52.059751	5.965601	3.458738	0.90915	0	0	145.8533	3.739992	4.526923	0	2R	
14	100	125.922698	69.101823	102.70774	64.155468	110.417539	69.057958	19.09174	123.15243	14.00898	10.98211	0.89935	0	0	143.0906	3.771109	4.284968	50	2R	
15	100	172.994611	67.385675	149.791174	61.754112	155.911131	90.582301	19.15599	170.29861	18.89145	15.41704	0.991135	0	0	142.5567	4.17154	4.785733	75	2R	
16	100	214.868573	57.433032	196.160971	50.700532	197.645285	109.861606	16.55914	213.2199	20.15432	16.57578	0.865701	0	0	133.0149	3.904982	4.317387	90	2R	

Figure 5.4 Processed Data Compilation Example

From this data, several plot were made in order to have a better visual on key aspects to the data. These aspects are data trends, outliers or any pattern that may result in the different test conditions. Two different types of scatter plots were made as mentioned in Chapter 3.

5.2.1 PFC Single EHR Tests Results

The results shown in this section are the most significant to the study of the EHR valve efficiency. Reporting all the results from all the tests is not necessary since all that we can learn about our system, we can learn it from the results to be shown. The remaining test data however, was still very useful. It was used to develop a working model of the EHR valve in the Simcenter Amesim environment. The development, work and validation of this model is not part of the document, however the model was a key tool, more on this will be elaborated in Chapter 6.

When an EHR valve is utilized in the field, it is done under full flow command. The EHR valve supplies as much pressurized flow as in can to the implement. The implement itself has local controls that distribute this flow. This was validated by the steady state data seen on the DLG test standard from section 2.3.2. Therefore, in order for us to better understand the efficiency in an actual working condition, our attention was heavily focused on studying the data from the tests that had a full command of flow, and different load levels.

The first set of tests examined are those completed under low temperature and low engine rpm. Tests in the forward direction for the EHR valve shown. One remote per circuit is presented since data did was consistent between different EHR valves within the same circuit.

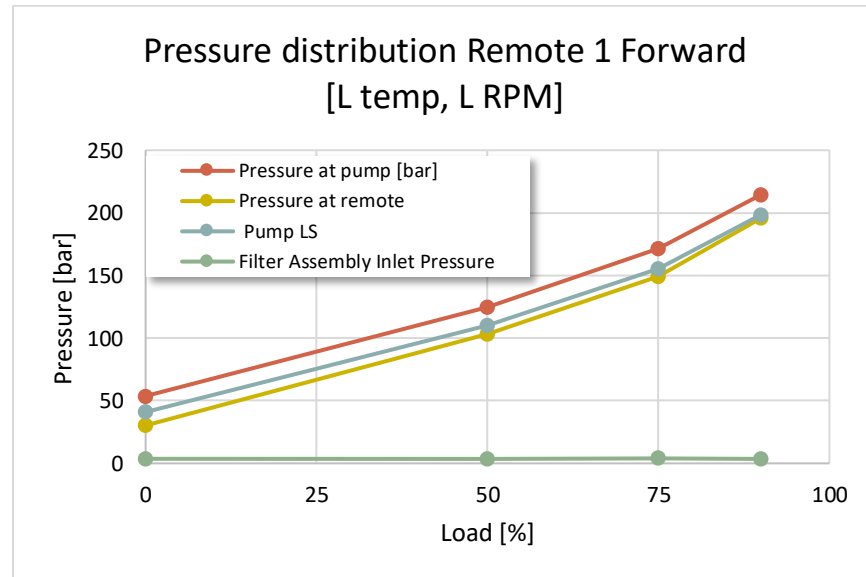


Figure 5.5 Pressure Distribution of EHR 1

The data plot in Fig. 5.5 shows how the different pressures in the system behave. From this type of plot, we can learn many points on how the system behaves. As an example, in the above plots, in all the tests where the load was at 0%, 50% & 75% the load sense signal is a bit higher than the actual load. This is unexpected since in load sensing theory [see section 2.1], the pressure at the LS port is the same one as the load. This was something that was looked into. The reason to why this behavior appears was discovered and will be explained in section 5.2.1.1 of this chapter.

With this pressure distribution, we can also learn the power distribution in the system since we measured flows. With this we can see in the plot below how the system behaves under the stated characteristics. The data in Fig. 5.6 behaves as expected, since the flow is constant, the higher the pressure seen at the load, then the higher the power that is required. Since it is the PFC pump, the flow to the EHR valve has to go through the steering priority valve first, and then to the EHR. The value of power consumed by the steering system is also plotted as proof that no

power was consumed by the steering system and would alter our results. It is clear that there is discrepancy between power input and power output. The same behavior is seen on both remote 1 & 2.

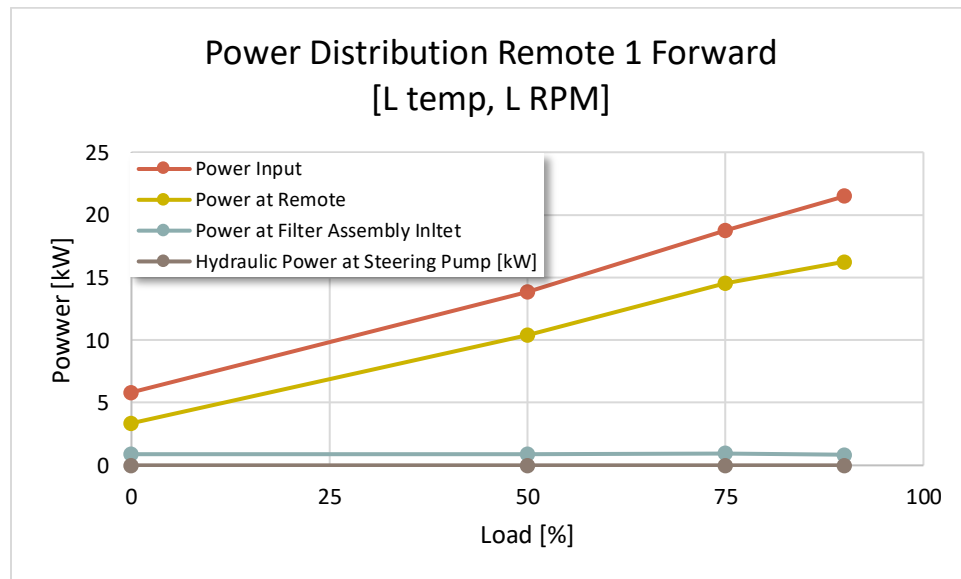


Figure 5.6 Power Distribution of EHR 1

To further validate that that is the trend, the same tests were analyzed for the TF pump circuit. As before, the results for the TF pump EHR valve 4 are shown when the test was taken at low temperature and low rpm.

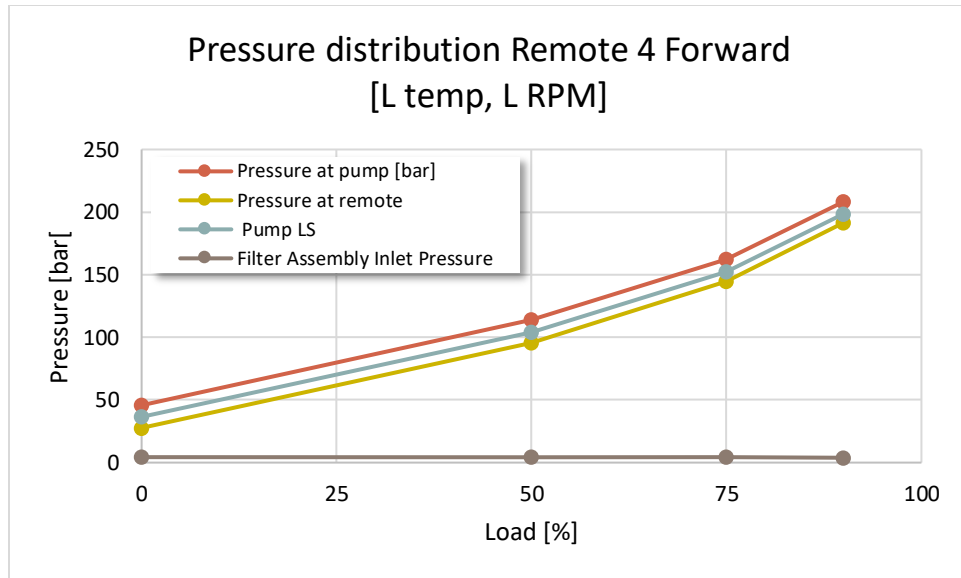


Figure 5.7 Pressure Distribution of EHR 4

Like the PFC pump circuit, the pressure data in Fig. 5.7 behaves in a similar manner. This is expected since the EHR valves are the same ones as the ones in the other circuit. Once again there is a small discrepancy in the LS signal compared to the load.

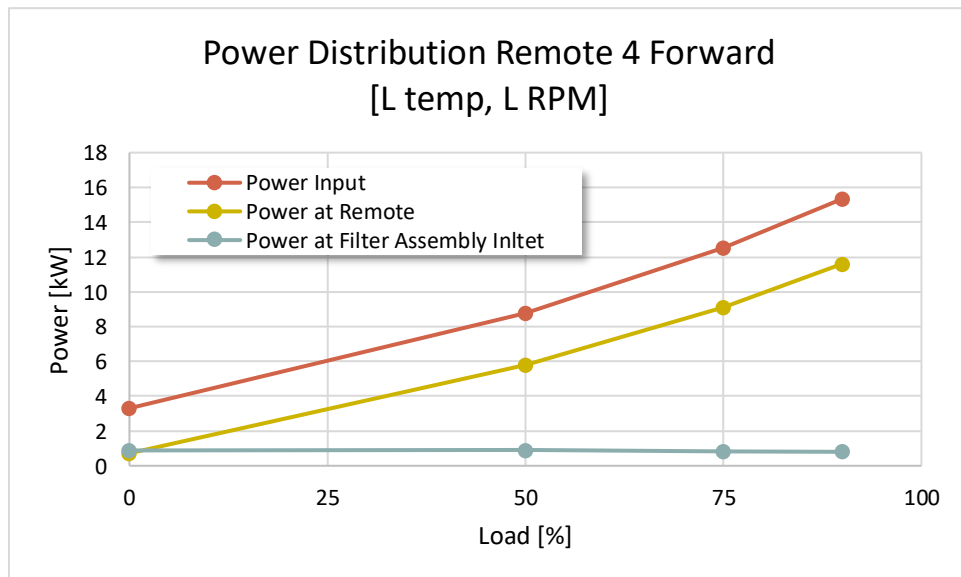


Figure 5.8 Power Distribution of EHR 4

Maximum flow coming from the TF pump is lower than the one of the PFC pump. Therefore, in Fig. 5.8 it is expected that the power yielded from the TF pump to be smaller. From the TF pump, flow goes and can first be delivered to the hitch valve and then the EHR valves. However, since the hitch valve is a command on or off valve, and not a priority like the one of the steering, there was no need to plot the power consumption from the hitch since it was never actuated. The distance from the TF pump to the EHR valves is shorter than the one in the PFC circuit, therefore not a lot of energy would be lost. However, we see that the remote power seems to be still considerably lower than the one inputted by the pump.

The EHR does seem to be losing energy in both circuits. To quantify the average value of energy loss at the EHR valve, all the data from the remotes in both circuits were taken into consideration. The average efficiency in any direction within the same circuit EHR valves was calculated and represented as an efficiency percentage. This efficiency percentage per EHR valve can be seen in the bar graph. The lower axis represents the load levels at which the EHR valves were tested and the vertical their respective efficiency.

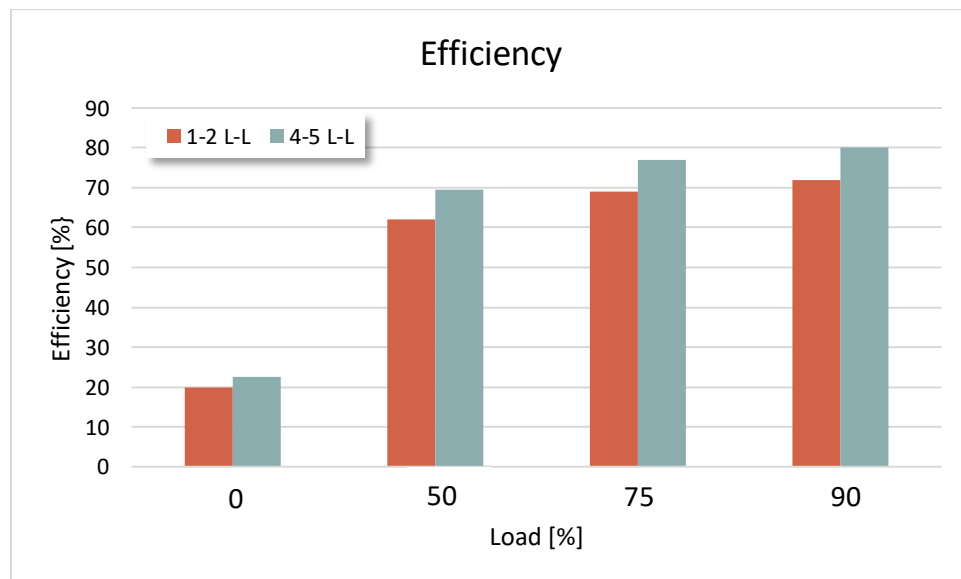


Figure 5.9 Average Efficiency of PFC & TF EHR Valves

The EHR valves mounted on both PFC and TF circuits are the same, they have the same model code from the supplier. The difference in percentage comes from the position and circuitry

difference. PFC EHR valves have more distance from the pump in the machine and also more restrictions since flow to the EHR must pass through the steering priority. Efficiencies of the TF EHR valves are considered to be the most accurate and closer to a real values of efficiency of only the valve, since the distance from the pump is relatively short and there are minimum restrictions of flow from the pump to the actual EHR.

The second set of tests examined are those completed under high temperature and low engine rpm. Tests in the forward direction will be shown for both remotes. The high temperature will show us the effect of oil viscosity in the tests.

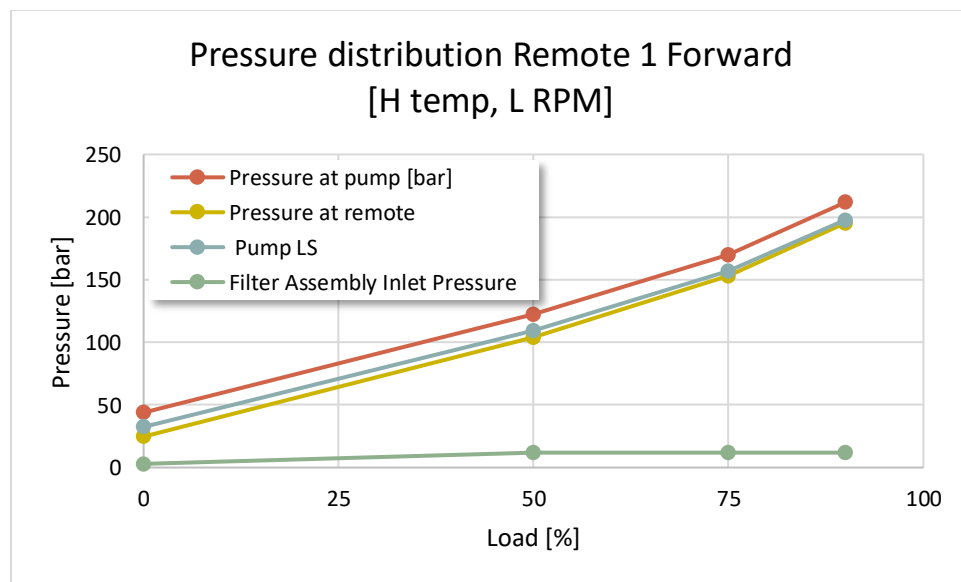


Figure 5.10 Pressure Distribution of EHR 1 (A) & EHR 2 (B)

The data trend in Fig. 5.10 remains almost identical to the low temperature trend in Fig. 5.5. All the previous points are also the same. Oil temperature doesn't seem to impact the behavior of the system in terms of pressure. The temperature does have an effect on the power and efficiency plots.

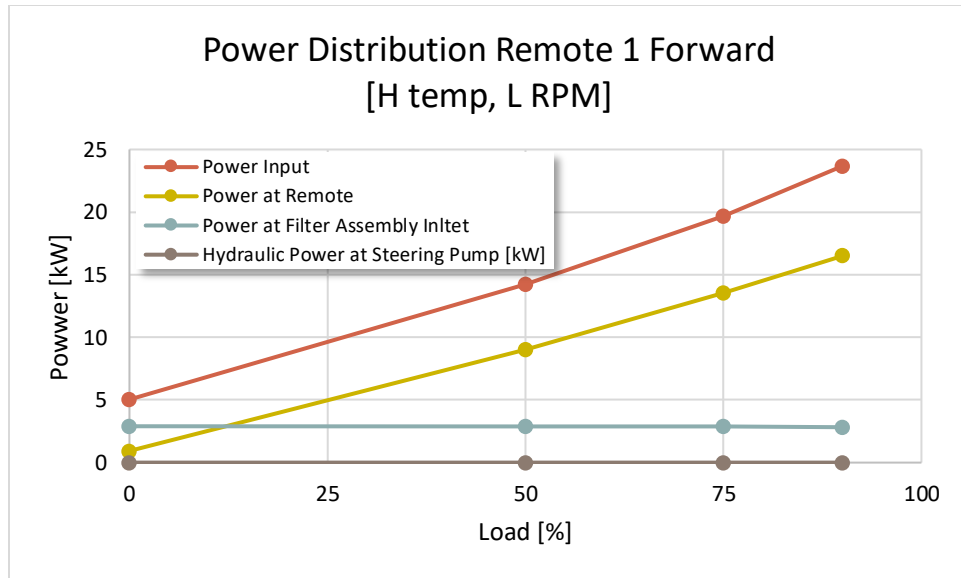


Figure 5.11 Power Distribution of EHR 1

The power input by the pump with hot oil compared with cool oil seems to be higher as shown in Fig. 5.11. With cool oil the highest power output from the PFC pump in Remote 1 is at 21.4 kW. When the oil is heated that power sits at 23.6 kW. From those 21.4 kW of power, 16.25 kW reached the EHR outlet. Making it have an efficiency of 75.9% with this operating condition. With hot oil, 16.4 kW of the 23.6 kW reached the outlet of the EHR. Dropping the efficiency down to 69.5%. Since it is only one specific point and one EHR valve in the two cases, we cannot fully state that the hotter the oil then the least efficient the EHR valve becomes. When we take all the rest of the data points and average them out we see a different behavior. Before explaining what that behavior is, we will analyze the TF EHR valves and see if the behavior is the same whenever we compare hot and cool oil at its maximum power yield.

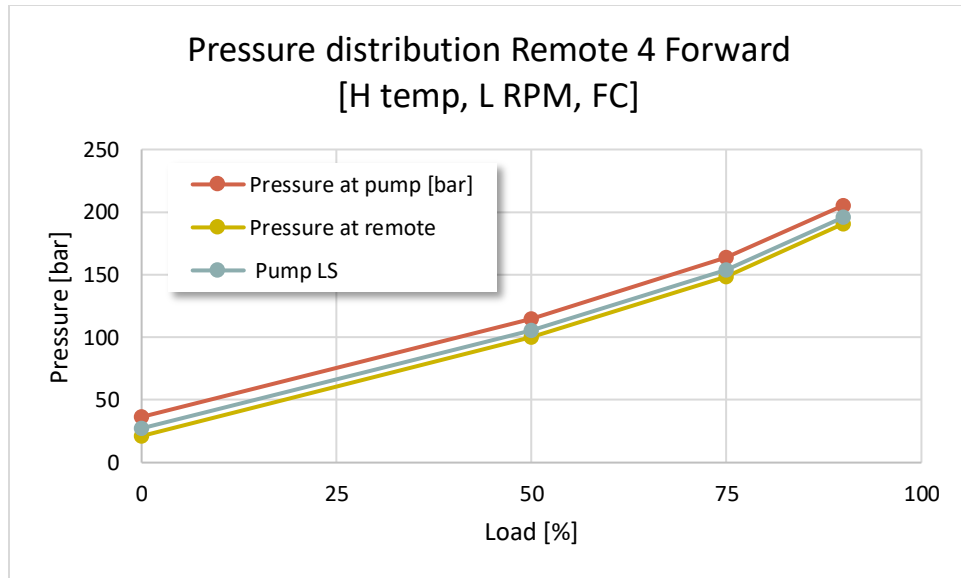


Figure 5.12 Pressure Distribution of EHR 4 (A) & EHR 5 (B)

Once more the trend of the pressure behavior in Fig. 5.12 is the same, nothing unusual or unexpected can be seen. The power scatter plots show better how the difference in temperature affects the TF EHR valve.

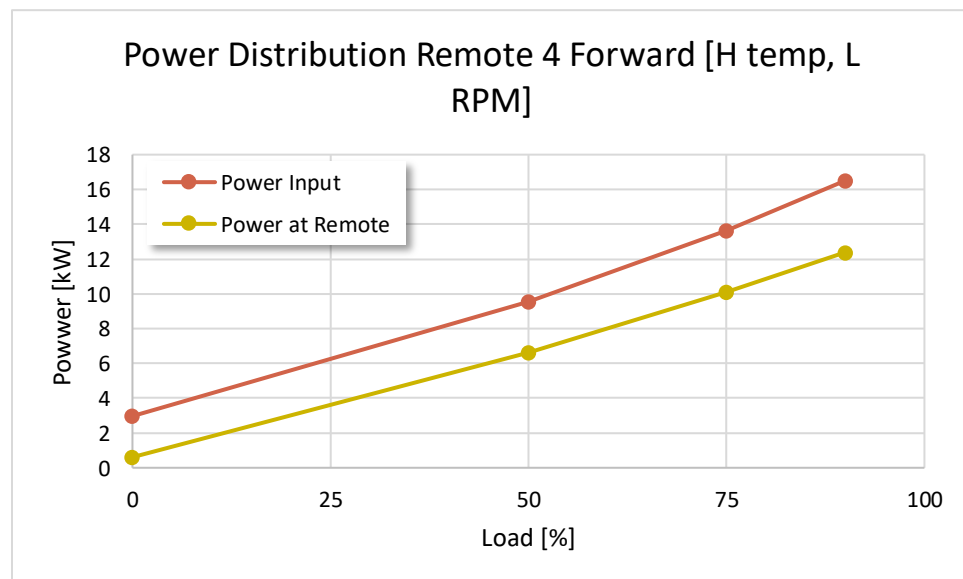


Figure 5.13 Power Distribution of EHR 4 (A) & EHR 5 (B)

By analyzing once more a single remote in this case EHR 4 within Fig. 5.13, and taking the highest output power from cool and hot oil, we can have an idea if these EHR valve will behave as the PFC EHR. With cool oil the highest power at the pump is 15.34 kW, and of that, 11.6 kW reach the EHR outlet. Making it have a 75.6% efficiency. This is in line with the efficiency of the other EHR valve in the PFC circuit. With hot oil, the highest power from the pump is 16.5 kW and of that, 12.38 kW reach the EHR outlet making it 75% efficient. The efficiency did decrease but that value is not as substantial as the one in the PFC EHRs.

The only difference is the fact that the PFC contains the steering priority valve. With this we can state that although the efficiency dropped in the PFC remote, the actual power delivered to the EHR valve remained almost the same, in both cool and hot cases, within the PFC EHR, the remote got around 16 kW of power. It can be stated that the fact that the oil has less viscosity, the leakages rise within the steering priority valve and thus the pump must input more power into the system so that the requested 16 kW from the EHR can still be met.

This is all just for one suction of the data, however when we take into consideration all of the data points available, the summary bar graph in Fig. 5.14 below is made.

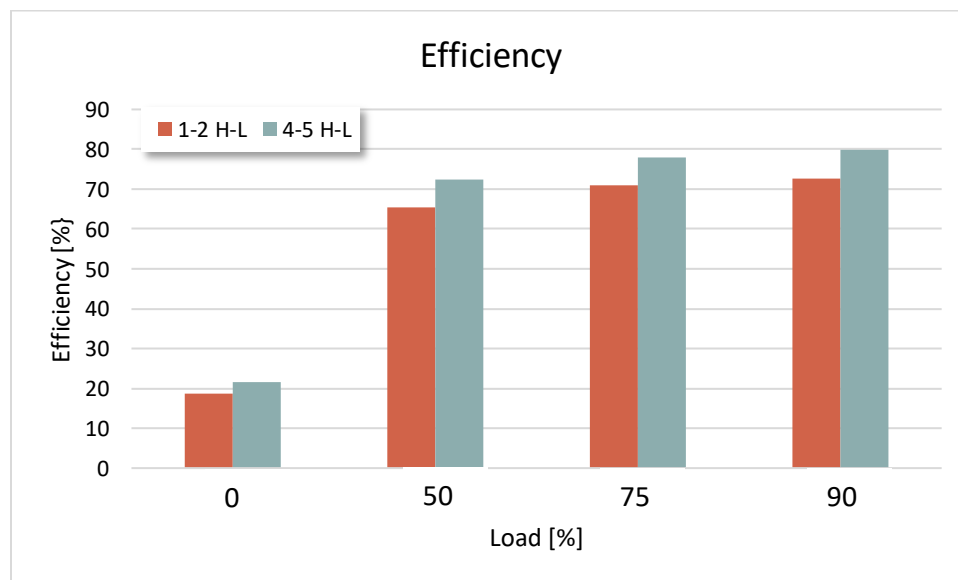


Figure 5.14 Average Efficiency of PFC & TF EHR Valves

With this, we can conclude that hot oil will make the system in general more efficient compared to low oil when all operating loads and EHR valves are taken into account. In both cool and hot oil we can see that TF EHR valves tend to be more efficient than the PFC EHR valves. This as stated before has to do with having a steering priority valve upstream the EHR valves in the PFC pump circuit. This may be further developed so that a solution where the steering system is independent from the EHR valves so that the system may be more efficient. With this, we completed the test results from single EHR at low rpm. Low rpm are usually not the working conditions of the machine since the pump will truly supply its maximum flow at high rpm.

The next data to be discussed will be high rpm with cool and hot oil. Testing at high rpm and cool oil proved to be a challenge since the machine is working at its fullest capacity and therefore produces heat at a faster rate. We will again analyze only the forward direction of the EHR valve.

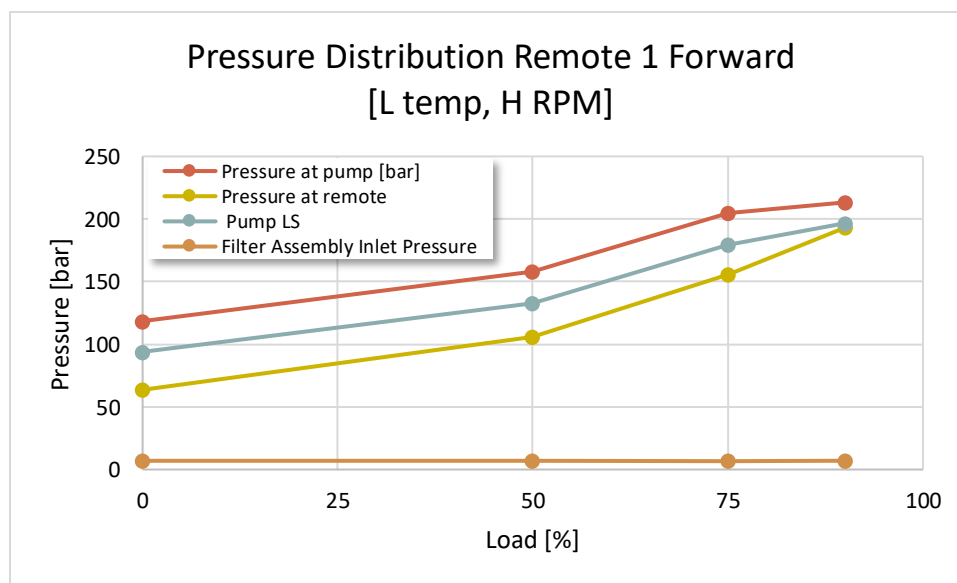


Figure 5.15 Pressure Distribution of EHR 1

The pressure behavior remained the same in Fig. 5.15 as with low rpm, the major difference is the gap between the pump LS and pressure at the EHR valve outlet line is now greater. That behavior was further looked into and will be explained further along in this section.

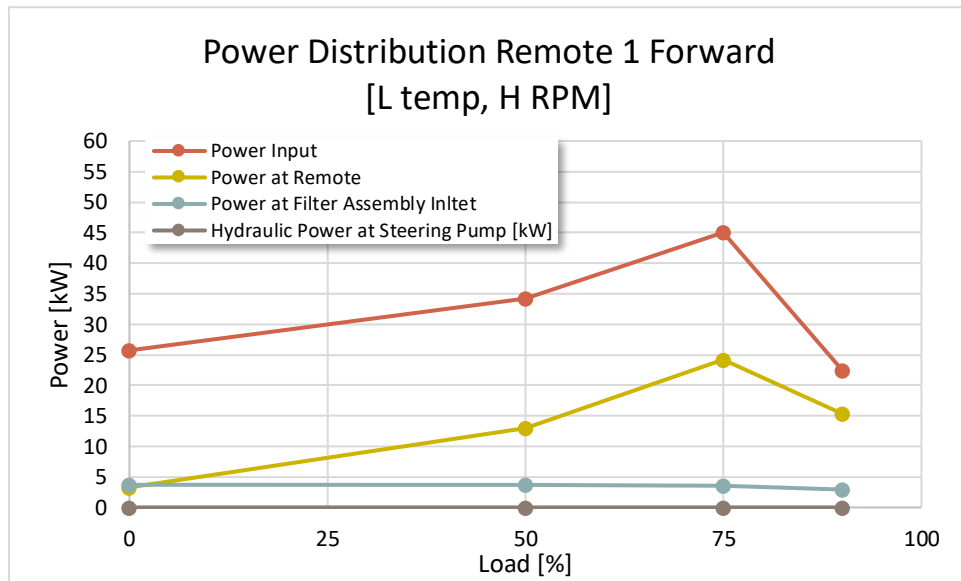


Figure 5.16 Power Distribution of EHR 1

With high rpm we notice a change in data trend in Fig 5.16 when compared to low rpm. Past 75% load, the power given by the pump starts to decrease. This behavior is in both EHR valves of the PFC pump. The explanation can be given using the aid of the pressure distribution plots [Fig 5.15]. We can notice that at 75% load, the pressure at the pump in both EHR valve plots is at around 200 bar. The level compared with low rpm is considerably higher. The pump is commanded by the LS line signal. As we see that signal is higher than the actual load, forcing the pump to stroke and yield higher pressure to be able to load sense. When the system load is set higher to 90%, the pressure starts crossing into the boundary of actuation of the pressure compensator. Therefore, the pump begins de-stroking and less power is inputted into the system. The reason why the LS line is higher than expected was difficult to discover. First, the data from the TF pump should be analyzed to see if they behavior is the same.

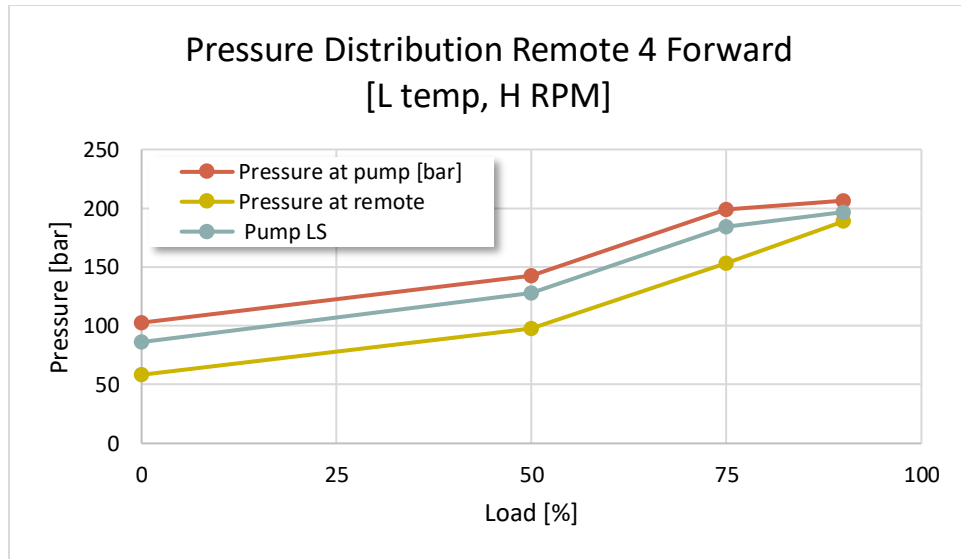


Figure 5.17 Pressure Distribution of EHR 4

With the LS line higher than the actual load at the EHR valve as shown in Fig 5.17, it is expected that the power plot will also decrease in the 90% load to EHR tests. The power distribution plots of the TF EHRs also have the same behavior. Since the PFC and TF are two separate circuits and they both have totally different layout, we can conclude that this behavior in Fig 5.18 is being caused by the EHR valve.

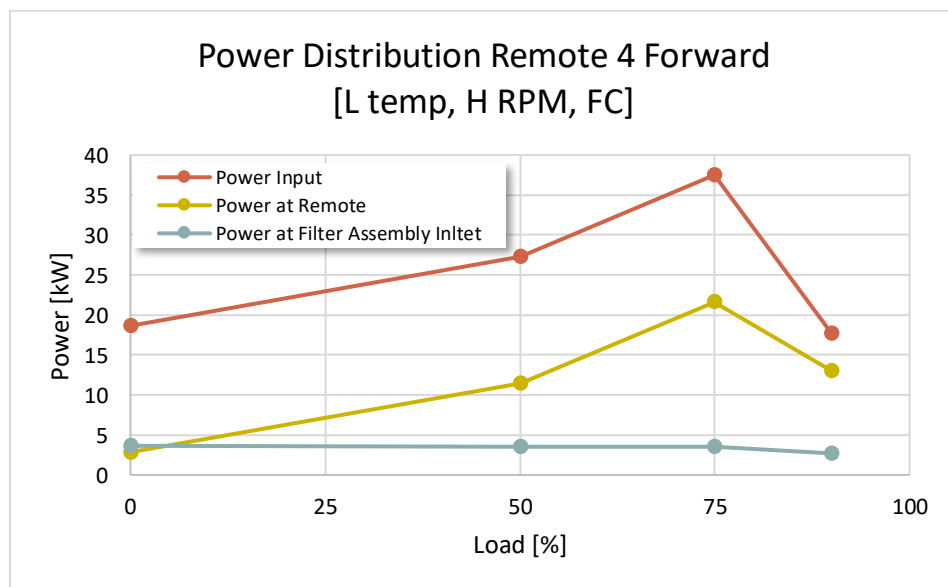


Figure 5.18 Power Distribution of EHR 4 (A) & EHR 5 (B)

Knowing the power distribution in both of the circuits, the bar graph in Fig. 5.19 lays out those values.

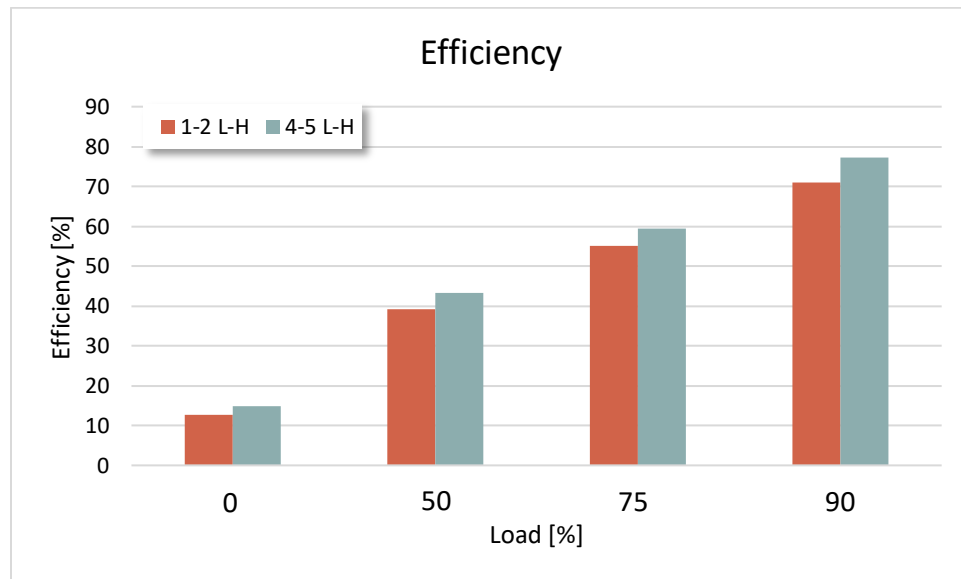


Figure 5.19 Average Efficiency of PFC & TF EHR Valves

In this case the efficiency levels at 90% load may be misleading, since at this load the pump is in pressure saturation as we have seen in the power plots. For our comparison we will use up to 75% load. When comparing the efficiencies of low and high rpm and both with low oil temperature, we see that at high rpms all of the remotes will be less efficient than at low rpms.

On average the EHR valves are 35-37% more efficient under low rpms. Only at 90% load do we see a similar behavior, which is expected since the pump is actually in pressure compensation so it will supply less flow in high rpm as compared to the other cases.

Table 5-1 EHR Efficiency Values- Low Oil Temp

Efficiency comparison: Low oil Temperature					
<i>Load</i>	0	50	75	90	
<i>EHR 1 & 2</i>	19.96	62.12	69.05	71.88	Low RPM
<i>EHR 4 & 5</i>	22.62	69.56	76.88	80.12	
<i>EHR 1 & 2</i>	12.70	39.07	55.17	71.05	High RPM
<i>EHR 4 & 5</i>	14.86	43.24	59.50	77.35	

Like mentioned before, having high rpms and cool oil is not a scenario in which the machine will behave under normal working conditions. The machine will most of its lifetime spend at high rpms and temperature. These are the final conditions at which single EHR tests we conducted and data was recorded and processed. The pressure behavior in Fig. 5.20 showed nothing new that may need explanation or further investigation.

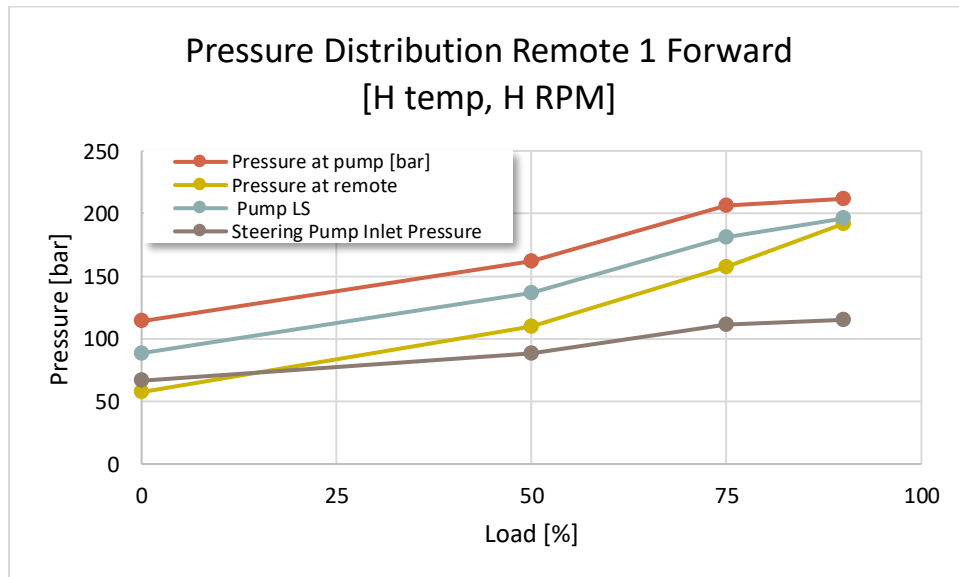


Figure 5.20 Pressure Distribution of EHR 1

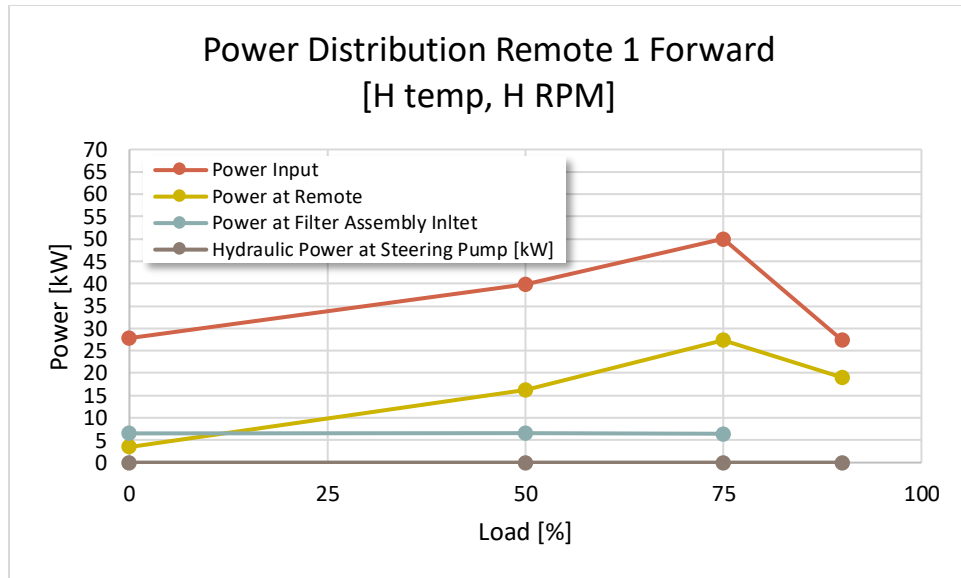


Figure 5.21 Power Distribution of EHR 1

The power distribution charts in Fig. 5.21 show the same behavior as with the other high rpm condition. In plot A of the figure above, data connection was lost to the pressure transducer of the filter and that data was not recorded. Based on its behavior on all the other remaining tests, it was decided that the test would be kept and it would be valid, since the power at the filter is generally constant and enough data exists to extrapolate a close estimate.

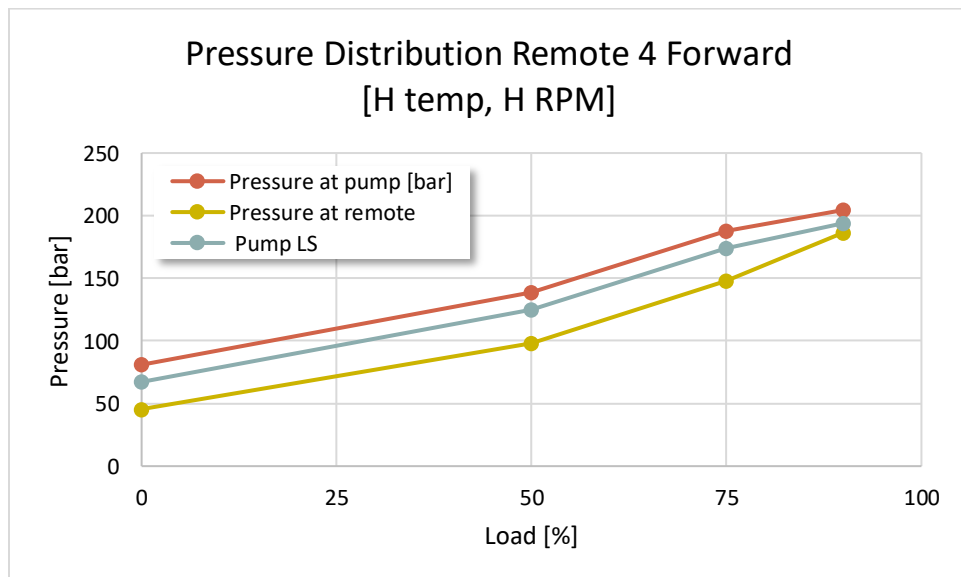


Figure 5.22 Pressure Distribution of EHR 4

Pressure data in Fig. 5.22 has normal trend and like EHR 1 & 2 the 90% loads tests reach the pressure saturation area of the TF pump. This will reflect in the power plots seen in Fig. 5.23 below.

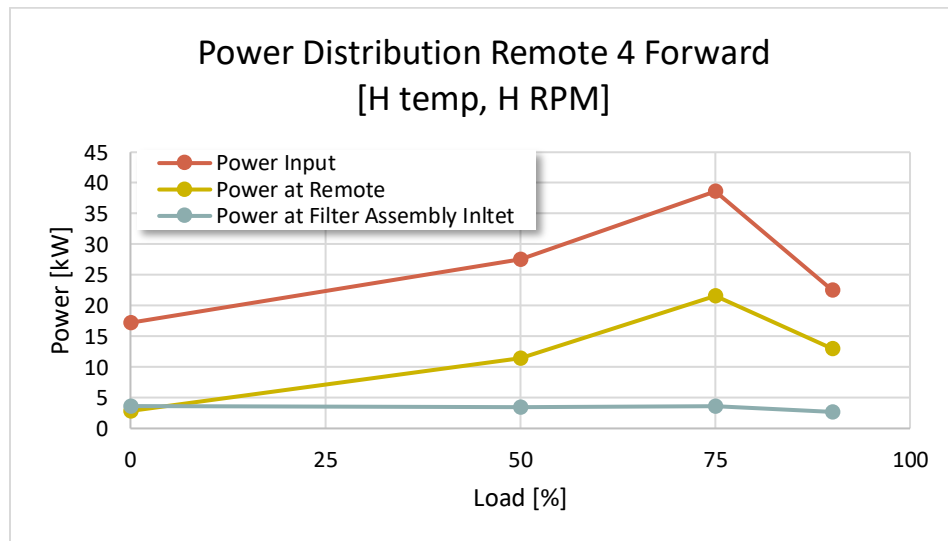


Figure 5.23 Power Distribution of EHR 4

With all the data plots fully elaborated, a similar analysis with the efficiencies by averaging out both directions of testing from all the EHR valves tested under the same circuit can be done and bar graph in Fig. 5.24 seen below was created.

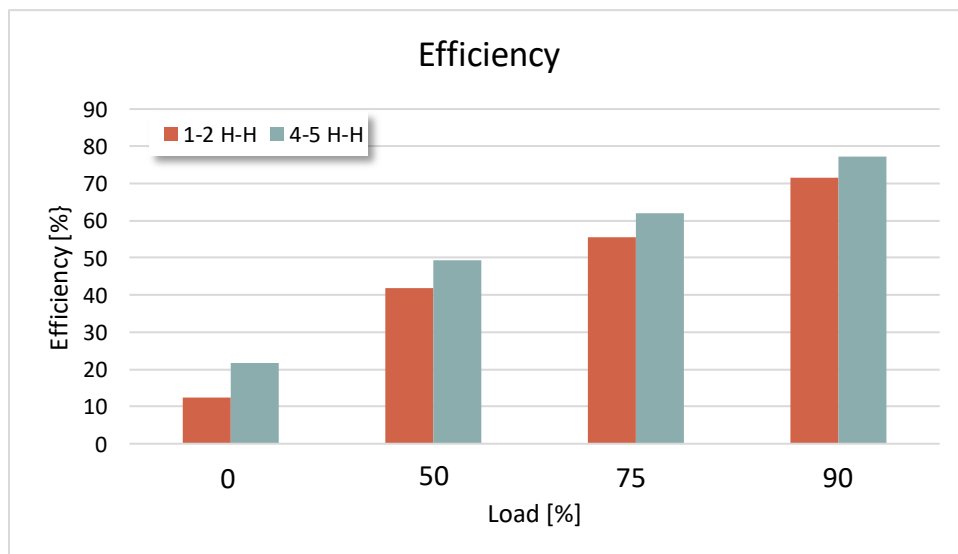


Figure 5.24 Average Efficiency of PFC & TF EHR Valves

As before, the same trend can be observed the figure above like in all of the bar graphs, as the load gets bigger, the EHR valve efficiency increases. However, we see a considerable drop in efficiency under high rpm compared to low rpm. A table has been made to express this difference. Table 5.2 shows that in general PFC remotes are 34% more efficient under low rpm than high, at high temperature. TF remotes are around 18% more efficient. The full 34% less efficiency should not all be attributed to the EHR valves; the steering priority valve has a lot of power loss. Under correct conditions, EHR valves in the TF circuit can reach almost 80% efficiency under certain conditions. The conditions however, are not close to normal operating conditions. Under normal operating conditions, the EHR valves can vary from 55% -70% efficiency.

Table 5-2 EHR Efficiency Values- High Oil Temp

<i>Efficiency comparison: High oil Temperature</i>					
<i>Load</i>	0	50	75	90	
<i>EHR 1 & 2</i>	18.63	65.30	71.03	72.76	Low RPM
<i>EHR 4 & 5</i>	21.53	72.46	78.00	79.93	
<i>EHR 1 & 2</i>	12.31	41.76	55.63	71.42	High RPM
<i>EHR 4 & 5</i>	21.75	49.40	61.91	77.19	

5.2.1.1 LS line and actual load Discrepancy

In this section the discrepancy that the data has when the LS line pressure is compared with the actual load will be briefly explained. As seen in all of the pressure curves of the single EHR results, the LS line pressure is a bit higher than the actual load itself, forcing the pump to go into even higher pressure than needed. This is not a normal LS system behavior. After further investigating the topic. It was discovered that the component being saturated at high flows was the quick connect couplers at the outlets of the EHR. Since it is an external component, the solution to this is straight forward, replace the current coupler with a larger size coupler. However, the implementation of this solution may be complicated. All the implements have standardized coupler sizes so that implements from different manufacturers may easily connect with any brand or model of agricultural tractors.

5.3 Multiple EHR Test Results

Multiple remote tests were much less tests compared to single EHR tests. However, they were more complex to run, since the set up took considerable amounts of time. In a simultaneous matter, the model of the EHR valve was being developed in another work. The first EHR valve circuit to be modeled was the TF circuit since it is the simplest of the two. This affected the order in which EHR test were ran. The multiple TF EHR valves test were taken and recorded first.

The EHR tests for this section were conducted with different loads per EHR valve. There are 4 different conditions at which the EHR valve were tested:

Table 5-3 Testing Conditions for Multiple EHR valve Tests

Testing Conditions
<i>Low oil temperature & low rpm</i>
<i>High oil temperature & low rpm</i>
<i>Low oil temperature & high rpm</i>
<i>High oil temperature & high rpm</i>

With every condition of testing, the same combination of loads was tested. The combination yielded 3 types:

Table 5-4 Load Combination Tested in Multiple EHR Valves

Testing Loads
<i>50 % & 75% Load</i>
<i>75% & 90% Load</i>
<i>90% & 50% Load</i>

The first set of results to be shown will be the test results of low temperature and low rpms. As before the first data introduced is the pressure distribution plots. Only the data of the forward direction will be shared since the data in the reverse direction is almost identical. One thing to mention is that these tests were all taken at 25% command to the remotes. As previously stated, the test that would use multiple EHR under normal LS operation could not be run at 100% command on both of the remotes due to the fact that there was flow saturation.

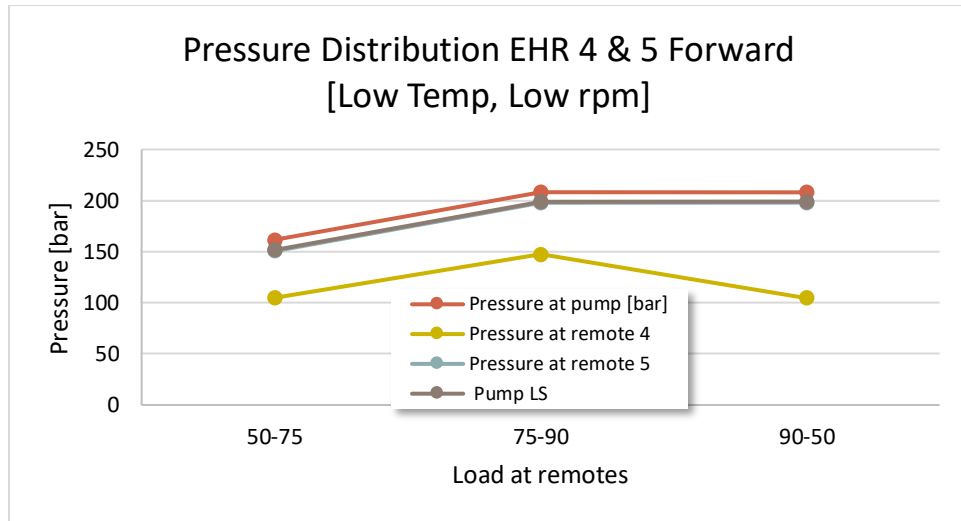


Figure 5.25 Pressure Distribution EHR 4 & 5 Forward

The pressure plot in Fig 2.25 shows the 3 combinations of load in its horizontal axis. Each pair of load represents the corresponding load percentage the EHR were set to. There is no specific order as to what EHR valve number received a particular load level. Everything is random. From this initial plot a significant difference can be noted. The LS line is now as should be, the same value as the highest load in the system. This indicates that the quick connect couplings are appropriately sized to at least handle 25% of the flow that the EHR can reach at low rpm.

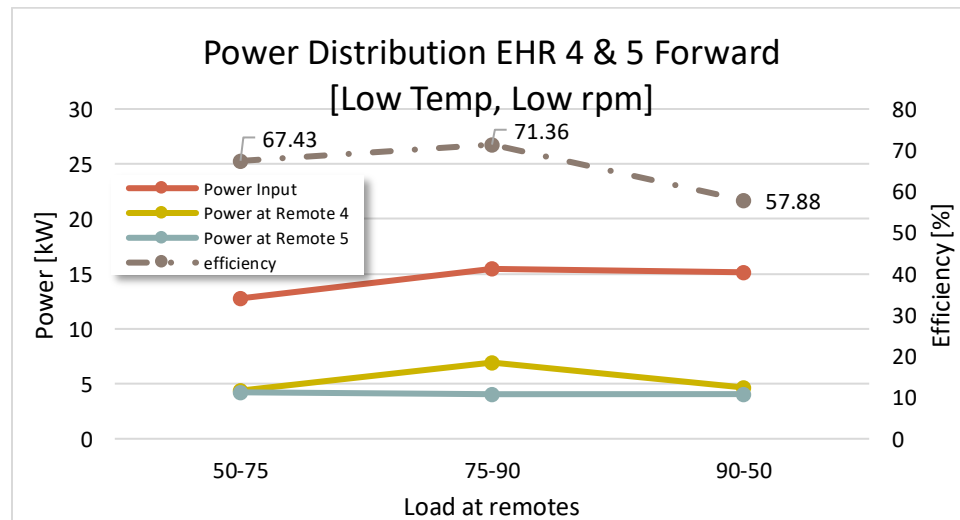


Figure 5.26 Power Distribution EHR 4 & 5 Forward

This will have a direct impact also in the power scatter plots [Fig 2.26], since now the pump is not forced to input unnecessary power to be able to meet the load requirements. In the power distribution plot, we can notice that whenever we have a combination of a high load and low load, the efficiency drops considerably, this of course is expected since the pressure compensator of the EHR with the lower load has to burn off all the excess pressure that the EHR with the highest load demands. When the loads tend to move closer together in value, the EHR valves become more efficient.

The second condition will now test under hot oil and low rpm. From all the previous tests already seen, hot oil should not affect drastically the pressure behavior of the system.

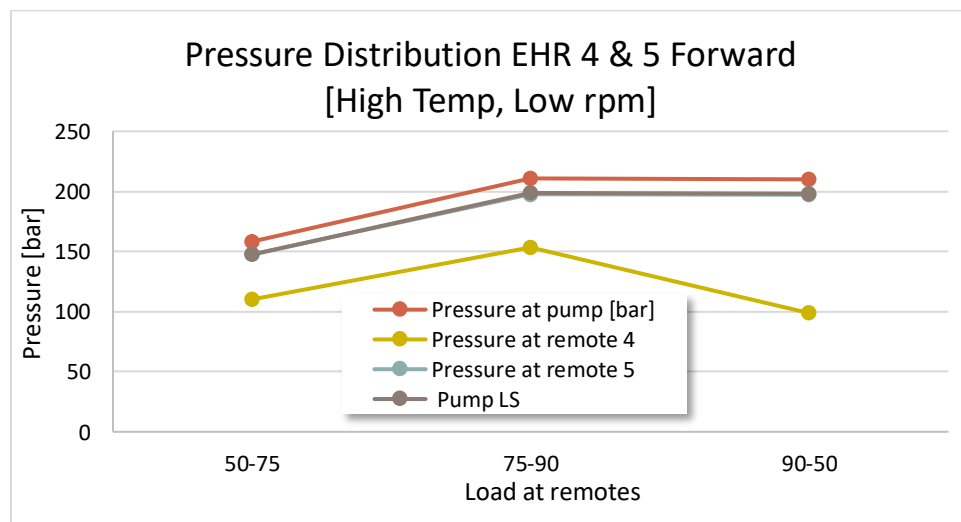


Figure 5.27 Pressure Distribution EHR 4 & 5 Forward

As with cool oil, the signal at the LS line of Fig. 5.27 is identical to the one coming from the highest load in the system. This is why pressure at remote 5 overlaps with the LS line in the plot. In the power plot, hot oil increased the efficiency of the system in a small quantity.

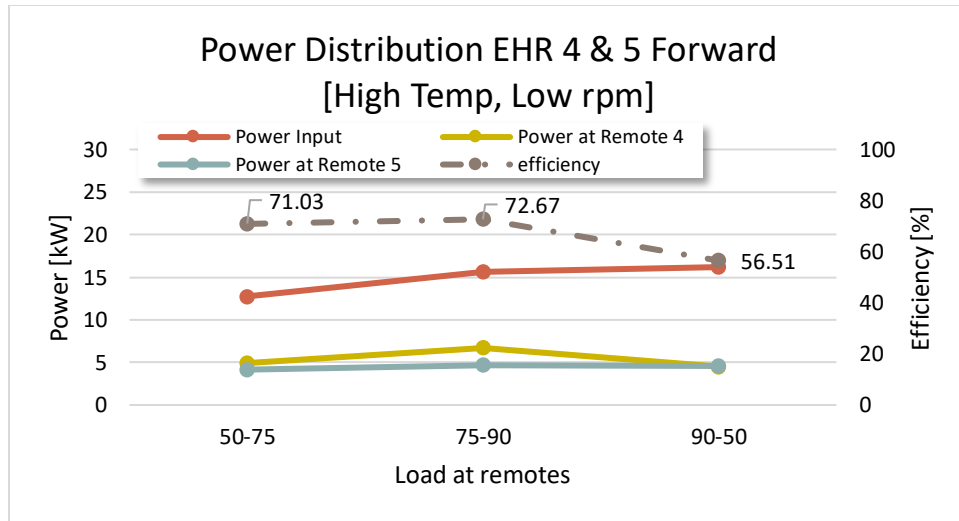


Figure 5.28 Power Distribution EHR 4 & 5 Forward

Results in Fig 5.26 & 5.28 gave much information about the machines behavior in low rpms and different oil temperatures. The quick connect coupling does not seem to interfere in the EHR performance at these flow levels. The third scenario of tests is when the rpms are high and oil temperature is low. High rpms are a much more frequent working scenario since the user of this or any tractor will normally want the maximum performance. The pressure distribution should not be affected. Still, the results are included in this work [Fig 5.29].

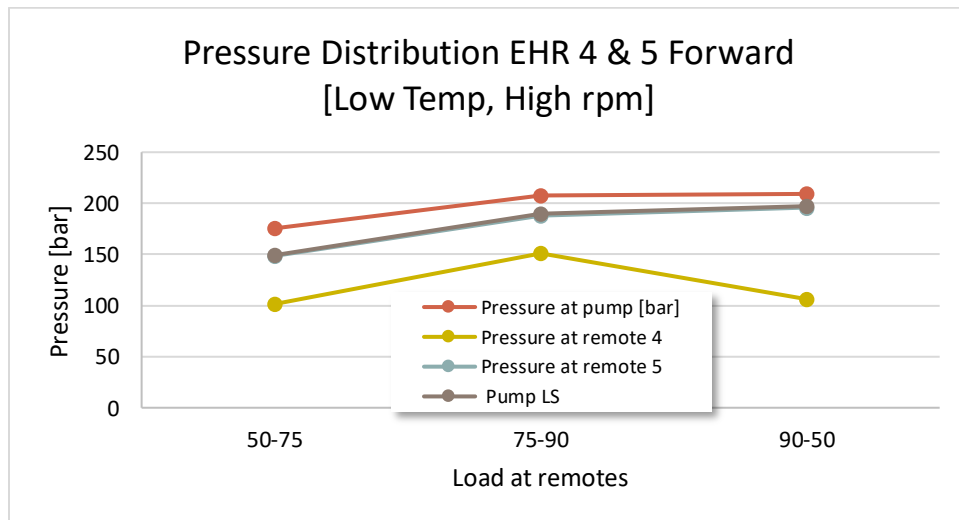


Figure 5.29 Pressure Distribution EHR 4 & 5 Forward

Once again the behavior of the single EHR valves seems to also be the same as in multiple EHR valves. In Fig 5.29, the higher the rpms or flow to the system, it will tend to be less efficient. Tests under 50 & 75% load lost a significant amount of efficiency, 5% when compared to the tests of low oil temperature and low rpms. Since the TF circuit is the one with less sources of external energy loss, the only other component in this circuit is the hitch, which was not actuated and its valve is closed center. From this, we can attribute the loss in efficiency to the EHR valve. The exact distribution of energy loss inside the EHR valve cannot be discovered experimentally with the current set up. However, a model was developed with the use of all the data acquired for this work. This model will be introduced in chapter 6.

We also notice the LS line value of Fig. 5.23 overlaps the highest load in the system, validating that the EHR quick coupling can also handle 25 % of the full flow that can pass through the EHR valve with high rpms.

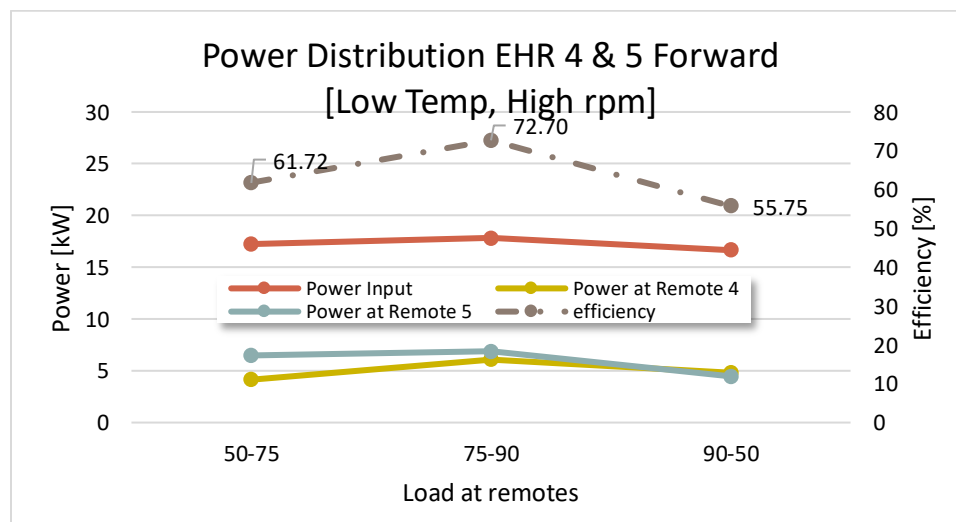


Figure 5.30 Power Distribution EHR 4 & 5 Forward

The final working condition is the one with high temperature and rpms. This is the closest scenario to a real life working cycle. Every hydraulic implement that maybe attached to the tractor has at least two working EHR valves at any given time and always demand the highest flow possible.

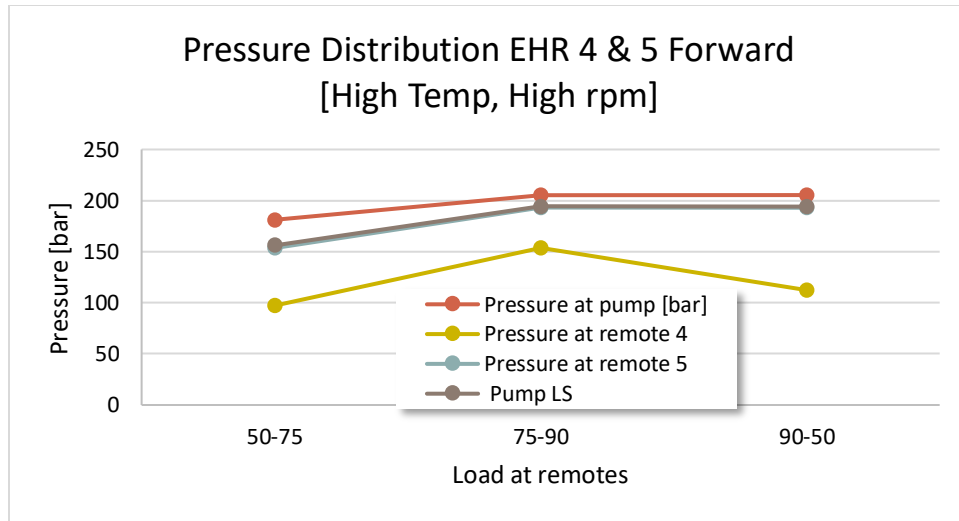


Figure 5.31 Pressure Distribution EHR 4 & 5 Forward

All the data for pressure plots for the TF circuits have now been shown and explained. Since the data from the PFC remotes did not vary in terms of behavior or prove to be significantly different in terms of efficiency, those results will not be shared in this work in the interest of time and not disclosing redundant data.

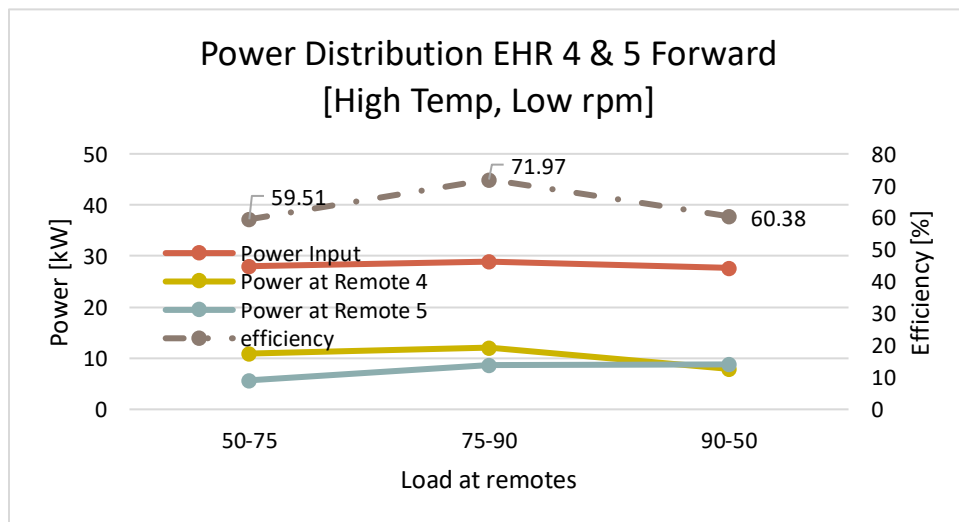


Figure 5.32 Power Distribution EHR 4 & 5 Forward

With the power distribution plots described in all conditions, it is learned that the EHR valve tend not work at their least efficient when ever one of any EHR is below 75% load. This

value further decreases as the rpms increase and also the temperature. The table below shows the average efficiencies between all the testing conditions and loads.

Table 5-5 Efficiency % Values of Multiple EHR Tests

<i>Efficiency % Values of Multiple EHR Tests</i>					
<i>Load</i>	L-L	H-L	L-H	H-H	Average Efficiency
50-75	67.43	71.03	61.72	59.51	64.92
75-90	71.36	72.67	72.70	71.97	72.17
90-50	57.88	56.51	55.75	60.38	57.63

The data of this table represents the conclusion of the test results and analysis of this work. The efficiency of the EHR can vary from 57-72% depending on the load conditions. As it can be seen, the closer the loads are to each other in value, the EHR valve seems to be more efficient. This is due to how load sensing systems work and its theory of operation.

5.4 Model Validation Through Experimental Characterization

The model introduced in section 2.2 of Chapter 2 was a direct result of the experimental characterization. The procedure is simple, validate a developed model of the EHR valves with the data collected and presented in chapter 5. The development of the model and its adequate considerations and procedure are not part of this work, however since the data from this work allowed for its validation, a brief explanation of the validation criteria along with validating figures may be presented in this section. A single EHR valve model from the TF [Fig 5.33] will be explained.

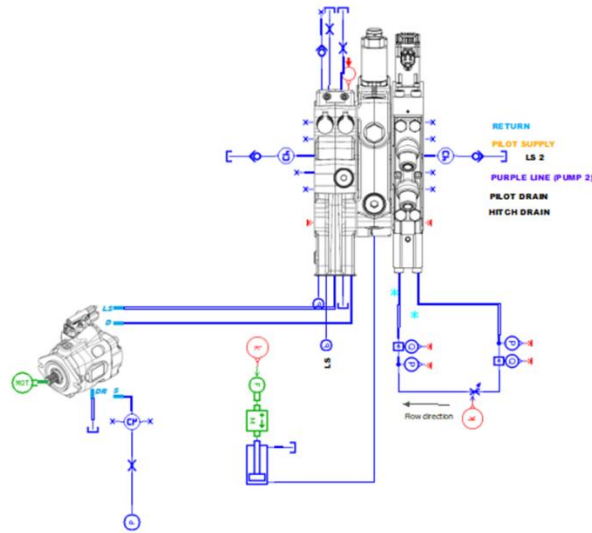


Figure 5.33 Single TF EHR Model Layout

This specific model layout contains the same components introduced in section 2.2 The pump was validated with experimental data from the supplier. Such data may not be disclosed. The rest of the components like hitch valve and EHR valve were each validated by experimental results. The focus is on the EHR valve, inside of the super component seen in the figure above, the general layout of the EHR valve components can be seen [Fig. 5.34].

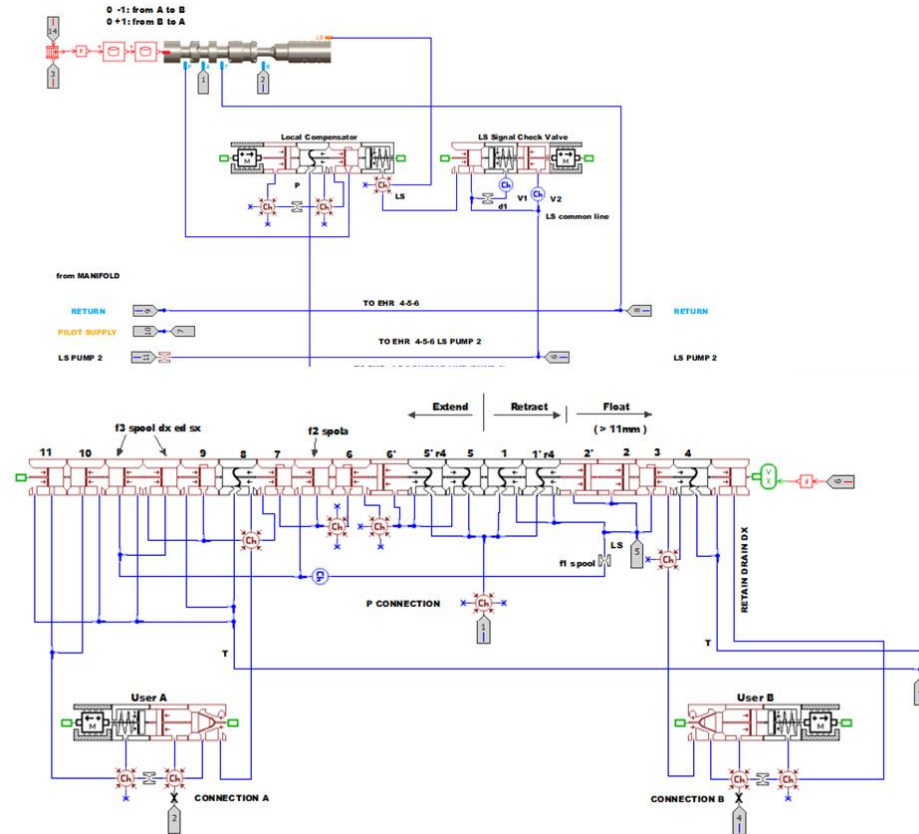


Figure 5.34 EHR Valve Model Layout

From Fig 5.34, all the inner components of the EHR valve can be easily identified. From top to bottom, we see the signals coming from the hitch valve model like pump flow. Flow enters the local compensator and then reaches the main spool. Which depending on direction for actuation will supply flow to one of the two lock check valves [user A or user B]. This is the exact same operation of the EHR valve discussed in chapter 3.

The model was tuned to align itself with the experimental characterization. Proof of the validation can be seen in Fig. 5.35. In this figure, different load settings are plotted in its lower axis. Its two vertical axis plot normalized values of pressure and flow for both experimental and simulation results. Results shown correspond to the reverse direction with high oil temperature and rpms. The simulation data in dashed line overlaps quite well the experimental results validating the model. In this manner, the model may be utilized to point where the energy within the EHR valve itself is distributed. Results of this findings can be seen in the Publication section.

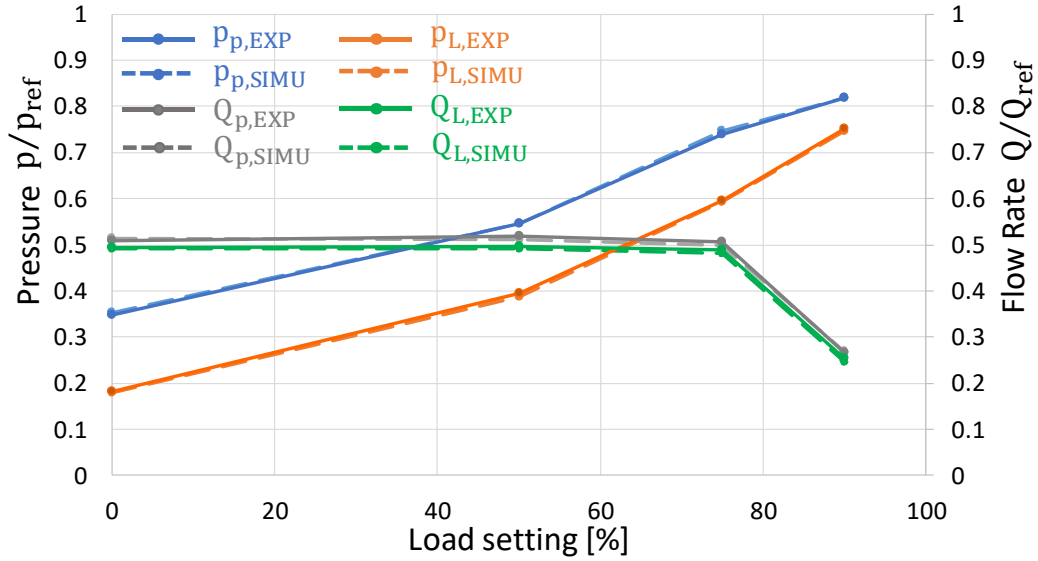


Figure 5.35 Single EHR Valve Test Results Comparison

Many other testing conditions were also validated. Although not included in this work, experimental characterization allowed for the full development of a working LS system simulation model of the reference machine to be validated. Study on the power distribution analysis, particularly EHR tests, provides important insights on the system component power consumption when the reference machine is operating under different working conditions. As a result, the system operates at a higher efficiency, which could be as high as 55.99% when handling a higher remote load at higher oil temperature. The non-symmetric structure of EHR main spool doesn't contribute much difference in system efficiency. When multiple remotes are activated, there's much higher power dissipated on the pressure compensator associated with the lower pressure user.

6. EHR VALVE IMPROVEMENTS

Chapters 4 and 5 elaborated a test plan and explained its results respectively. The contents of this chapter is to explain more in detail the discoveries that the testing and data led to. One major unwanted behavior in the system was the presence of flow saturation in our EHR valve circuit. This behavior did not allow for any test above 25% to demonstrate how the EHR valves would behave with this command under normal LS theory.

6.1 Flow saturation in PFC and TF pumps

The test plan elaborated in chapter 4 was originally planned to be ran only at full command per EHR valve when testing simultaneous EHR valves. However, when testing, the values of flow compared to previous values seen in single EHR valve tests, the behavior was not as expected. After analyzing the data, it was discovered that if two or more EHR valve were commanded, the system would be placed in a flow saturation scenario. This flow saturation behavior was present in all testing conditions, even in high rpms whenever more than 25% command was given simultaneously to multiple EHR.

The reason for this behavior comes from the way LS systems work. As learned in section 2.2, flow to an actuator is based only on operator command when using LS systems. With this in mind, one can unknowingly command a value of flow and place the system in flow saturation.

Table 6-1 Flow Saturation Data

Full Command- Multiple Remotes- Low RPM and Temp					
PFC Pump		Remote 1		Remote 2	
Flow [LPM]	Pressure [bar]	Flow [LPM]	Pressure [bar]	Flow [LPM]	Pressure [bar]
71.2	136	0	116.5	65.3	77.2
Power [kW]		Power [kW]		Power [kW]	
15.9		0		12.6	

Figure 6.1 shows data taken from a random test taken. When using full command, it is observed that our pump yields its maximum flow available at low rpms. EHR 2 has the least load, and therefore receives all of the available flow from the pump. The rest of the flow is used to make up leakages in all of the other systems. This in our reference machine can represent a problem.

The operator can unknowingly command too much flow from the EHRs valves and place the system in flow saturation. In our reference machine, there can be two scenarios in which flow saturation may present itself.

Scenario 1

In this scenario, and possibly the scenario most likely to be encountered, the machine is at low or full RPM. High rpms place the pump at its maximum flow capacity. In this set up, flow saturation can come from commanding two or more EHR on the same circuits with 100% flow command. In the case of the PFC pump, the bigger of the two, around $140 \frac{L}{min}$ at full rpm are expected. A single EHR valve is designed to be able to handle $130 \frac{L}{min}$ when full command is given. As soon as another EHR valve from the same circuit with 100% command is actuated, the system will flow saturate.

Scenario 2

The flow requested by a single user is higher than that of the maximum pump flow. For this scenario, the machine is at idle speed. At low rpms, the flow from the PFC pump is at most $60 \frac{L}{min}$. As previously stated, EHR valves can request up to $130 \frac{L}{min}$ when at full command.

Since scenario two has a relatively simple solution, increase engine rpms, attention was focused in solving scenario 1. The challenge of this problem, is to detect a flow saturation condition and override operator command with the appropriate command to distribute the flow available in the proportion wanted by the operator.

Flow sharing is the capability of a system to maintain desired operating behavior at a lower speed, since there is not enough flow to fully supply the demand. To deal with the flow saturation scenarios in our reference machine, a flow sharing solution was proposed. Flow sharing will maintain the flow command proportion to the users, while avoiding to flow saturate the pump. A simple example is if an operator demands $10 \frac{L}{min}$ & $5 \frac{L}{min}$ to independent but equal size actuators respectively, the flow proportion is 2:1. This means one actuator is to travel twice as fast compared to the other. If the pump may only give $10 \frac{L}{min}$ max, then the system is in flow saturation since the demand is $15 \frac{L}{min}$ from the pump.

Flow sharing will then be used to distribute the flow available on both actuators but in the original 2:1 proportion while also not saturating the pump. Hence, one actuator would theoretically and ideally receive $6.6 \frac{L}{min}$ and the other $3.3 \frac{L}{min}$. This allows for correct operation at lower speeds.

A flow sharing algorithm was designed and implemented in our reference machine since the EHR valves are electronically commanded. Flow saturation has been defined only in numeric terms. In order to be able to design an electronic control system that will override the commands given to the EHR valves when in flow saturation and reduce those commands until desired flow distribution is achieved the behavior of load sense systems under flow saturation must be studied.

6.2 EHR Flow Sharing as a Solution to Flow Saturation

The problem of flow saturation was solved by implementing an electronic control algorithm that would detect a flow saturation condition and override the operator command to avoid this condition. Two approaches were proposed, designed, implemented and validated on the machine. Both approaches only required the addition of pressure transducers to the actual system in order to be able to have feedback to the algorithm to detect a flow saturation condition. Explained in section 3.3, flow saturation in multiple users presents whenever $Q_{u1} + Q_{u2} + \dots + Q_{u_n} > Q_{pump}$ is met.

6.2.1 Approach 1: Pump Based Feedback

This approach seeks to monitor the value of the load sense margin s from figure 3.7 by taking the difference between pump outlet pressure and LS line.

$$s = p_p - p_{LS} \quad 6.1$$

The value of s is a known value. Every LS pump has its LS margin spring (s) set between 20-30 bar. This is to keep energy losses as minimum as possible while keeping the LS pump in a good stability condition. When a pump is flow saturated, it can no longer generate the required pressure to hold equation 6.20 true, as previously stated, the pump pressure is $p_p = s = \Delta p_x$ where:

$$s > \Delta p_x \quad 6.2$$

Any time the pump is flow saturated the value of Δp_x will diverge from that of s . The first approach is to design an electronic controller that will act on the areas of O1 and O2, so that the equation 6.3 is true.

$$s - \Delta p_x = 0 \quad 6.3$$

By knowing the values of equation 6.2, whenever the pump is in flow saturation can be known. Action are made so that the difference is driven down to 0, therefore achieving correct LS theory in our system.

The first step into implementing this controller into the actual machine is to proof the concept. The model validated by all the experimental data taken form the tests was used as the first step into validating the flow sharing algorithm. Modifications to the model were made to be able to simulate flow saturation conditions. Figure 6.5 shows the model created for TF EHR valves.

The EHR valves were commanded in simulation in such a way so that flow saturation may occur. As in the experimental tests, the model also entered a flow saturation condition with a command higher than 25%. Figure 6.6 below illustrates the model in a flow saturation scenario.

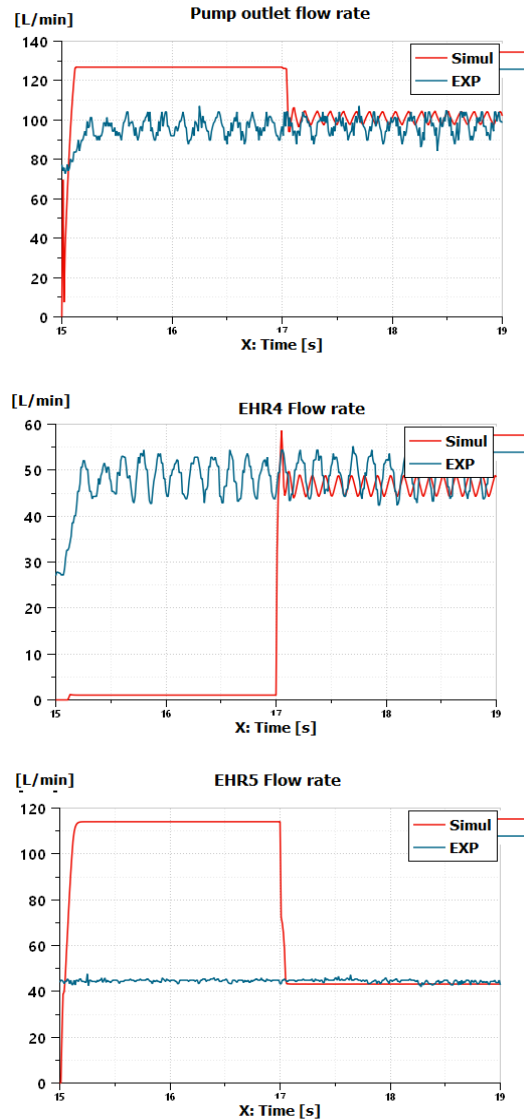


Figure 6.1 Flow Saturation vs No Saturation Model Simulation

In the three graphs experimental data is in blue and the simulation data in red. From second 15 to second 17, the model was purposely given EHR command that would place it in flow saturation. From seconds 17 to 19, the command was changed back to 25% command. The blue line shows experimental data in a non-flow saturation behavior for all the time span. This is to

have a reference of how the machine is supposed to behave whenever it is not in flow saturation. It also serves as proof that the model is loyal to the machine behavior whenever it is not flow saturating. In this manner, certainty that the model reflects the correct behavior of the machine whenever it goes into flow saturation is assured. The oscillations in the experimental data come from the behavior of the loading relief valves. This behavior was replicated as much as possible in simulation. Since it comes from an external relief valve, as long as the simulation data overlapped as much as possible the experimental data, the amplitude of the oscillations was overlooked.

Table 6-2 Simulation Parameters

Saturation Test	Remote 1	Remote 2
Load	50% [100 bar]	75% [150 bar]
CMD	100%	100%

Table 6.1 states the commands and loads given to the remote from seconds 15-17. After second 17 the command was changed to 25% command. Looking at simulation data, from second 15 to 17, the system is in flow saturation, one EHR receives all the available flow from the pump while the other has minimum flow available.

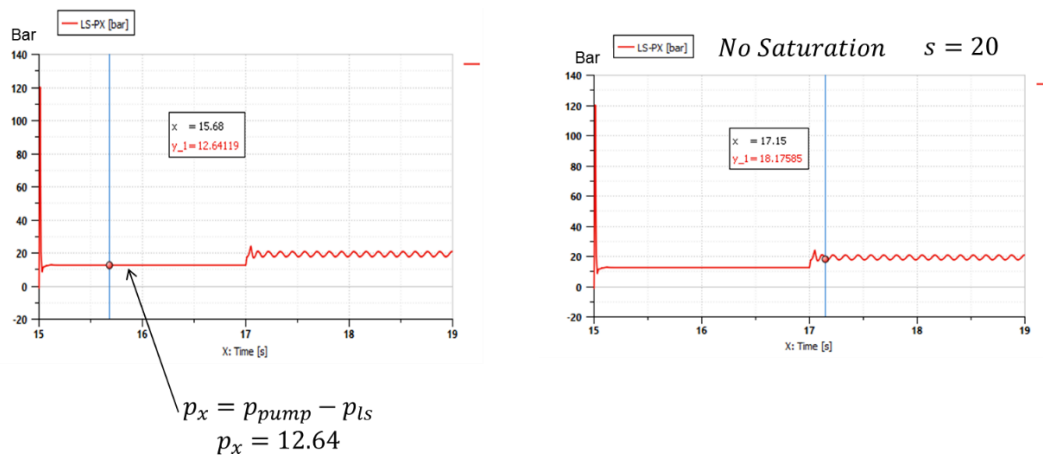


Figure 6.2 Validation of $s > p_x$

During this simulation, the values of p_x were calculated and recorded. During the time of flow saturation, the value of $p_x = 12.64$ bar. When it is not saturated, the value approaches the

setting of $s^* = 20 \text{ bar}$. With this equation 6.21 is validated. Multiple simulation scenarios were tested. All with the purpose to verify that the model went into flow saturation in the correct scenarios.

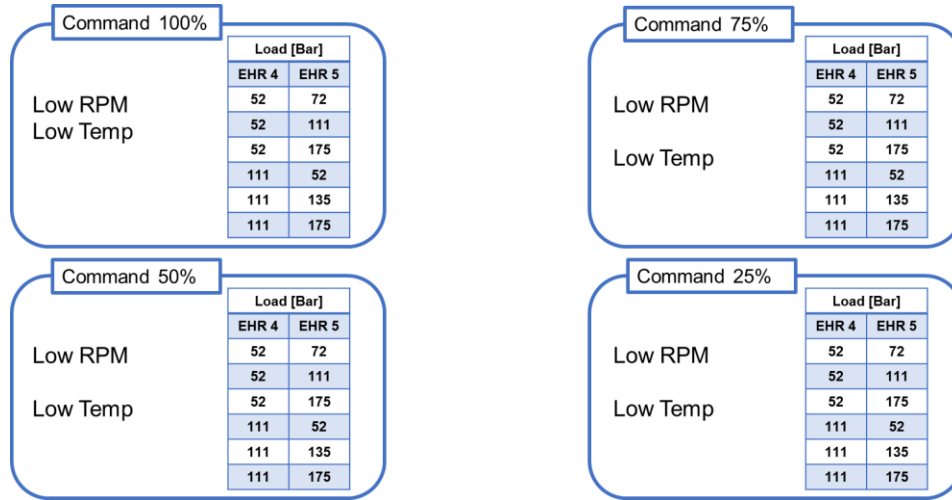


Figure 6.3 Testing Parameters for Flow Saturation Simulation

The figure above shows all simulated scenarios in the TF EHR circuit model. As expected, the table below shows that in every command other than 25% the system is in flow saturation.

Table 6-3 Simulation Test Results

Cmd	Load	EHR 4 LPM	EHR 5 LPM
100%	52 & 72 bar	65	0
	52 & 111 bar	65	0
	52 & 175 bar	65	0
75%	52 & 72 bar	65	0
	52 & 111 bar	65	0
	52 & 175 bar	65	0
50%	52 & 72 bar	65	0
	52 & 111 bar	65	0
	52 & 175 bar	65	0
25%	52 & 72 bar	35	30
	52 & 111 bar	35.7	27
	52 & 175 bar	35.6	24.4

The second step, after getting the model to flow saturate was to implement the control algorithm in the model and test such algorithm. Figure 6.9 below displays the control algorithm and signal flow to be implemented.

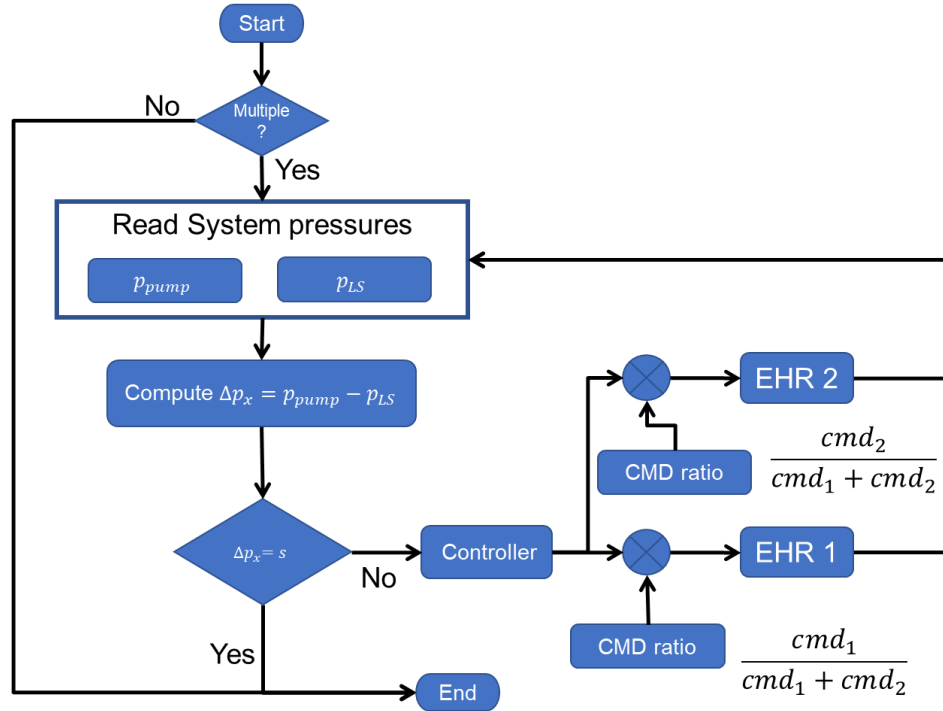


Figure 6.4 Flow Sharing Algorithm Flow Chart

The algorithm is based on the pressure feedback of pump outlet pressure and load sense line. It will first detect if multiple EHR are being used. If yes, it will proceed to calculate the value of Δp_x . If this value is the same as s , then the system is not flow saturating. If it is different than the controller is activated and will output a command signal that will be corrected based on the initial command ratio desired by the operator. From that the system will again read the pressure and compute a new value of Δp_x . It will cycle until the value of $\Delta p_x = s$.

The controller to be implemented now has to be chosen. The purpose of flow sharing is to remove the pump from a flow saturating condition. This type of control does not require fast response times and precise control since as stated before, EHR valves operate in steady state even when on the machine does dynamic working cycles.

The controller chosen to be implemented in the algorithm is a PID controller. This type of controller generates a control signal that is proportional to the system error, its time integral and its time derivative. A PID controller is often modeled in one of the following two forms [##]:

$$G_c(s) = K_p + \frac{K_i}{s} + \frac{K_D}{s} \quad 6.4$$

$$G_c(s) = K_p \left(1 + \frac{1}{T_i s} + T_D s \right) \quad 6.5$$

PID has 3 types of gains, proportional, integral and derivative gains. The proportional term affects system error and stiffness. Integral terms eliminate system steady state error. The derivative term is for damping oscillatory response. The configuration for the PID control structure will be a cascade compensation.

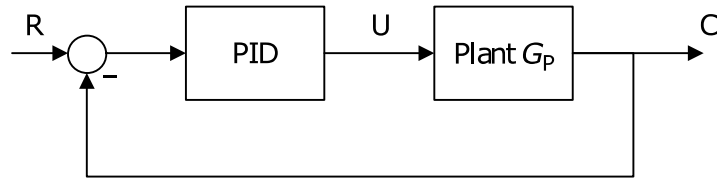


Figure 6.5 Cascade Structure for PID Controllers

In this case our plant will be the EHR model developed. Our Input R is the set point of s^* and our output C will be the value of Δp_x . To this simple cascade structure, augmentation to command U is made with a multiplication based on the command ratio that has been set by the operator. The command ratio is the ratio between the original command input of the operator. This is to ensure that when flow sharing, the flow distributes in the manner that the operator wants.

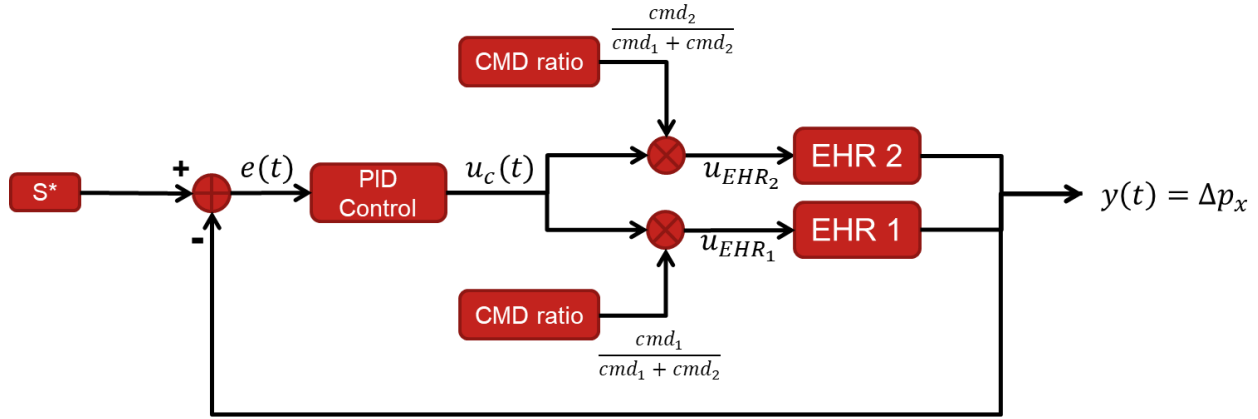


Figure 6.6 PID Control Structure

Figure 6.11 displays the control structure implemented in the EHR model. Assuming the operator give simultaneous EHR valves a command with a given ratio that creates flow saturation, given a known reference signal s^* , (also known as s) the PID control will command signal U_c . This signal will be multiplied by the command ratio that was previously set by the operator and then sent to the EHR valves overriding the initial command of the operator. Once this is done, a comparison is made and if the output value of Δp_x starts to approach the value of s^* , the error $e(t)$ will go to 0 and the controller will not modify the command signal anymore and keep the command that allows for $e(t)=0$.

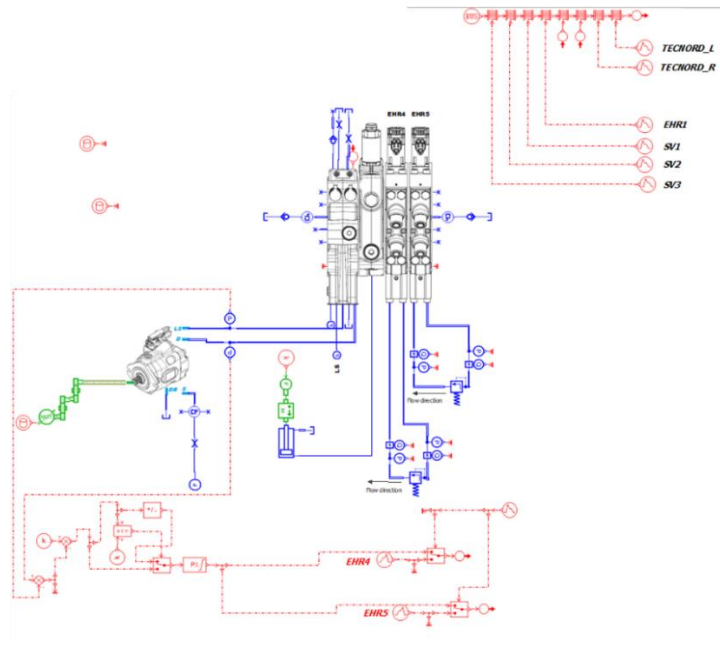
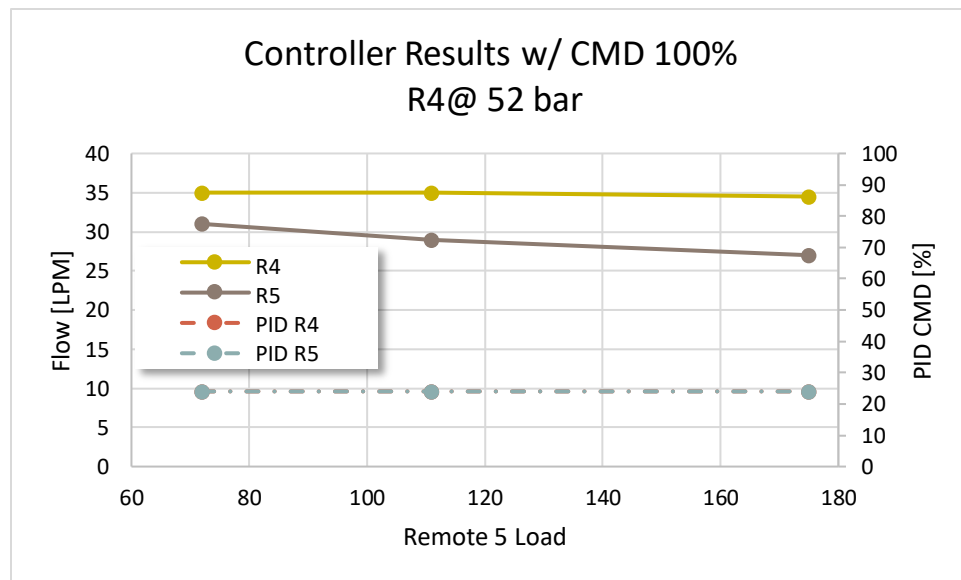
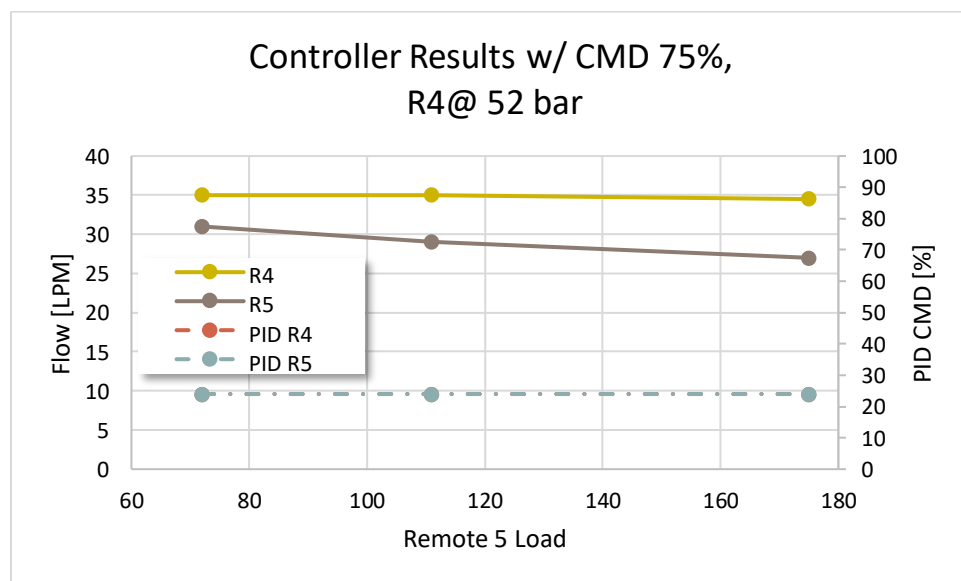


Figure 6.7 Simulation Model with PID Control Implementation

The model with the PID controller can be seen in the figure above. Once the control structure was implemented. The same tests shown in figure 6.8 were ran. The data seen below is the one obtain from the tests at 100% command and 75% command with remote 4 at a constant 52 bar load and remote 5 with different load levels.



A



B

Figure 6.8 Controller Simulation Results with 100% (A) & 75% (B) Command

The value of the PID gains in the model cannot be disclosed in this document. Only the tuning process can be stated, this process was done manually. Every simulation took around a minute to complete, making the manual tuning a favorable approach. With the tests results validating the approach and flow sharing algorithm, the controller can be tested on the actual machine to provide final validation.

6.2.1.1 Machine Implementation and Validation

The flow sharing control algorithm was implemented in the same LabVIEW code that was used for data acquisition. As stated before this first approach only requires two pressure signals, pump outlet and load sense line. These signals were already available in the machine, since they were used for testing the EHR valves.

From a software perspective, the LabVIEW code was updated with a dedicated flow sharing control tab. Within this tab the signal into the EHR could be altered as needed. If no alteration is required, the bypass lever button would not be pressed. If the command from the lever was to be altered, the bypass button would be pressed. From there, the signal could be altered manually or by the PID Flow sharing control. This update can be seen in the figure of the front panel below.

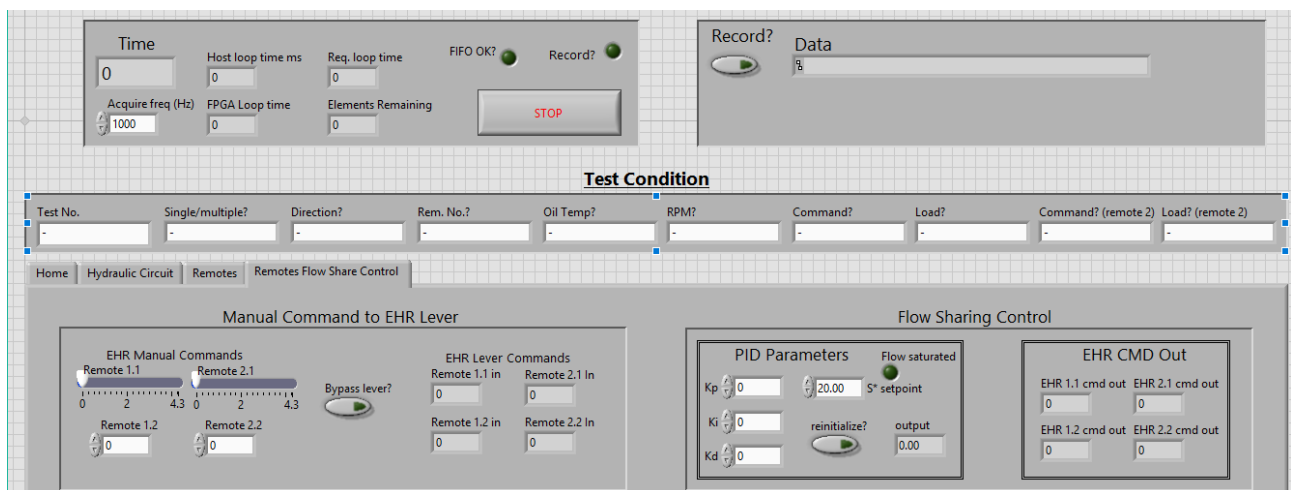


Figure 6.9 Host Code Front Panel Update

Within this new front panel, the different parameters for the PID control can be set. The respective gains for the controller can also be set along with the reference value input. A visual indicator of when the system detects flow saturation was placed. When this visual indicator is on, the controller overrides any command given by the levers or manually from inside the code. Read outs of the command being sent to the CAN controller are also present. The actual vi behind the main panel includes extra implementations not shown in figure 6.16.

In order to not saturate the bandwidth of the remotes by having the PID give commands at a fast rate. An output rate limiter was placed at the output of the PID vi. This limiter restricts the command per second being given by the PID. The final implementation of the PID code into LabVIEW is shown in figure 6.16.

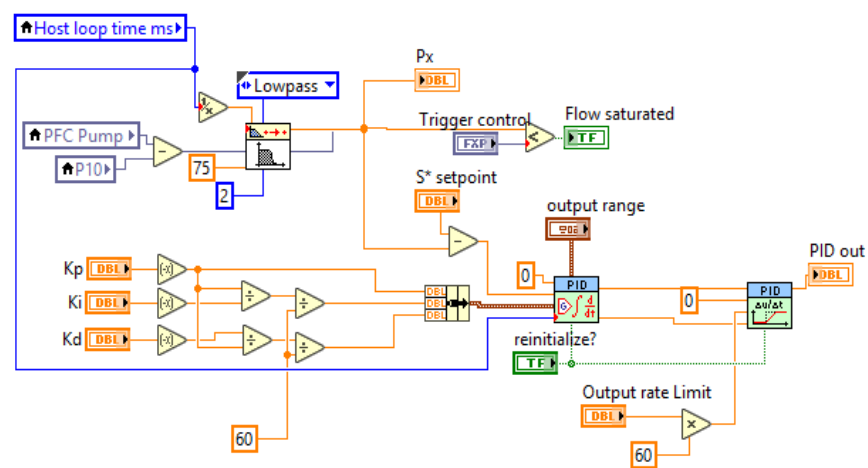


Figure 6.10 PID Vi Implementation

Once the Vi was implemented in LabVIEW and working correctly, tests were run in the machine to test the controller structure and approach. A test with its time based plot is shown below. This test demonstrates the behavior of the system whenever the flow share control is active. At the start of the test; the system is in flow saturation. For the duration of the test the output flow of the pump remains the same. The flows at the EHR valves change in behavior. When the test started, from seconds 30-40 the controller was off. At second 40, the controller was activated.

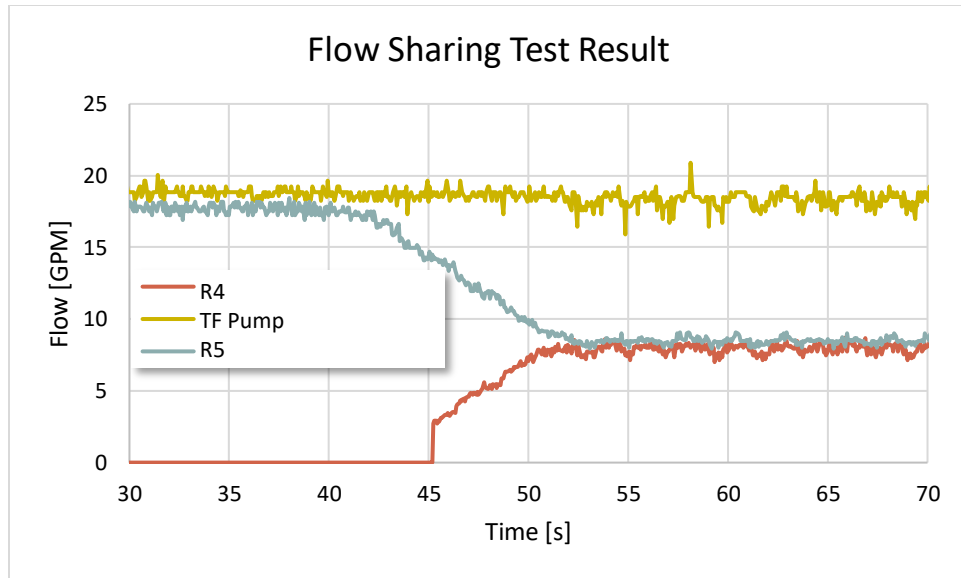


Figure 6.11 RAW Data Flow Sharing Control Test Results

Once the controller was active it can be seen that EHR 5 starts decreasing in flow amount and begins sharing the flow with EHR 4, until a steady state of flow sharing is achieved. One thing to notice is the amount of time to reach the steady state point for the controller is at around 12 seconds. This is acceptable since the operating conditions of the EHR valves are at steady state. Also, a farmer will not start moving the machine until the EHR valves and the implements connected have reached a steady state condition.

The final gains were tuned to have the system reach a steady state flow sharing condition as fast as possible. The final gains are: $k_p = 0.005$, $k_i = 6 \times 10^{-6}$, $k_d = 0.05$. These gain allowed for the fastest performance without overshoot and minimizing oscillations in the system. Figure 6.19 shows the system reaching a steady state point in a much faster manner. It takes around 4 seconds [13-17s] for the system to stabilize.

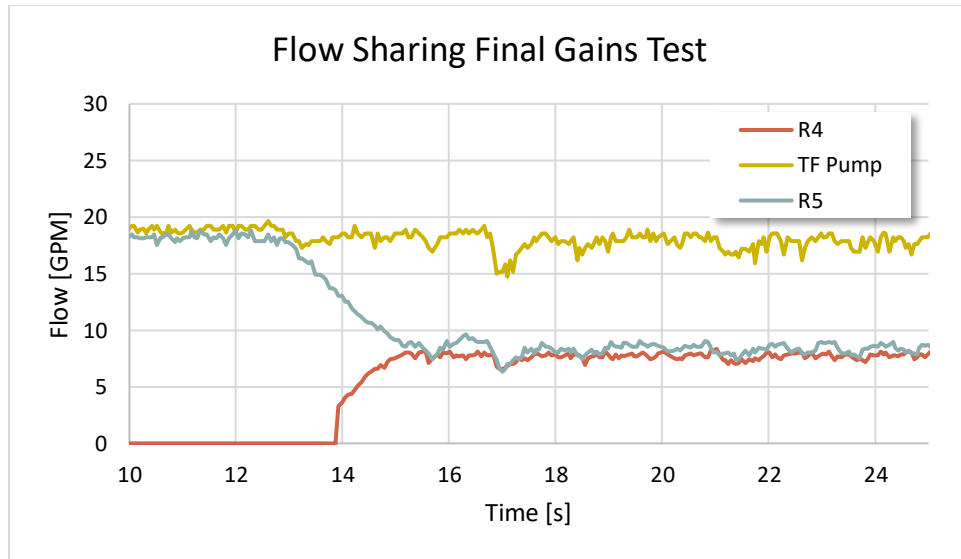
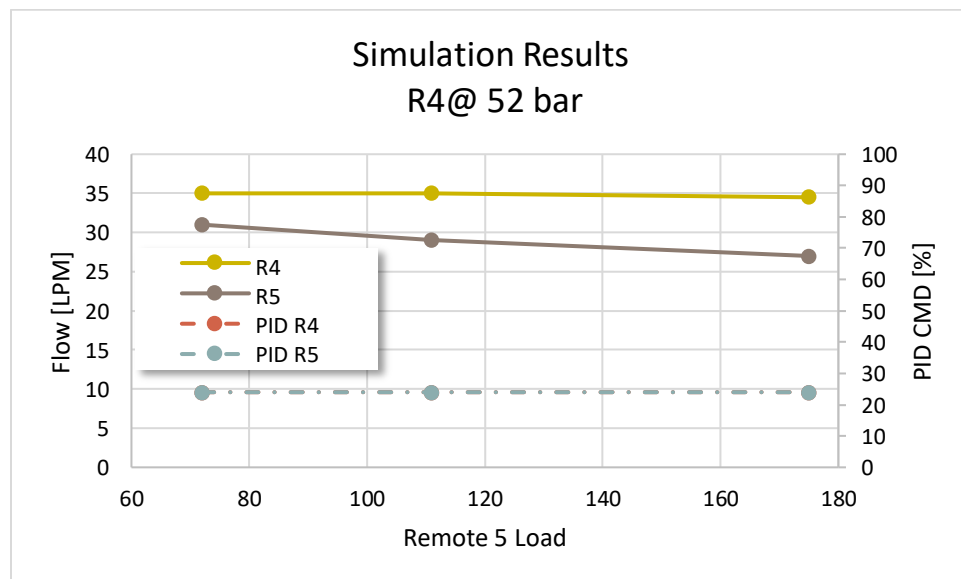
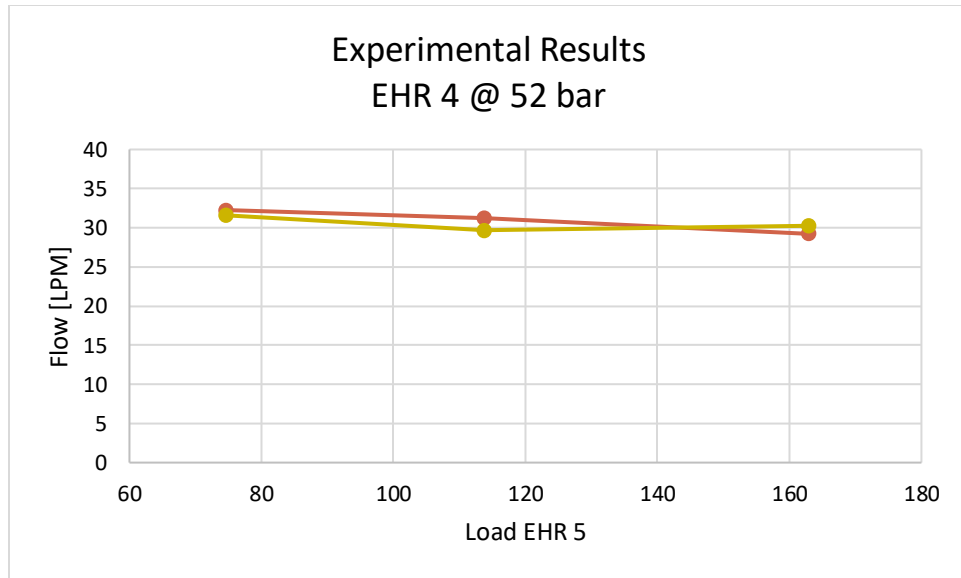


Figure 6.12 Flow Sharing with Final Gains Test Results

A final validation needed to be made by comparing experimental data with simulation data. A total of 12 experimental test were taken to validate the simulation data. These 12 tests were all at low engine RPM. Temperature was not monitored for these tests. Test were taken at low rpm for practical reasons. The tests are taken in a faster manner and the machine does not produce noise. All of the tests had the same command ratio. The all started with a 100 % command. All of the tests validated simulation results.



a.) Simulation



b.) Experimental

Figure 6.13 Flow Sharing Controllers Simulation vs Experimental Results

In the simulation results shown above, the flows to the remotes have a discrepancy when they are compared to the experimental results. This is due to the fact that in simulation the controller was allowed to go to a reference value of $s^* = 20$. In experimental testing the actual value of $s^* = 26 \text{ bar}$. This 6 bar difference did not permit the simulation tests to fully exit the flow saturation zone. This discovery was corrected before moving on into approach 2.

Approach one allows for correct flow saturation correction. It requires the most minimum instrumentation of the two approaches. It is also an inexpensive solution that can be implemented in both future and already released models of tractors. Existing machinery can be upgraded with the required sensors and also the EHR UCM CAN software can be easily updated to incorporate the flow sharing algorithm.

6.2.2 Approach 2: EHR Spool Pressures Feedback

The second approach that was proposed is based on monitoring the pressure drop across the EHR valve. Recalling load sense theory on multiple actuators, the pressure drop across the control orifices O_1 & O_2 is given by the following expressions:

$$\begin{aligned}\Delta p_{O1} &= p_{x1} - p_{u1} \\ \Delta p_{O2} &= p_{x2} - p_{u2}\end{aligned}\tag{6.6}$$

During normal operating conditions, the flow across both orifices is given by the area command, this is possible since the pressure drop across the orifices is constant. That constant pressure drop is the setting of the spring s_c of the compensators C1 and C2 seen in figure 3.7. All load sense systems that are in non-flow saturation conditions and have multiple actuators behave identically and meet this criteria:

$$\begin{aligned}\Delta p_{Ox} &= s_c \\ \Delta p_{O_{x+1}} &= s_c\end{aligned}\tag{6.7}$$

The assumption is that the spring setting is the same for all present compensators. For the flow sharing controller in this approach, the individual measurement across each present control orifice will be measured and compared to the fixed setting of the compensator spring value s_c .

$$s_c - \Delta p_{Ox} = 0\tag{6.8}$$

If the condition of equation 6.8 is met across all working orifices in a load sense system, then the system is not under flow saturation. If $s_c > \Delta p_{Ox}$ then the system is in flow saturation. For this method to work, feedback of the value of p_x and p_u per EHR valve are needed.

Before exploring this method any further, the possibility of obtaining a measurement of p_x is explored.

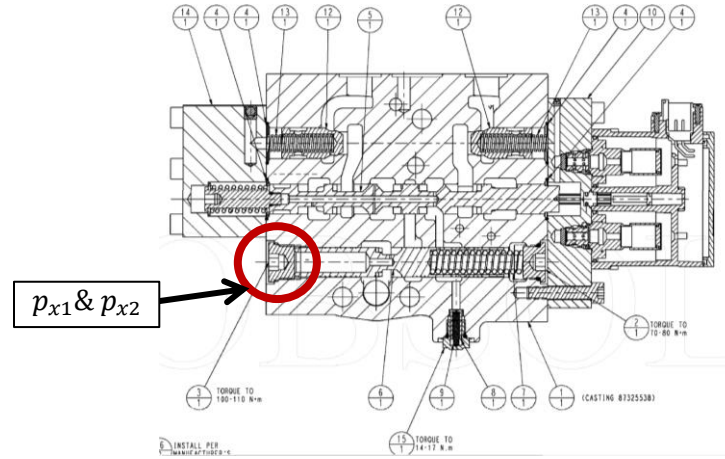


Figure 6.14 Location for Pressure Transducer Placement for p_x Measurement

After studying the cross section of the EHR valves. A service port that allows for the measurement of p_x was found. It has just enough available space for the mounting of a pressure transducer on all working EHR. The value of the load could not be taken directly from inside the EHR valve, however, the load may be measured by the external pressure transducers that were used to take data for all the tests. With this approach, two pressure transducer per EHR are needed. This may prove to be a disadvantage since with approach 1 only two sensors are needed in total. With the availability of dedicated pressure transducers per EHR valve, other than approach 2 being possible, other advantages arise. The two sensors per remote can keep track of the internal efficiency in real time during all of the machine life cycle.

With the correct estimation of flow through the working area, data that has not been available to the farmer before may now be within reach. An energy consumption study may now be available through the HMI in the cabin. Energy consumption data may now be stored and compared every season. This data can be used to estimate incoming fuel costs in upcoming agricultural seasons.

The same steps for approach 1 were taken. It has been established that the model can show flow saturation conditions. With this in mind, the value of the pressure drop across the EHR valves when the system is in saturation was monitored. It was validated that the pressure drop Δp_{ox} across the EHR valve that was not receiving the required flow was less than the value of s_c .

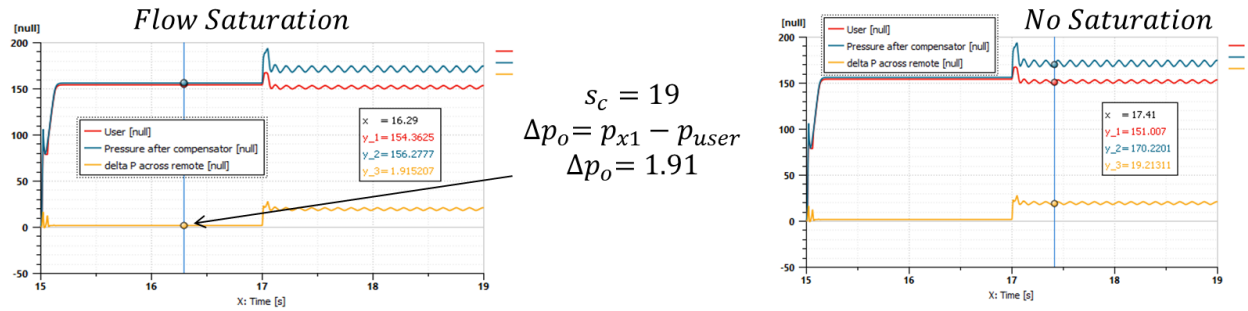


Figure 6.15 Validation of $s_c > p_x$ when in Flow Saturation

The model was restructured to accommodate measurements of the pressure drop across the main spool of the EHR valves. In a flow saturation condition the constant pressure drop of $s_c = 19 \text{ bar}$ is lost. The flow sharing algorithm that was implemented is the same on as the one explained in figure 6.10. Once again the controller chosen was a PID control and the control structure follows the same as figure 6.12. The only difference is the reference signal now becomes the compensator spring setting and the output is the lowest value of pressure drop across all working EHR valve spools. Since the control structure is the same as before, the test shown for approach 2 will be with different command ratios. The command ratios were proposed: 0.25, 0.50 & 0.75.

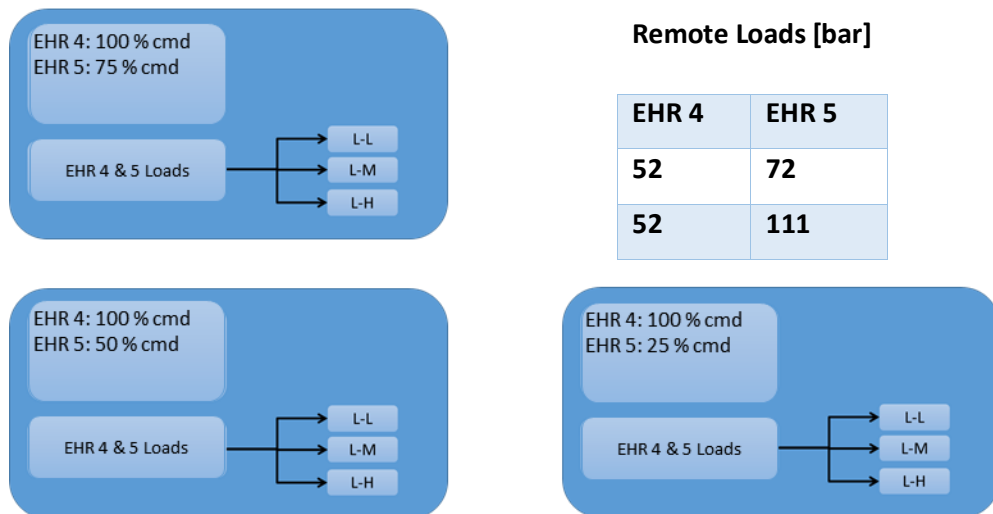


Figure 6.16 Simulation Flow Sharing Test Conditions Approach 2

All ratios were tested with the flow control algorithm. The simulations lasted 20 seconds each. The first half of the simulation the control was off and the system was in flow saturation. After second 10, the controller was enabled. On all tests the controller worked and was able to flow share while also maintaining the original ratio given. For these tests EHR 4 was kept at a constant load and EHR 5 changed loads. The resulting commands of these tests can be seen in the table below.

Table 6-4 Flow Sharing Command Results- Simulation

Load at remotes		Command to remote	
R1	R2	R1	R2
52	72	0.39	0.01
	111	0.39	0.01
	175	0.39	0.01
	72	0.33	0.16
	111	0.33	0.16
	175	0.33	0.16
	72	0.28	0.21
	111	0.28	0.21
	175	0.28	0.21

The commands all respect the initial ratio given. These commands generated the flow plot below. In this plot, the resulting flow at the EHR valves is seen. Each same color line represents a different remote with a given command ratio.

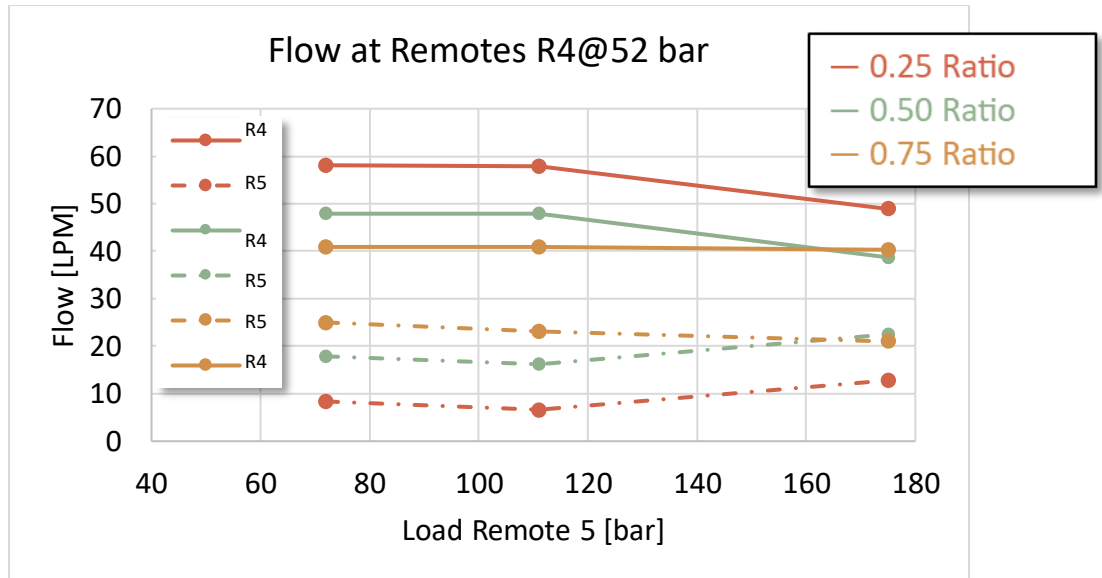


Figure 6.17 Flow Results of Flow Sharing Tests Approach 2

The approach is valid in simulation. The algorithm may be applied in the reference machine now. The LabVIEW code was updated with the new approach and a new front panel was designed.

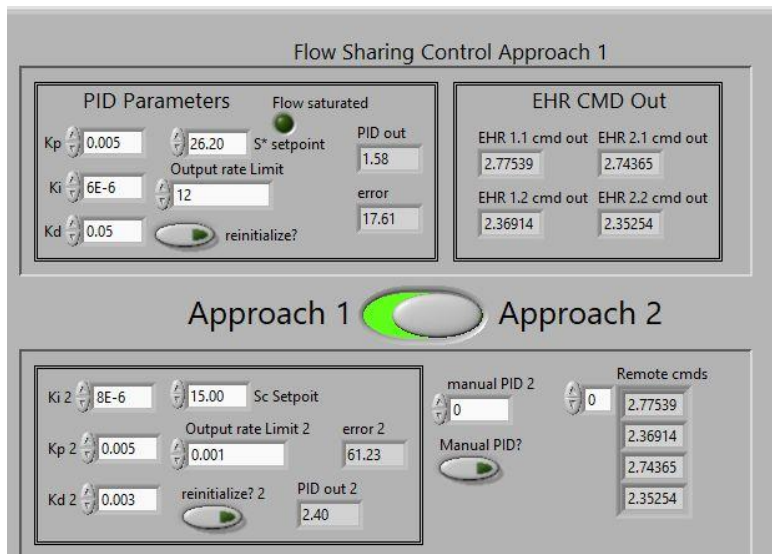


Figure 6.18 Final Updated Front Panel of Host Code

The panel includes a selector between the two approaches. The gains did not have to be retuned since the system responded well also with these gains. Since the approach 2 takes a different reference signal, using the same gains on both methods is a coincidence. If the gains did not make the system behave adequately, gain tuning had to be remade. The vi was modified with a section

to detect the EHR valve that has the least pressure drop across its main spool. This signal was used as feedback to compute the error in the control structure.

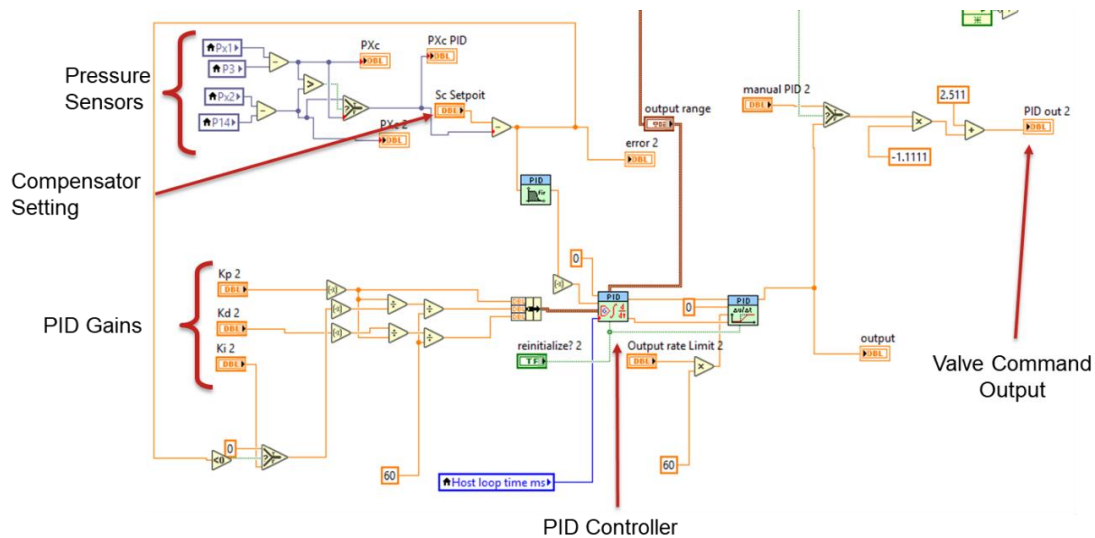


Figure 6.19 Flow Sharing Controller LabVIEW Implementation- Approach 2

With the PID for approach 2 completely implemented the same tests were run in the machine as the ones in simulation. After testing the data was processed and organized in the plot seen below.

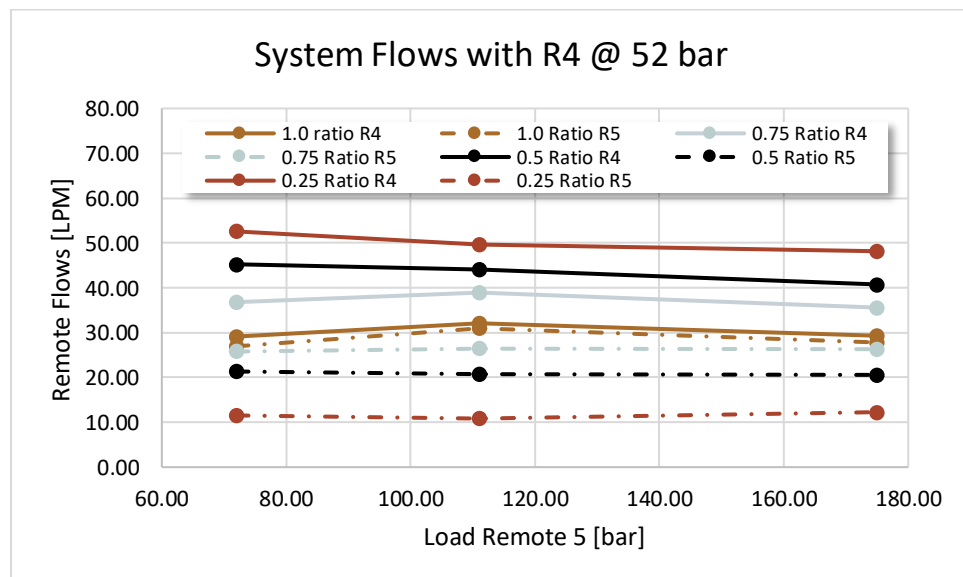


Figure 6.20 Experimental Test Results Flow Sharing Approach 2

The experimental test results validate the implementation of approach 2 in the EHR valves to eliminate flow saturation scenarios. Both approaches worked and eliminated flow saturation of the system whenever the flow sharing control was on. The control structure of a PID is a correct path into getting any of the two approaches commercially available in the reference machine. Due to timeline restrictions, the exploration of controllers with a high complexity was not realized. The opportunity stands for future work and development for the flow sharing algorithm.

7. CONCLUSION AND FUTURE WORK

At the start of this work the knowledge of the hydraulic circuits efficiency behavior was nearly null. The time invested in this work has bestowed great knowledge and experience in both hydraulic systems and agricultural tractors and its implements. It is clear that agricultural tractors are at its peak of state of the art technology. That technology may still be improved.

This work has exposed certain energy efficiency points that may be corrected for future designs of the EHR valves. This work represents much investigative effort spanning two years of hard work and collaboration with peers and advisors. This work focused heavily on machine instrumentation and test plan development. All the high pressure circuits present in the tractor were instrumented to be able to study all of the hydraulic energy efficiency. The pages of this work focused mainly on the high pressure EHR valves. The hitch, steering and suspension system also had test plans developed and test taken by this works author. All of this data aided in the generation of a full model in Simscape Amesim of all the high pressure hydraulic circuits.

All of the tests allowed to make an energy efficiency analysis on all the systems, in this work specifically the efficiency of the EHR valves was addressed. The second focus of this work resulted in the discovery of a potential sources of energy loss inside the EHR valves or their respective circuits. A flow saturation behavior was also investigated. Two different approaches to implement a flow sharing algorithm were implemented on the reference machine. These two approaches were first validated with the working simulation model developed in the first year. The approaches were also tested and validated in the machine. All the necessary hardware and software was designed and installed.

The result of this study is identification of energy losses within the EHR valves circuits. The implementation of flow sharing algorithms that augment the EHR performance. It opened up scenarios for potential different technologies.

7.1 Future Work

With the study of this work, potential technologies may be implemented in the EHR valve circuits to further increase efficiency. Electronic load sensing pumps may allow for further energy efficiency. With electronic load sensing the LS margin may be modified to consume the least amount of energy given a working cycle.

The separation of the steering circuit from the EHR valves may bring even further efficiency and performance benefits. A redesign of the hydraulic circuits with the use of the developed models will aid in optimizing the layout of the hydraulic components to maximize efficiency and performance. A steer by wire implementation will aid drastically the performance of the steering since the steering priority valve was found to be a major source of energy loss. By making the priority valve an electric algorithm, no energy loss will be present.

Instrumenting the machine to be able to handle flow saturation with advanced controllers will prove to be a great benefit for the end user of the machine. The duration of the degree being pursued by this work was not enough to fully explore all of these possibilities. However, there is no doubt that this work will continue to be developed. This work has laid the foundation stone to many more opportunities and possibilities. May this work assist in future research endeavors.

APPENDIX A: TESTING PROCEDURE

To start the experimental testing, the same procedure must be followed in each test. The reference machine has to be in similar working conditions to ensure testing consistency and data comparison. Before starting any tests, the machine has to be prepared. For machine preparation, the following steps were made:

Machine preparation

- Start machine and let run to stabilize machine temperature [engine temperature]
- Ensure machine has no unnecessary loads [external electrical loads]
- Place machine parking lock before running tests [automatic]

Once the machine was ready and the oil was at a desired testing temperature the hydraulic system was prepared following the next steps:

Hydraulic circuit preparation

- Connect the external hydraulic circuit specified on the ISO schematic above.
- Record specs of hoses used in circuit. [L1 & L2]
- Ensure only hydraulic load is coming from system to be tested [no steering, suspension change, hitch movement, etc.]
- Adjust loading valve to correct pressure level.
- Run “Practice tests” (if necessary) to stabilize oil temperature to desired testing temperature

Finally, after all the require steps to prepare the machine and hydraulics, the tests were ready to be run. The way of recording the data and steps of commanding the EHR valves are explained below:

Test Running [Constant Command- Different load]

- Check desired load for test
- Start DAQ system
- Start Recording while machine is on standby
- Bring Machine to desired RPM
- Command desired flow to remote until a steady state condition is reached
- Once steady state condition is reached an average value of data between a ΔT will be used for power consumption calculation

- Stop command and data recording at least 10 s of steady state is observed.
- Bring machine to IDLE
- Stop DAQ system

Test Running [Constant Load- Different Command]

- Set constant desired load
- Start DAQ system
- Start Recording while machine is on standby
- Bring machine to desired RPM
- Command desired flow to remote until a steady state condition is reached
- Once steady state condition is reached an average value of data between a ΔT will be used for power consumption calculation
- Stop command and data recording at least 10 s of steady state is observed.
- Bring machine to IDLE
- Stop DAQ system

APPENDIX B: SINGLE EHR TEST TABLES

Test	Single\ multiple	Direction [F/R]	Remote Number	Oil Temperature [Hi/Lo]	RPM [Hi/Lo]	Command	Load
1	S	F	1	L	L	FC	0
2	S	F	1	L	L	FC	50
3	S	F	1	L	L	FC	75
4	S	F	1	L	L	FC	90
5	S	R	1	L	L	FC	0
6	S	R	1	L	L	FC	50
7	S	R	1	L	L	FC	75
8	S	R	1	L	L	FC	90
9	S	F	2	L	L	FC	0
10	S	F	2	L	L	FC	50
11	S	F	2	L	L	FC	75
12	S	F	2	L	L	FC	90
13	S	R	2	L	L	FC	0
14	S	R	2	L	L	FC	50
15	S	R	2	L	L	FC	75
16	S	R	2	L	L	FC	90
17	S	F	4	L	L	FC	0
18	S	F	4	L	L	FC	50
19	S	F	4	L	L	FC	75
20	S	F	4	L	L	FC	90
21	S	R	4	L	L	FC	0
22	S	R	4	L	L	FC	50
23	S	R	4	L	L	FC	75
24	S	R	4	L	L	FC	90
25	S	F	5	L	L	FC	0
26	S	F	5	L	L	FC	50
27	S	F	5	L	L	FC	75
28	S	F	5	L	L	FC	90
29	S	R	5	L	L	FC	0
30	S	R	5	L	L	FC	50
31	S	R	5	L	L	FC	75
32	S	R	5	L	L	FC	90

Test	Single\multiple	Direction [F/R]	Remote Number	Oil Temperature [Hi/Lo]	RPM [Hi/Lo]	Command	Load
65	S	F	1	L	H	FC	0
66	S	F	1	L	H	FC	50
67	S	F	1	L	H	FC	75
68	S	F	1	L	H	FC	90
69	S	R	1	L	H	FC	0
70	S	R	1	L	H	FC	50
71	S	R	1	L	H	FC	75
72	S	R	1	L	H	FC	90
73	S	F	2	L	H	FC	0
74	S	F	2	L	H	FC	50
75	S	F	2	L	H	FC	75
76	S	F	2	L	H	FC	90
77	S	R	2	L	H	FC	0
78	S	R	2	L	H	FC	50
79	S	R	2	L	H	FC	75
80	S	R	2	L	H	FC	90
81	S	F	4	L	H	FC	0
82	S	F	4	L	H	FC	50
83	S	F	4	L	H	FC	75
84	S	F	4	L	H	FC	90
85	S	R	4	L	H	FC	0
86	S	R	4	L	H	FC	50
87	S	R	4	L	H	FC	75
88	S	R	4	L	H	FC	90
89	S	F	5	L	H	FC	0
90	S	F	5	L	H	FC	50
91	S	F	5	L	H	FC	75
92	S	F	5	L	H	FC	90
93	S	R	5	L	H	FC	0
94	S	R	5	L	H	FC	50
95	S	R	5	L	H	FC	75
96	S	R	5	L	H	FC	90

Test	Single\multiple	Direction [F/R]	Remote Number	Oil Temperature [Hi/Lo]	RPM [Hi/Lo]	Command	Load
97	S	F	1	H	H	FC	0
98	S	F	1	H	H	FC	50
99	S	F	1	H	H	FC	75
100	S	F	1	H	H	FC	90
101	S	R	1	H	H	FC	0
102	S	R	1	H	H	FC	50
103	S	R	1	H	H	FC	75
104	S	R	1	H	H	FC	90
105	S	F	2	H	H	FC	0
106	S	F	2	H	H	FC	50
107	S	F	2	H	H	FC	75
108	S	F	2	H	H	FC	90
109	S	R	2	H	H	FC	0
110	S	R	2	H	H	FC	50
111	S	R	2	H	H	FC	75
112	S	R	2	H	H	FC	90
113	S	F	4	H	H	FC	0
114	S	F	4	H	H	FC	50
115	S	F	4	H	H	FC	75
116	S	F	4	H	H	FC	90
117	S	R	4	H	H	FC	0
118	S	R	4	H	H	FC	50
119	S	R	4	H	H	FC	75
120	S	R	4	H	H	FC	90
121	S	F	5	H	H	FC	0
122	S	F	5	H	H	FC	50
123	S	F	5	H	H	FC	75
124	S	F	5	H	H	FC	90
125	S	R	5	H	H	FC	0
126	S	R	5	H	H	FC	50
127	S	R	5	H	H	FC	75
128	S	R	5	H	H	FC	90

Test	Single\multiple	Direction [F/R]	Remote Number	Oil Temperature [Hi/Lo]	RPM [Hi/Lo]	Command	Load
129	S	F	1	L	L	25	90
130	S	F	1	L	L	50	90
131	S	F	1	L	L	75	90
132	S	R	1	L	L	25	90
133	S	R	1	L	L	50	90
134	S	R	1	L	L	75	90
135	S	F	2	L	L	25	90
136	S	F	2	L	L	50	90
137	S	F	2	L	L	75	90
138	S	R	2	L	L	25	90
139	S	R	2	L	L	50	90
140	S	R	2	L	L	75	90
141	S	F	4	L	L	25	90
142	S	F	4	L	L	50	90
143	S	F	4	L	L	75	90
144	S	R	4	L	L	25	90
145	S	R	4	L	L	50	90
146	S	R	4	L	L	75	90
147	S	F	5	L	L	25	90
148	S	F	5	L	L	50	90
149	S	F	5	L	L	75	90
150	S	R	5	L	L	25	90
151	S	R	5	L	L	50	90
152	S	R	5	L	L	75	90

Test	Single\multiple	Direction [F/R]	Remote Number	Oil Temperature [Hi/Lo]	RPM [Hi/Lo]	Command	Load
153	S	F	1	H	L	25	90
154	S	F	1	H	L	50	90
155	S	F	1	H	L	75	90
156	S	R	1	H	L	25	90
157	S	R	1	H	L	50	90
158	S	R	1	H	L	75	90
159	S	F	2	H	L	25	90
160	S	F	2	H	L	50	90
161	S	F	2	H	L	75	90
162	S	R	2	H	L	25	90
163	S	R	2	H	L	50	90
164	S	R	2	H	L	75	90
165	S	F	4	H	L	25	90
166	S	F	4	H	L	50	90
167	S	F	4	H	L	75	90
168	S	R	4	H	L	25	90
169	S	R	4	H	L	50	90
170	S	R	4	H	L	75	90
171	S	F	5	H	L	25	90
172	S	F	5	H	L	50	90
173	S	F	5	H	L	75	90
174	S	R	5	H	L	25	90
175	S	R	5	H	L	50	90
176	S	R	5	H	L	75	90

Test	Single\multiple	Direction [F/R]	Remote Number	Oil Temperature [Hi/Lo]	RPM [Hi/Lo]	Command	Load
177	S	F	1	L	H	25	90
178	S	F	1	L	H	50	90
179	S	F	1	L	H	75	90
180	S	R	1	L	H	25	90
181	S	R	1	L	H	50	90
182	S	R	1	L	H	75	90
183	S	F	2	L	H	25	90
184	S	F	2	L	H	50	90
185	S	F	2	L	H	75	90
186	S	R	2	L	H	25	90
187	S	R	2	L	H	50	90
188	S	R	2	L	H	75	90
189	S	F	4	L	H	25	90
190	S	F	4	L	H	50	90
191	S	F	4	L	H	75	90
192	S	R	4	L	H	25	90
193	S	R	4	L	H	50	90
194	S	R	4	L	H	75	90
195	S	F	5	L	H	25	90
196	S	F	5	L	H	50	90
197	S	F	5	L	H	75	90
198	S	R	5	L	H	25	90
199	S	R	5	L	H	50	90
200	S	R	5	L	H	75	90

Test	Single\multiple	Direction [F/R]	Remote Number	Oil Temperature [Hi/L0]	RPM [Hi/L0]	Command	Load
201	S	F	1	H	H	25	90
202	S	F	1	H	H	50	90
203	S	F	1	H	H	75	90
204	S	R	1	H	H	25	90
205	S	R	1	H	H	50	90
206	S	R	1	H	H	75	90
207	S	F	2	H	H	25	90
208	S	F	2	H	H	50	90
209	S	F	2	H	H	75	90
210	S	R	2	H	H	25	90
211	S	R	2	H	H	50	90
212	S	R	2	H	H	75	90
213	S	F	4	H	H	25	90
214	S	F	4	H	H	50	90
215	S	F	4	H	H	75	90
216	S	R	4	H	H	25	90
217	S	R	4	H	H	50	90
218	S	R	4	H	H	75	90
219	S	F	5	H	H	25	90
220	S	F	5	H	H	50	90
221	S	F	5	H	H	75	90
222	S	R	5	H	H	25	90
223	S	R	5	H	H	50	90
224	S	R	5	H	H	75	90

APPENDIX C: MULTIPLE EHR TEST TABLES

<i>Test</i>	Single\ multiple	Direction [F/R]	Remote Number	Oil Temp [Hi/L0]	RPM [Hi/L0]	Command A	Load A	Command B	Load B
1	M	F	AB	L	L	25	50	25	75
2	M	F	AB	L	L	25	75	25	90
3	M	F	AB	L	L	25	90	25	50
4	M	R	AB	L	L	25	50	25	75
5	M	R	AB	L	L	25	75	25	90
6	M	R	AB	L	L	25	90	25	50
7	M	F	CD	L	L	25	50	25	75
8	M	F	CD	L	L	25	75	25	90
9	M	F	CD	L	L	25	90	25	50
10	M	R	CD	L	L	25	50	25	75
11	M	R	CD	L	L	25	75	25	90
12	M	R	CD	L	L	25	90	25	50

<i>Test</i>	Single\ multiple	Direction [F/R]	Remote Number	Oil Temp [Hi/L0]	RPM [Hi/L0]	Command A	Load A	Command B	Load B
13	M	F	AB	H	L	25	50	25	75
14	M	F	AB	H	L	25	75	25	90
15	M	F	AB	H	L	25	90	25	50
16	M	R	AB	H	L	25	50	25	75
17	M	R	AB	H	L	25	75	25	90
18	M	R	AB	H	L	25	90	25	50
19	M	F	CD	H	L	25	50	25	75
20	M	F	CD	H	L	25	75	25	90
21	M	F	CD	H	L	25	90	25	50
22	M	R	CD	H	L	25	50	25	75
23	M	R	CD	H	L	25	75	25	90
24	M	R	CD	H	L	25	90	25	50

Test	Single\multiple	Direction [F/R]	Remote Number	Oil Temperature [Hi/L0]	RPM [Hi/L0]	Command A	Load A	Command B	Load B
25	M	F	AB	L	H	25	50	25	75
26	M	F	AB	L	H	25	75	25	90
27	M	F	AB	L	H	25	90	25	50
28	M	R	AB	L	H	25	50	25	75
29	M	R	AB	L	H	25	75	25	90
30	M	R	AB	L	H	25	90	25	50
31	M	F	CD	L	H	25	50	25	75
32	M	F	CD	L	H	25	75	25	90
33	M	F	CD	L	H	25	90	25	50
34	M	R	CD	L	H	25	50	25	75
35	M	R	CD	L	H	25	75	25	90
36	M	R	CD	L	H	25	90	25	50

Test	Single\ multiple	Direction [F/R]	Remote Number	Oil Temp [Hi/L0]	RPM [Hi/L0]	Command A	Load A	Command B	Load B
37	M	F	AB	H	H	25	50	25	75
38	M	F	AB	H	H	25	75	25	90
39	M	F	AB	H	H	25	90	25	50
40	M	R	AB	H	H	25	50	25	75
41	M	R	AB	H	H	25	75	25	90
42	M	R	AB	H	H	25	90	25	50
43	M	F	CD	H	H	25	50	25	75
44	M	F	CD	H	H	25	75	25	90
45	M	F	CD	H	H	25	90	25	50
46	M	R	CD	H	H	25	50	25	75
47	M	R	CD	H	H	25	75	25	90
48	M	R	CD	H	H	25	90	25	50

REFERENCES

- [1] Casoli, P., Anthony, A., and Ricco, L., "Modeling Simulation and Experimental Verification of an Excavator Hydraulic System - Load Sensing Flow Sharing Valve Model," SAE Technical Paper 2012-01-2042, 2012
- [2] Zimmerman, J.D., Pelosi, M., Williamson, C.A., & Ivantysynova, M.P. (2007). Energy Consumption of an LS Excavator Hydraulic System.
- [3] Wu, D. (2003). Modeling and experimental evaluation of a load-sensing and pressure compensated hydraulic system.
- [4] Benevelli A., Zardin B., Borghi M. 2012. Independent metering architectures for agricultural tractors auxiliary utilities. Proceedings of the 7th Ph.D. Symposium on Fluid Power, Reggio Emilia, 27-30 June 2012.
- [5] Borghi, M. , Zardin, B. , Pintore, F. , & Belluzzi, F. (2014). Energy Savings in the Hydraulic Circuit of Agricultural Tractors. Energy Procedia, 45 . doi: 10.1016/j.egypro.2014.01.038
- [6] Diaz Lankenau, F. (2017) The Mechanics of Tractor Performance and Their Impact on Historical and Future Device Designs.
- [7] OECD, "Standard Code for the Official Testing of Agricultural and Forestry Tractor Performance,"
- [8] Tian, X., Cruz, J., Vacca, A., Fiorati, S., and Pintore, F.. "Analysis of Power Distribution in the Hydraulic Remote System of Agricultural Tractors Through Modelling and Simulations." Proceedings of the ASME/BATH 2019 Symposium on Fluid Power and Motion Control. ASME/BATH 2019 Symposium on Fluid Power and Motion Control. Longboat Key, Florida, USA. October 7–9, 2019. V001T01A042. ASME.
- [9] Borghi M., Zardin B., Mancarella F. 2010. Energy Dissipation Of The Hydraulic Circuit Of Remote Auxiliary Utilities Of An Agricultural Tractor. Proceedings of the Bath/ASME Symposium on Fluid Power & Motion Control FPMC 2010, 15th-17th September, 2010, Bath, UK.
- [10] Gao, Y., Cheng, J., Huang, J., & Quan, L. (2017). Simulation Analysis and Experiment of Variable-Displacement Asymmetric Axial Piston Pump. Applied Sciences, 7(4), 328.
- [11] Grott, Matteo (2010) Design of Suspension Systems and Control Algorithms for Heavy Duty Vehicles. PhD thesis, University of Trento
- [12] Johnston, D. N., & Plummer, A. R. (Eds.) (2010). Fluid Power and Motion Control: FPMC 2010. Centre for Power Transmission and Motion Control.

- [13] Macmillan, R.H. (2002). The mechanics of tractor-implement performance: theory and worked examples: a textbook for students and engineers.
- [14] O. Degrell and T. Feuerstein, "DLG-Powermix-A practical tractor test," DLG test centre for agricultural machinery, Groß-Umstadt, Germany, pp. 1–4, 2003.
- [15] P. Casoli, A. Vacca, A. Anthony, and G. L. Berta, "Numerical and Experimental Analysis of the Hydraulic Circuit for the Rear Hitch Control in Agricultural Tractors," in 7th International Fluid Power Conference, 2010, pp. 1–13.
- [16] R. McIntosh, J. Matthews, G. Mullineux, and A. J. Medland, "Energy Dissipation of the Hydraulic Circuit of Remote Auxiliary Utilities of an Agricultural Tractor," Fluid Power Motion Control, vol. 48, no. 6, p. 563, 2010. Standards, vol. 2, no. July, p. 91, 2012.
- [17] Wei, C. M., Lian, J. Y., & Li, J. J. (2011). The Modeling Analysis and Dynamics Simulation of Load-Sensing Hydraulic Systems. Advanced Materials Research, 317–319, 307–313.
- [18] Zhang, J., Zhang, T. Z., & Cheng, L. J. (2014). Dynamic Simulation Research Based on AMESim Load-Sensing Pump. Applied Mechanics and Materials, 687–691, 195–200.

PUBLICATION

Proceedings of the ASME/BATH 2019
Symposium on Fluid Power and Motion Control
FPMC2019
October 7-9, 2019, Longboat Key, FL, USA

FPMC2019-1686

ANALYSIS OF POWER DISTRIBUTION IN THE HYDRAULIC REMOTE SYSTEM OF AGRICULTURAL TRACTORS THROUGH MODELLING AND SIMULATIONS

Xin Tian¹, Josias Cruz Gomez, Andrea Vacca
Purdue University
West Lafayette, IN, USA

Stefano Fiorati, Francesco Pintore
CNH Industrial Italia
Modena, Italy

ABSTRACT

Agricultural tractors make massive use of hydraulic control technology. Being fuel consumption a big concern for agricultural applications, tractors typically use the latest state-of-the-art technology to allow efficient fluid power actuation. Nevertheless, the quantification of the energy loss within the hydraulic system of such applications represents an important step to drive the development of the current technology with cost-effective solutions.

In this paper, the load sensing (LS) circuit that typically equips of the hydraulic remotes is taken as reference. A simulation model has been developed within the Amesim software with the aim of accurately predict the operation of the system including the energy flow from the hydraulic supply to the hydraulic user. The paper particularly details the models of the LS pump and the hydraulic remote valves. Within the research, experimental tests on a reference tractor were designed and executed to allow the model validation. The comparison between the experimental results and the simulation data shows the validity of the model. Furthermore, the model allows highlighting the energy losses in the different components of the system as well as identifying the most favorable operating conditions of the system with respect to energy efficiency. The model can be used in support of future research aimed at formulating a more efficient solution for the hydraulic circuit of agricultural tractors.

Keywords: load-sensing system, mid-size tractor, model development and validation, experimental test, power dissipation.

NOMENCLATURE

A	flow area	[m ²]
A_p	FC piston cross-sectional area	[m ²]
A_h	hitch control LPC spool cross-sectional area	[m ²]
b	coefficient of viscous friction	[N/(m/s)]
B	bulk modulus	[Pa]
c_q	flow coefficient	[-]
D	piston diameter	[m]
e	eccentricity	[m]
f	viscous friction force	[N]
F_{si}	spring force on the spool	[N]
F_i	pressure force on the spool	[N]
F_{jeti}	flow/jet force on spool	[N]
K	jet force multiplier	[-]
k_{jet}	jet force coefficient	[-]
lc	contact length	[m]
m	control piston mass	[kg]
n	pump shaft rotation speed	[r/s]
p	pressure	[Pa]
Δp	pressure drop	[Pa]
p_p	pump outlet pressure	[Pa]
p_{LS}	pump load sense line pressure	[Pa]
p_{in}	low pressure circuit port pressure	[Pa]
Q_p	pump outlet flow rate	[m ³ /s]
rc	radial clearance	[m]
s	pump pressure margin	[Pa]
s_c	pre-compensator spring setting	[Pa]

T_e	effective pump shaft torque	[Nm]
v	spool velocity	[m/s]
V_D	pump measured displacement	[m ³ /r]
w	coefficient of windage	[N/(m/s) ²]
x	control piston displacement	[m]
\dot{x}	control piston velocity	[m/s]
\ddot{x}	control piston acceleration	[m/s ²]
x_{lap}	underlap	[m]
x_{min}	underlap corresponding to minimum flow area	[m]
ρ	fluid density	[kg/m ³]
θ	jet angle of the fluid	[°]
η_v	pump volumetric efficiency	[%]
η_{hm}	hydro-mechanical efficiency	[%]
μ	absolute viscosity	[kg/m s]
EHR	electro-hydraulic remote	
FC	flow compensator	
LS	load sensing	
LPC	local pressure compensator	
PC	pressure compensator	
Subscripts		
$i = 1$	FC spool	
$i = 2$	PC spool	
$i = 3$	control piston	
$i = 4$	hitch control valve LPC spool	

INTRODUCTION

Improving the energy efficiency of the current state of the art hydraulic actuation systems has been one of the main drivers for research in fluid power technology for the last decades. Although the fluid power system is often only a sub-system of an off-road vehicle, energy efficiency improvements on the hydraulic system can still lead to major fuel saving advantages. For this purpose, many system architectures have been proposed to reduce energy dissipations within the hydraulic systems, which is one of the possible areas for system improvements, yet keeping a good compromise between cost and performance. The work by Murrenhoff et al. [1] provides an extensive review of the current state-of-art technology. In this work, it is highlighted how architectures derived from the principle of hydraulic individualization, such as displacement control, offer the best energy efficiency performance, although they have a limitation related to cost. The possible concepts of individual hydraulic architectures were exploited in the review paper by Weber et al [2]. As stated in the Murrenhoff's work cited above, the load-sensing (LS) system architecture is nowadays often considered as the best compromise between cost and efficiency, although its limitation is represented by the load interferences between the hydraulic functions connected to the same hydraulic supply. With this rationale, high productivity machines such as agricultural tractors are often equipped with LS systems,

sometimes with more supply pumps to limit the number of hydraulic functions connected to a single pump.

Having a state of art LS system installed on a hydraulic tractor is often considered as a manufacturer choice aimed at offering the user the best compromise between fuel consumption of the hydraulic system and cost. However, for complex systems with numerous hydraulic functions such as agricultural tractors, it can be difficult to make considerations about the optimal sizing of the hydraulic components, as well as to identify possible margins of improvement. This is due not only to the complexity given by the possible combinations at which the different functions can be used but also because the duty cycle of these functions during the actual use of the tractor is highly variable.

The present study focuses on the analysis of the LS system that powers the hydraulic remotes of many states of art tractors, and it contributes to the subject of characterizing its energy consumption, to drive possible improvements aimed at a lower fuel consumption without compromising performance in terms of power transmission to the hydraulic functions.

The hydraulic remotes are part of the high-pressure system of the tractor, which is usually connected to the steering, power beyond and suspension circuit. This system is one of the most demanding systems in terms of power requests. Therefore an increase in the energy efficiency of such a system can lead to a significant benefit to the end user and the environment.

The approach used in this work involves the combined use of simulation and experimental testing on an actual machine. This allows obtaining a simulation model validated on the basis of experimental results which are representative of the actual use of the tractor. The simulation model allows giving an insight into the power flow within the hydraulic system so that the main sources of power dissipation can be identified.

The approach proposed in this paper is often used for the analysis of the energy efficiency of hydraulic control systems. The authors' research center published studies for the analysis of the circuit losses in hydraulic cranes [3] (with particular attention to counterbalance valves) and of aerial platforms [4]. In both cases, a representative drive cycle was identified and a lumped parameter simulation model of the system was used to determine possible improvements of the system to reduce energy consumption. In both cases, the hydraulic circuit taken as reference was simpler than a LS system. Closely related to LS systems for agricultural tractors are instead the references [5], [6], [7] and [8], in which the Amesim commercial software was used to perform a detailed modeling of the LS directional valve and the LS pump, and to evaluate alternative architecture or control solutions to improve energy efficiency. Both [9] and [10] involves similar studies on different components of the high-pressure circuit of an agricultural tractor, and they particularly aim at understanding the influence of design and control parameters involved in the determination of the vehicle dynamic behavior ([9]) and analyzing the performance of the hydrostatic steering system for agricultural tractors ([10]).

With respect to the past cited work, this contribution has some original aspects related to the overall modeling of the LS system that controls the hydraulic remotes. Most importantly,

tests were designed and performed on an agricultural tractor to validate the model under realistic conditions. Finally, the paper details the performance of the system in terms of power distribution and energy efficiency.

The structure of the paper is as follows: Section 2 first introduces the reference system; after that, the modeling approach and pump dynamic behavior validation are detailed in Section 3. Section 4 explains the experimental plan and test procedure. Successively the comparison between experimental test results and simulation results are shown in Section 5 and finally, the system power distribution is analyzed in Section 6. The conclusion section enlightens the positive results and discusses the perspectives of future developments.

2. HYDRAULIC REMOTE SYSTEM

The reference system for this study is shown in the simplified ISO schematic of Fig. 1. The circuit includes a flow supply unit (LS pump), the hitch cylinders control valve, the electro-hydraulic (EH) pre-compensated directional valves for the hydraulic remotes. The hitch valve is composed of a local pressure compensator (C), and two proportional flow control solenoid valves respectively for commanding the raise and the lower of the hitch cylinder. The remote valve (EHR) unit includes a proportional 5/4 directional spool valve electronically

controlled, a local pressure compensator, and lock check valves. The four different positions of the EHR are the neutral position, the extend position (left), the retract position (right), and the float position (far right). All the EHR sections have working ports equipped with a poppet-type lock check (R and E), which are installed to prevent the settling of a load (in neutral) because of the possible leakages at the EHR main spool and to prevent a partially raised cylinder from dropping when the remote valve is operated.

The actual circuit in an agricultural tractor connects the LS pump and the returns to a low-pressure circuit (15-20 bar). This is not shown in Fig. 1, where the tank symbol is used in place of the connection to the low-pressure circuit. The LS pump integrates two elements for the control of its displacement: the pressure compensator (PC) and the flow compensator (FC). The pressure regulated by these two valves is sent to the control piston that adjusts the displacement of the swash plate LS pump. More details on the architecture of LS pumps can be found in [11].

As typical in a LS system, a LS pilot line connects all the functions (for the case of Fig. 1 the hitch valves, the hydraulic remotes) to FC, and the check valves operating as logic elements selects the highest load to be sent to the FC. The pump adjusts

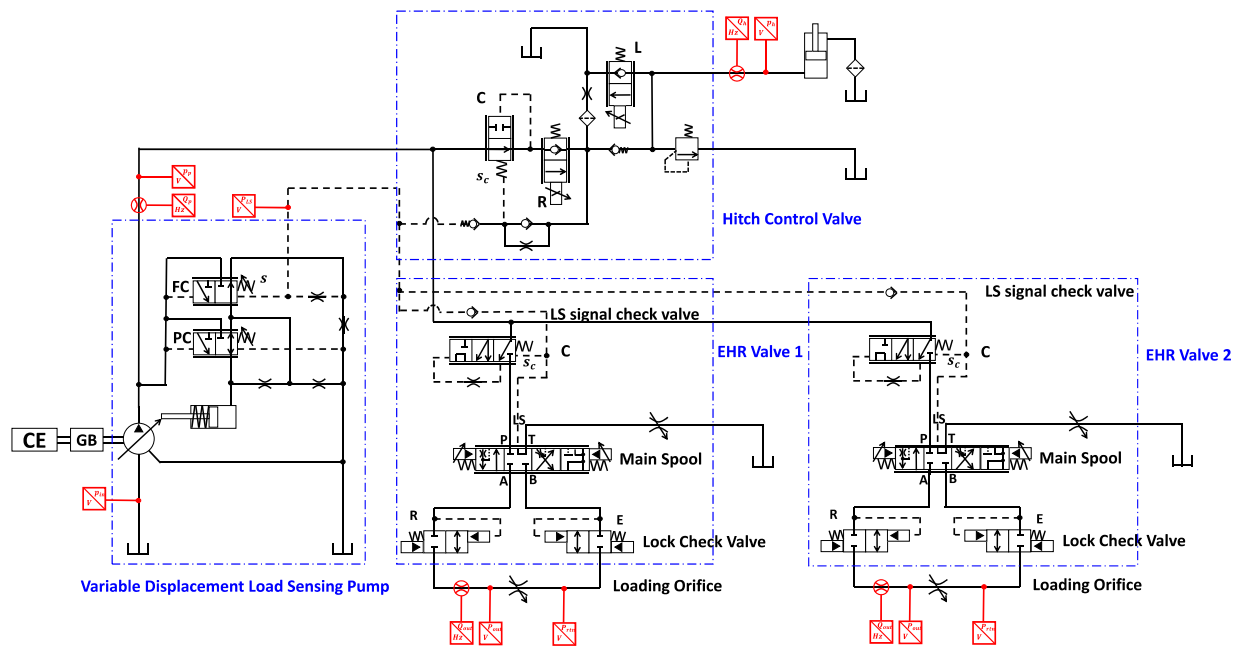


FIGURE 1: SCHEMATIC OF LOAD SENSING ELECTRO-HYDRAULIC REMOTE CONTROL SYSTEM

its displacement to maintain its outlet pressure above this maximum pressure:

$$p_p = p_{LS} + s \quad (1)$$

where s is also referred to as pump pressure margin. This number (about 25 bar in the considered machine), is significantly above the setting s_c of the pre-compensators (C) used at each hydraulic function (for the reference machine, s_c is about 9 bar). This allows having a pressure drop $\Delta p = s_c$ at each working function. In this way, the opening of the valve at each function univocally determines the flow rate sent to the function itself:

$$Q = c_q \cdot A \cdot \sqrt{\frac{2|\Delta p|}{\rho}} \cdot \text{sign}(\Delta p) \quad (2)$$

This allows having control of the flow independently on the load pressure, with a minimum over pressurization of the flow supply. This is the main advantageous feature of a LS system, compared to other hydraulic control methods based on hydraulic valves.

The simultaneous actuation of multiple users connected to the supply pump generally causes an increase of the pressure drop at the compensators (C) that equalize the Δp at each control valve section. The more is the pressure difference among the function, the more is the pressure loss (and consequently the power loss) at the compensator.

The actual behavior of a LS system needs to consider additional aspects related to the pressure losses in lines, fluid compressibility, a setting of the springs, internal leakages, etc. For this reason, the ideal behavior of the system briefly described in these paragraphs is only approximated by an actual system. From this point of view, a detailed numerical model permits to quantify the deviations from the ideal behavior, and particularly the actual losses present in the system.

Since the system of Fig. 1 will be used as reference also in the following sections of the paper, the schematic of the Fig. 1 also anticipates the sensors that are introduced for the measurements of the power flow within the system. This would be further explained in the Experimental Validation section (Section 4).

3. HYDRAULIC SYSTEM MODELING

This section describes the modeling of the system of Fig. 1 through a lumped parameter approach. The hydraulic system is composed of three main components including the LS pump, the hitch control valve, and the EHR remote sections.

The modeling approach takes into consideration the past work done on similar systems, as it will be described in the following sub-sections, which also details the model implementation through conceptual diagrams. For the actual implementation, the commercial software Siemens Simcenter Amesim was utilized.

3.1 Detailed Modelling of the Pump

The pump model reproduces a LS variable displacement swash plate axial piston pump. The complete pump modeling is separated into four subsections: the pressure compensator (PC), the flow compensator (FC), the control piston, and the pump model.

The model implementation has similarities to what has been discussed in [4] and [7]. These models separate the pump behavior from the displacement adjustment system behavior. The rationale behind this conceptual separation is that the pump dynamics are mostly affected by its regulators [12]. Therefore, steady-state modeling of the pump, considering both hydromechanical efficiency and volumetric efficiency, can be coupled to a dynamic model of the flow regulators. Besides the dynamic behavior, also the flow consumption in the regulators is considered. This is because, particularly when the pump operates at low displacements, the FC significantly contributes to power loss due to flow consumption (i.e. low flow requests or pump standby).

With respect to the past literature, particularly with reference [13], the main difference is that the study of this paper presents a simplification of the pump regulators and control pistons, so that the model can be easily adapted to several different pump designs.

The conceptual model of the entire LS pump system is shown in Fig. 2. The flow compensator (FC) plays the most important role of offsetting the pump displacement for a set preload by regulating the swash plate angle. The spool equilibrium on FC spool (Eq. 3) ensures that the pump outlet pressure is a fixed differential pressure higher than the sensed system dominant pressure in the load sensing line. In this way the flow through the spool is modulated, and so is the pump displacement. The functioning of the FC as shown in Fig. 2 is that the pump outlet pressure enters the FC spool through chamber A from chamber M. The pressure entering the spool would work on the area to create a force on the left side of the spool. On the other side of the spool, there acts the load sensing line pressure through chamber C and the FC spring. The sum of these two forces, the load sensing pressure force and spring force, is the value used to counter the force applied by pump pressure. Thus, the force balance of the spool is maintained. When the pump outlet pressure is higher than the sensed pressure in chamber B, the FC spool would displace right creating a flow path between chambers A and B. The flow passing through chamber B has the function of varying the pump swash plate angle by entering chamber N, in which way the pump displacement would be regulated. The FC drain line directs the flow to the tank from chamber B when the pressure balance on FC spool is interrupted. When the pump pressure is higher than $p_{LS} + s$, the flow rate through the path is increasing while decreasing in the other case.

The pressure compensator (PC) in the pump acts as a high-pressure relief valve to protect the system from over pressurization. The highest pressure allowed in the system is decided by the PC spring preload. Pump outlet pressure enters the spool through chamber X from chamber M, creating a spool force on the left side of the PC by acting on the area. This force

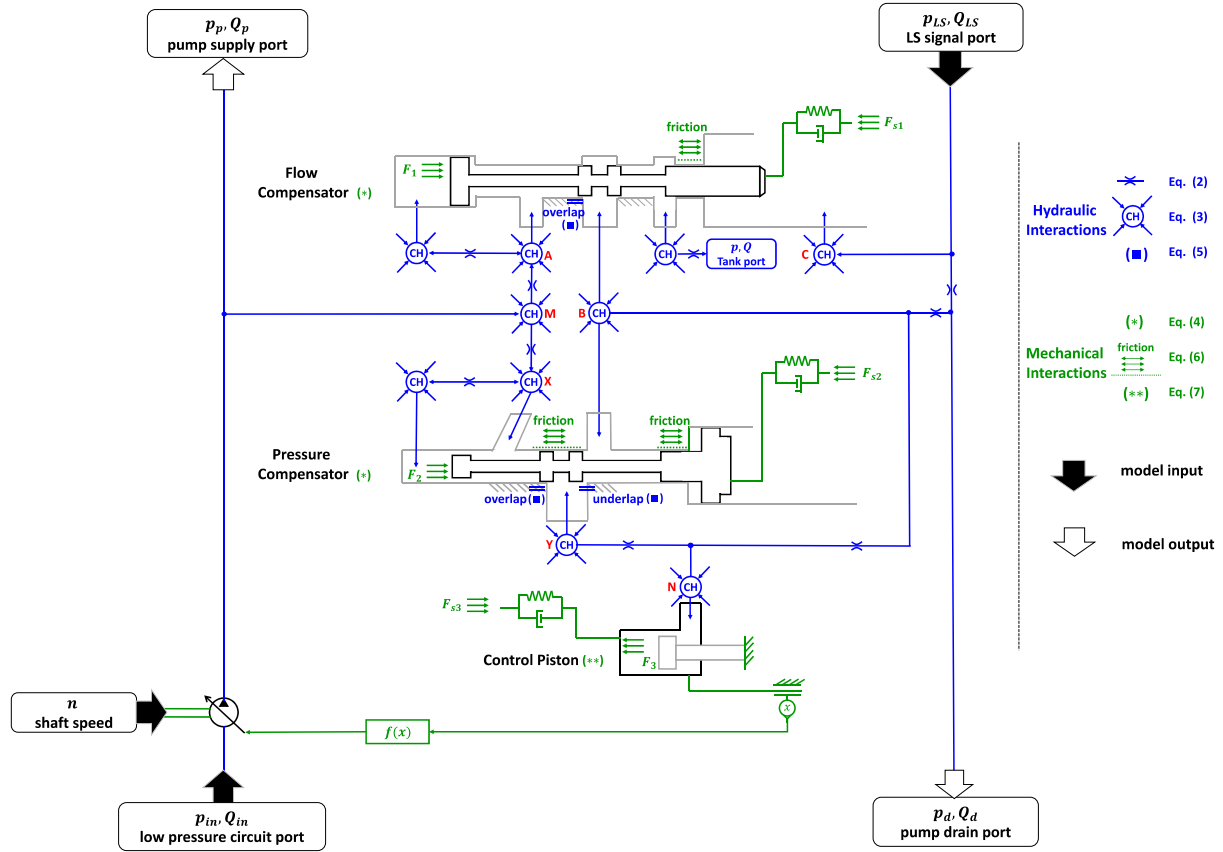


FIGURE 2: SCHEMATIC OF VARIABLE DISPLACEMENT LOAD SENSING PUMP

works against the spring force and flows force on the right side, creating a relief pressure setting. When the pump pressure is higher the PC relief setting, the PC spool will displace right against its spring to create a flow path between chamber X and Y, allowing the full pump pressure to be applied to the pump control piston. In this way, the pump would be destroyed very rapidly from full stroke to a sufficient value for balancing the PC spool. The swash plate stabilizes to provide the flow sufficient to make up for the internal leakages.

Both PC and FC interact with the swash plate to determine the pump displacement in the LS pump; therefore, the accurate prediction of the swash plate motion would be a key point to represent such a LS pump. Here for simplicity, instead of using two pistons constructing the flow characteristics of the pump, which provides a second order relationship between swash plate angle and piston as in [13], a linear relationship between control

piston displacement and swash plate angle has been derived as $f(x)$ in Fig. 2 and Eq. 8. The experimental results available (see Section 3.2) permitted to tune not only the dynamic parameters, but also the static parameters such as the linear relationship between control piston displacement and swash plate angle.

The calculations shown in Fig. 2 are given by the following equations.

- Internal volumes:

$$\frac{dp}{dt} = \frac{B(p) \cdot Q(p)}{V(p)} \quad (3)$$

- Spool equilibriums:

$$\begin{aligned} F_1 &= F_{s1} + p_{LS} \cdot A_p + F_{jet1} \\ F_2 &= F_{s2} + F_{jet2} \end{aligned} \quad (4)$$

- Jet forces [14][15]:

$$F_{jeti} = K_i \cdot 2 \cdot c_q \cdot A_i \cdot \Delta p_i \cdot \cos\theta \quad (i = 1, 2) \quad (5)$$

$$K_i = k_{jet_i} \cdot \frac{1}{2} \left[\tanh \left(\frac{2(x_{lap_i} - x_{min_i})}{x_{min_i}} \right) + 1 \right] \quad (i = 1, 2)$$

- Viscous friction forces:

$$f = -b \cdot v \quad (6)$$

- Control piston:

$$\ddot{x} = \frac{1}{m} \cdot (F_{s3} - F_3 - f \cdot \text{sign}(\dot{x}) - b \cdot \dot{x} + w \cdot \dot{x}|\dot{x}|) \quad (7)$$

- Linear relationship:

$$f(x) = 1 + \frac{x}{0.0185} \quad (8)$$

The model of the pump energy efficiency parameters was created by using an ideal pump model and by using experimental values for the hydro-mechanical and volumetric efficiency maps, where the calculations are expressed in Eqs. 9 and 10. These values were obtained from steady-state experiments performed on the pump.

$$\eta_v = \frac{Q_p}{n \cdot V_D} \times 100\% \quad (9)$$

$$\eta_{hm} = \frac{(p_p - p_{in}) \cdot V_D}{2\pi \cdot T_e} \times 100\% \quad (10)$$

3.2 Pump Dynamic Behavior Validation

To verify the dynamic behavior of the pressure and flow compensators in the complete pump model, experimental results gathered according to the test procedure provided in [16] were used. The basic test set up is depicted in Fig. 3. The pressure transducer at the pump outlet records instantaneous pressure against time.

The response time and recovery time for the FC are defined with the operation of rapid energizing and de-energizing the signal shutoff valve on the pump load sensing signal line. When

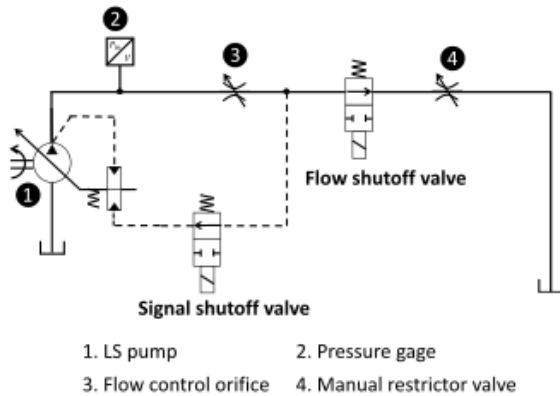


FIGURE 3: TEST SET UP FOR PRESSURE-FLOW COMPENSATOR PERFORMANCE

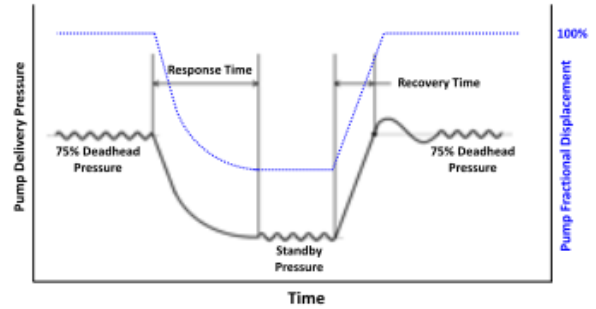


FIGURE 4: FLOW COMPENSATOR RESPONSE AND RECOVERY

it is energized, the pump signal line is disconnected from the 75% deadhead pressure. Since there's no more command for flow or pressure sensed by the LS pump, the pump de-strokes by minimizing the swash plate angle to deliver little flow, making up for internal leakages. After the transient, the LS pump would behave under standby pressure mode as depicted in Fig. 4. The pump remains in the standby pressure mode until the signal shutoff valve is de-energized. When that occurs, the pump signal line is connected to the system pressure again. LS pump starts working at a delivery pressure (75% deadhead pressure) which is a pressure margin higher than the pressure of the user. The time in milliseconds between the start of the pump pressure drop and the subsequent reaching of the standby pressure is defined as the FC response time while the time between the start of the pump delivery pressure rise and the initial reaching of the 75% deadhead pressure is FC recovery time.

The PC response and recovery time are defined associated with closing and opening the flow shutoff valve on the pump delivery line. When the flow shutoff valve is closed instantly, the pressure in the system builds up until it reaches the pressure compensator setting. PC spool shifts against its spring and destrokes the pump rapidly to protect the system from being over pressurized. The LS pump works under deadhead pressure mode

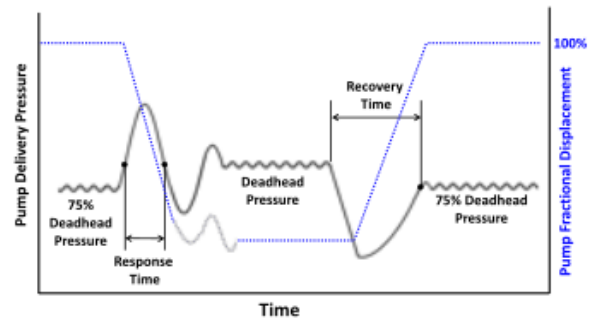


FIGURE 5: PRESSURE COMPENSATOR RESPONSE AND RECOVERY

TABLE 1
AGREEMENT ON THE SIMULATION-EXPERIMENTAL
COMPARISON (%)

Flow Compensator	
Load Pressure	99.79
Low Standby Pressure	83.22
Response Time	99.66
Recovery Time	97.34
Swash Plate Angle	98.61
Pressure Compensator	
Load Pressure	95.08
High Standby Pressure	99.29
Response Time	22.25
Recovery Time	97.93
Swash Plate Angle	98.89

after the transient as depicted in Fig. 5. The LS pump would remain in the deadhead pressure mode until the flow shutoff valve is open again, under which condition the system pressure drops back to the 75% deadhead pressure. Swashplate angle increases reaching full strokes of the pump. During this transient, the time in milliseconds between the instantaneous pressure crossing of deadhead pressure on the pressure rise and its subsequent reaching of deadhead pressure on the pressure drop when tested is defined as PC response time. The PC recovery time is the time in milliseconds between the start of pump delivery pressure drop and the subsequent reaching of system load setting pressure on the first rise of the instantaneous pressure curve when tested.

Table 1 shows the agreement between simulation and experimental results of the tests. The exact values in milliseconds or the plots showing the actual time response are not shown for respecting confidentiality agreements with the pump manufacturer. The FC and PC behaviors are demonstrating consistency between experiments and simulations regarding most of the results with marginal agreement for PC response time. For the purpose of this study, the steady state behavior of

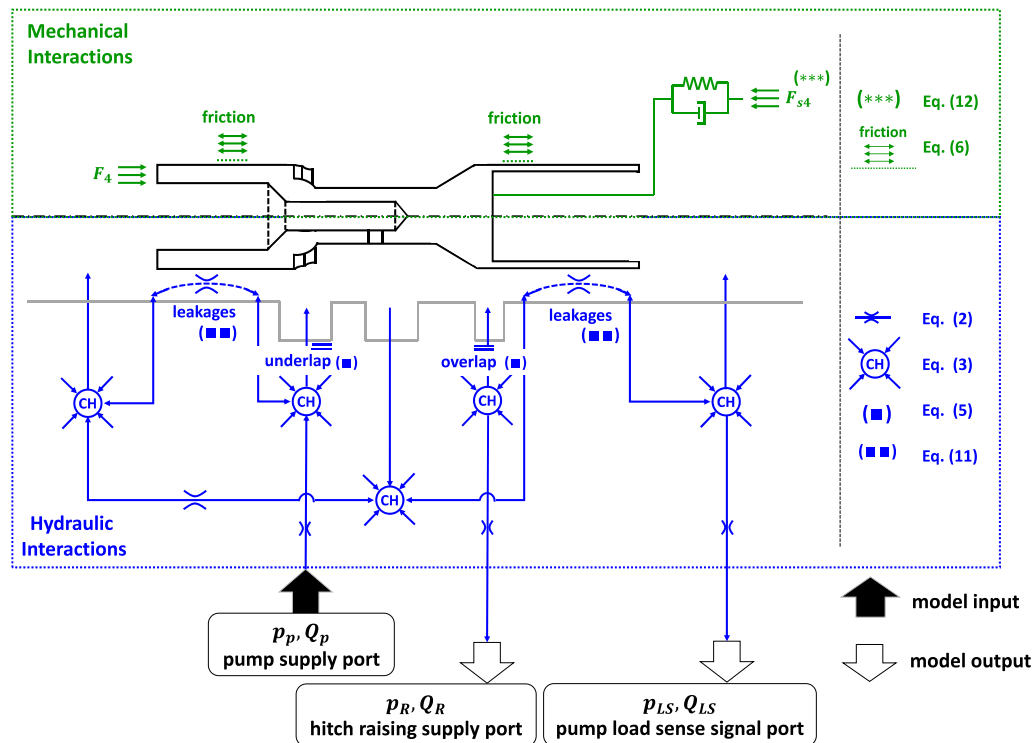


FIGURE 6: SCHEMATIC OF LOCAL COMPENSATOR IN HITCH CONTROL VALVE

the system is of the authors' interest, this discrepancy in response time on PC spool does not cause hesitation to carry out this pump in system simulations, as long as the other steady state terms are delivering good comparisons. Moreover, a deadhead pressure mode is not the condition under which the pump is expected to operate normally.

3.3 Modeling of the EHR Valve

The model for the EHR valve used in this work is very similar to the model developed in [5] and also utilized for system considerations in [6], [17] and [18]. The reference [5] has devoted much attention to the description of the metering characteristics of the proportional valve spool, the component that is responsible for determining the flow rate and hence the energy dissipation introduced by it. Applying the model developed in [5] to the system studied here directly helped speeding up the model development.

3.3 Modeling of the Hitch Control Valve

In this work, the functionality of a hitch control valve is performed with emphasis to the local pressure compensator (LPC), whose behavior is highly affected by the operating conditions in terms of flow and pressure. The main control sections are instead modeled by considering the static data area vs current given by the valve manufacturer, found to be not much affected by the operating conditions.

This approach differs from the one in [19] where the attention was posed equally to all the components of the hitch control valve. LPC keeps Δp constant; consequently, the flow rate is a function only of the solenoid valve metering area (and not of the load pressure). This fixed pressure is set by the preload of spring in LPC. When multiple users are activated in the system, LPC would introduce an additional pressure drop to maintain the desired load pressure on the hitch. The modeling approach is depicted in Fig. 6 and the equations implemented in the model is the same as the ones used in Fig. 2. Here, the leakages in the spool are modeled following Eq. 11 and 12.

- Leakages, gap laminar flow

$$Q = \Delta p \cdot \frac{\pi \cdot D \cdot rc^3}{12 \cdot \mu \cdot lc} \cdot \left[1 + 1.5 \cdot \left(\frac{e}{rc} \right)^2 \right] \quad (11)$$

- Spool equilibrium:

$$F_4 = F_{s4} + p_{LS} \cdot A_h + F_{jet4} \quad (12)$$

4. EXPERIMENTAL TEST PLAN FOR SYSTEM MODEL CALIBRATION

An experimental activity was carried out to characterize the energy flow within all the main high-pressure hydraulic sub circuits as well as for model validation purposes. This section details the tests specifically performed for the hydraulic remotes and the rear hitch.. Among different test standards for agricultural tractors, test procedures described in Nabraska [20] and DLG PowerMix [21] standards, which usually help design tests verifying hydraulic output power, are taken as reference to aid in acquiring repeatable data in stationary tests.



FIGURE 7: REFERENCE MACHINE DURING EHR TESTS

In particular, the Nebraska standard aided in how to express the hydraulic power data obtained in power input and power available at the user. This led to an understanding of what sensors would be required to yield such data. The DLG PowerMix test helps solve the problem when data between each cycle of farming maneuvers is not comparable.

It is important to mention that the reference machine used to conduct the experimental tests is a CNH Industrial high horse power tractor, which does not have all the required instrumentation to acquire data. Cross-referring to the test standards procedure and sensors required to fulfill each test plan, a set of necessary sensors and their location is obtained as shown in Fig. 1. For the tests performed in this research, the machine is instrumented with a total of 12 sensors, 4 flow meters and 8 pressure sensors (Fig. 7) with their characteristics are listed in Table 2. Once the machine finishes instrumentation, DAQ system design and implementation are made. The DAQ system,

TABLE 2
CHARACTERISTICS OF THE SENSORS USED

	Pressure Sensors	Flow Meters
Range	0 – 275 bar, 0 – 70 bar, 0 – 14 bar	12 – 300 L/min
Non-linearity	$\leq \pm 0.5\%$ Full scale	$\pm 1\%$ Full scale
Input	14 – 30 VDC	None
Output Type	Analog DC voltage	Self-generating sine pulse
Output Range	0 – 10 VDC	0 – 600 Hz
Sensing Method	Capacitive	Magnetic pickup with inline turbine

based on NI Hardware and software is called upon to record the data for the test.

For simulating loads to the EHR valves, a variable setting pressure relief valve is used. Instead, hitch was loaded with an external cylinder. The loads being tested, and the command given to the EHR valve and hitch can be seen in Table 3. The first section of the table focuses on a full command to the EHR valve and hitch with different loads. The second section maintains a constant load and explores different commands given to the EHR. A key point to notice is that the hitch is only tested during rising maneuvers. This is because when the hitch is lowered, it lowers by its gravity then no flow is requested from the pump. Low and high temperatures and RPMs ensure that the machine is tested in sufficiently different working conditions. Here high RPM refers to 2900r/min of pump engine speed and 1200 r/min for low RPM. Also, around 25 °C for low temperature and 65°C for high temperature.

TABLE 3
DIFFERENT CONTROLLED VARIABLES AND TEST
CONDITIONS FOR SINGLE REMOTE TEST & HITCH VALVE

100% Flow Command			
EHR: (Retraction/Extension, High/Low oil temperature)			
HITCH: (Rising, High/Low oil temperature)			
0% Load	50% Load	75% Load	90% Load
90% Load			
EHR: (Retraction/Extension, High/Low oil temperature)			
HITCH: (Rising, High/Low oil temperature)			
25% Flow command	50% Flow Command	75% Flow Command	

Tests involving multiple EHRs have also been conducted with the main goal to characterize the behavior of the LS system of the high-pressure circuit with multiple users.

5. MODEL VALIDATION RESULTS

To reproduce the tests described in the previous section in simulation. The hydraulic circuit model of the system of Fig. 1 was integrated by additional components: the gearbox between the engine and the pump providing a speed conversion ratio, a variable orifice reproducing the load at the hydraulic remote, a hitch cylinder carrying a certain load connected at the hitch control valve.

To prove that the model is well validated, four parameters representing the behavior of the system are considered for the comparisons for remote tests: LS pump delivery pressure, pump delivery flow rate, remote load pressure, and flow rate on the load. Two more sensors, pump LS line pressure, and hitch cylinder pressure are also studied for hitch tests.

Due to the length constraint of the paper, only representative test results under high oil temperature with high RPM are analyzed here. This is also the case under which the tractor is

operated most often in reality. From the experimental tests, it is studied that the EHR main spool is not symmetric by design. In order to have a comprehensive understanding and validation of the system model behavior, different flow directions are performed. The remote valve is performing retracting maneuver when flow coming to the loading orifice through lock check valve R and flows back to EHR through E (as labeled in Fig. 1). The extension maneuver is performed when the flow reverses (from E to R).

The results for the first set of considerations in the remote test plan, where load settings on remote valves are varying are shown in Fig. 8 and 9. Figure 8 shows retracting while Fig. 9 represents extending. The vertical axes are the absolute value of pressure/ flow rate divided by a reference pressure/flow rate chosen to make the scale clear and readable. Great matching is marked by steady-state results from the model, which implies that the models built for remote tests are validated well at this point. It's worth noting that when the load pressure is 0%, 50%, and 75%, the pump is under "single user" flow saturation, which explains the similar flow rate value delivered from the pump. Increasing the load pressure furthermore to 90%, the pump would be under pressure saturation since the system is

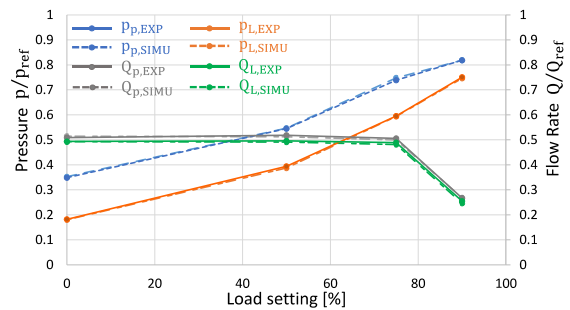


FIGURE 8: SINGLE REMOTE TEST RESULTS COMPARISON: Different load settings, Full command, Retraction, High oil temperature, High RPM

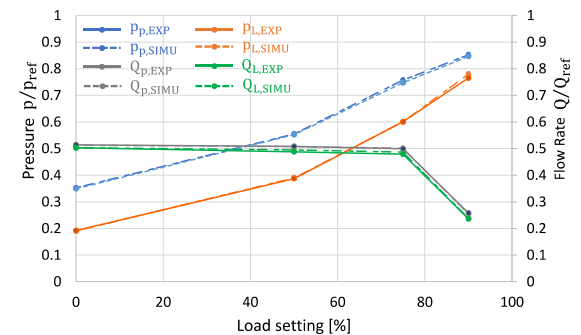


FIGURE 9: SINGLE REMOTE TEST RESULTS COMPARISON: Different load settings, Full command, Extension, High oil temperature, High RPM

functioning under deadhead pressure mode. This result emphasizes the explanation before as the pump PC is trustworthy enough to carry out steady state tests even while the transient response holds a marginal agreement with measurement.

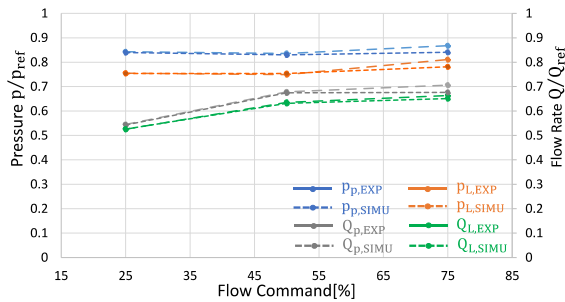


FIGURE 10: SINGLE REMOTE TEST RESULTS COMPARISON: Different flow commands, 90% load, Retraction, High oil temperature, High RPM

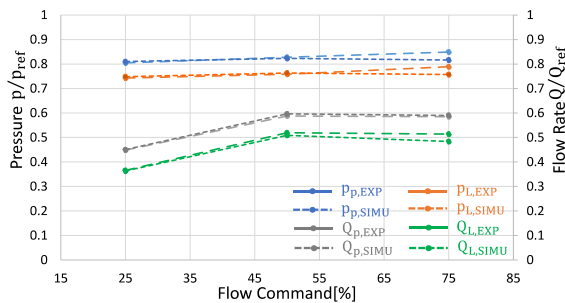


FIGURE 11: SINGLE REMOTE TEST RESULTS COMPARISON: Different flow commands, 90% load, Extension, High oil temperature, High RPM

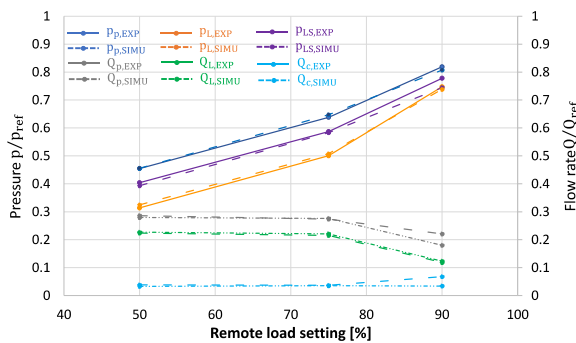


FIGURE 12: HITCH WITH SINGLE REMOTE TEST RESULTS COMPARISON: Different load settings on remote (Hitch cylinder raising, Full command, Extension, High oil temperature, High RPM)

Figure 10 and 11 are showing results when flow command is varying. The agreement between simulation and experimental results is satisfactory under 25% and 50% flow command situations. There exists a mismatch for 75% flow command. This could be explained that under 75% flow command and 90% load requirement, the LS pump used in the system is under both pressure saturation (PC effect) and “single user” flow saturation (FC effect). The behavior of the model under both saturation occurrences is certainly the most challenging condition for validating EHR model. However, the well-matched operating conditions still hold confidence to the model and it's possible to analyze the energy dissipation introduced by EHR in the hydraulic circuit up to this point.

Test results comparisons for hitch control valve activated with one remote are shown in Fig. 12. During the test procedure here, a certain fixed amount of load is raised up by hitch cylinder with raising solenoid valve activated, while the load setting on remote is varying. The results show a great match between simulation and measurement results while some small mismatches at 90% load. This can be explained in the same way as discussed in Fig. 9. Nevertheless, authors have great confidence to carry on component power distribution in the system, which is discussed in the following section.

6. SYSTEM POWER DISTRIBUTION CHARACTERIZATION

Using the validated system models, power dissipation distribution introduced by every single component in the hydraulic circuit could be analyzed, along with system efficiency. Here for brevity, only the remote cases are considered. Besides a single remote user involved in the system, multiple remotes could be activated together. Still, the pump would provide the pressure to the system responding to the highest loaded user. Now the pump delivery flow rate would be the sum of the flow rates requested by all the users (provided the maximum flow rate that the pump can supply is not exceeded).

6.1 Single Remote Test Result Analysis

Particular attention has been devoted to the comparisons between different flow directions, different oil temperatures, and different load settings while all the other variables are kept the same for each comparing. In Fig. 13, as the captions suggest, useful power serving for needs (green bar) and power dissipated at different sections are represented as a percentage of the total power supplied at the pump mechanical shaft during the tests. In other words, the volumetric and mechanical efficiencies of the pump are taken into consideration when implying system overall efficiency which is equal to the percentage of useful power on a remote. With a non-symmetry design of the main spool, even with not much difference in system efficiency between extension and retraction but the power distributions are different for two cases. As one may notice, the power consumed at EHR local pressure compensator (LPC) is not equal to zero, which is what is expected from the single user test. This is because of the insufficient high cracking pressure of LPC which is set by the preload of spring in it. Ideally, this spring preload setting is the

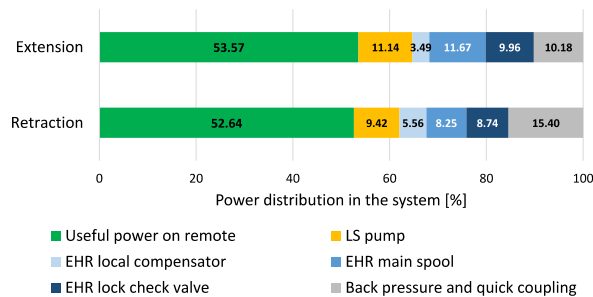


FIGURE 13: POWER DISTRIBUTION COMPARISON BETWEEN DIFFERENT FLOW DIRECTIONS FOR SINGLE REMOTE TEST (Full command, 75% Load, High RPM, High oil temperature)

same as the spring setting of FC in a LS pump to minimize the power dissipation on LPC. Nevertheless, the LPC cracking pressure is set slightly higher than that of the FC in the pump to ensure complete opening of LPC spool in reality.

System power distribution under high and low oil temperatures is depicted in Fig. 14. The efficiency of the system is slightly higher when running with higher temperature. This result is of benefit to users since most of the agricultural work on the tractor would be carried out when the oil temperature is high. One potential cause of lower efficiency when the oil is cooler can be contributed to the higher viscosity of the fluids, which leads to higher viscous friction, and hence more viscous flow losses occur inside the pump as we can see the pump is consuming more under this case.

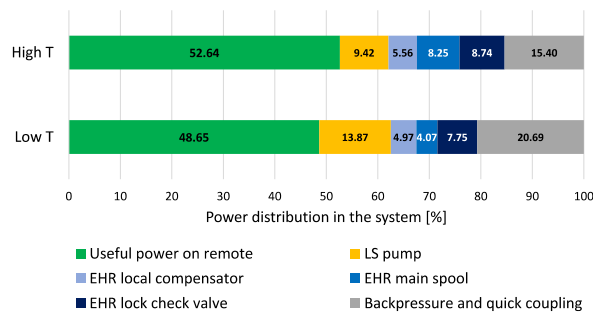


FIGURE 14: POWER DISTRIBUTION COMPARISON BETWEEN LOW AND HIGH OIL TEMPERATURES FOR SINGLE REMOTE TEST (Full command, 75% Load, Retraction, High RPM)

The last pair for different load settings on the remote is shown in Fig. 15, which implies the conclusion that the higher the load pressure, the more efficient the system would be. This conclusion also holds if simulation results with 0% and 50%

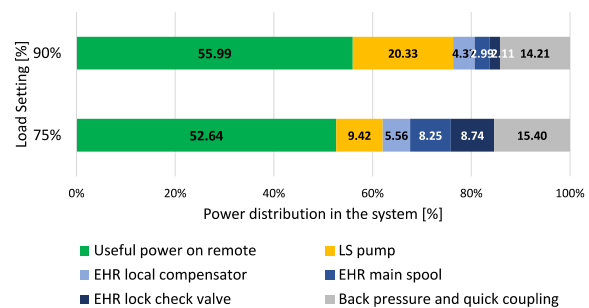


FIGURE 15: POWER DISTRIBUTION COMPARISON BETWEEN DIFFERENT LOADS FOR SINGLE REMOTE TEST (Full command, Retraction, High RPM, High oil temperature)

loads are compared with 75% and 90%. The increase of power dissipation on the LS pump when the pressure raises from 75% to 90% is attributed to the fact that the pump is under pressure saturation for the latter case. The swash plate angle is minimized under deadhead pressure mode which leads to higher power dissipation on LS pump itself.

6.2 Dual Remote Test Result Analysis

When dual users are active in the system, the two users are both requiring full retracting flow but load settings are different between them as shown in Fig. 16. Instead of focusing on the overall system power distribution as before, the attention is paid to the two EHR valves with their loading conditions. Now the power dissipations are determined as the percentage of the power

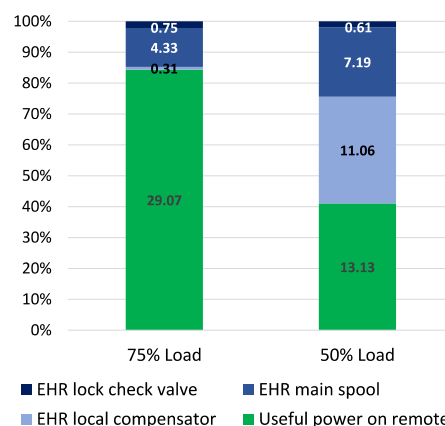


FIGURE 16: POWER DISTRIBUTION COMPARISON BETWEEN DIFFERENT LOADS FOR DUEL REMOTES TEST (Full command, Retraction, High RPM, High oil temperature)

available at the input of each EHR. A critical aspect of the load sensing system is evidenced under this study that the LPC inside EHR associated with lower user pressure is dissipating a relevant high amount of power available through it as explained before.

CONCLUSION

The paper has presented the analysis of the power flow within the high-pressure hydraulic system of an agricultural tractor. The reference machine is a CNH Industrial high horse power tractor and the approach of analysis includes both simulation and testing. A nonlinear lumped parameter model of the hydraulic system was developed using Simcenter Amesim modeling environment, building in-house models for every component of the system. Modeling is divided into three main parts named after the LS pump, the hitch control valve and the remote valve at different For the LS pump, the modeling of pressure compensator and flow compensator allows reaching a good agreement between simulation results and experimental data for both steady-state and dynamic behavior.

Experimental tests on the reference machine were performed through a test plan purposely developed within this research, and tests included different loads, oil temperature and engine speed. These tests were aimed at measuring both input and output hydraulic power within the system, permitting a gross analysis of the power loss through the system. More importantly, the test permitted to validate the model, so that the model can be used for in-depth studies of the power flow throughout the hydraulic system.

Study on the power distribution analysis, particularly remote tests, provides important insights on the system component power consumption when the reference machine is operating under different working conditions. As a result, the system operates at a higher efficiency, which could be as high as 55.99% when handling a higher remote load at higher oil temperature. The non-symmetric structure of EHR main spool doesn't contribute much difference in system efficiency. When multiple remotes are activated, there's much higher power dissipated on the LPC associated with the lower pressure user.

This study allows making considerations about possible improvements of the system, by identifying the components and the conditions more inconvenient from the point of view of energy efficiency.

ACKNOWLEDGMENTS

The authors would like to acknowledge the active support of this research by Siemens PLM software. This work has been developed with the help of Simcenter Amesim platform provided by Siemens.

REFERENCES

- [1] H. Murrenhoff, "An Overview of Energy Saving Architectures for Mobile Applications," *9th Int. Fluid Power Conf.*, no. 1, pp. 21–26, 2014.
- [2] D. B. Beck, D. E. Fischer, D. G. Kolks, D. J. Lübbert, D. S. Michel, and D. M. Schneider, "Novel System Architectures by Individual Drives," *10th Int. Fluid Power Conf.*, pp. 29–62, 2016.
- [3] G. F. Ritelli and A. Vacca, "Energetic and dynamic impact of counterbalance valves in fluid power machines," *Energy Convers. Manag.*, vol. 76, pp. 701–711, 2013.
- [4] A. Vacca, G. Franzoni, and F. Bonati, "An Inclusive, System-Oriented Approach for the Study and the Design of Hydrostatic Transmissions: The Case of an Articulated Boom Lift," *SAE Int. J. Commer. Veh.*, vol. 1, no. 1, pp. 437–445, 2010.
- [5] M. Borghi, B. Zardin, F. Pintore, and F. Belluzzi, "Energy Savings in the Hydraulic Circuit of Agricultural Tractors," in *Energy Procedia*, 2014, vol. 45, pp. 352–361.
- [6] M. Borghi, B. Zardin, F. Mancarella, and E. Specchia, "Energy consumption of the Hydraulic Circuit of a Mid-Size Power Tractor," in *7th International Fluid Power Conference*, 2010, pp. 37–50.
- [7] F. Pintore, P. D. Ing, and A. Benevelli, "Modelling and Simulation of the Hydraulic Circuit of an Agricultural Tractor," in *8th FPNi Ph. D Symposium on Fluid Power*, 2014, pp. 1–11.
- [8] M. Borghi, B. Zardin, and F. Pintore, "Energy Saving in the Hydraulic Circuit for Agricultural Tractors: Focus on the Power Supply Group," vol. 1, pp. 29–35, 2015.
- [9] G. Panetta, F. Mancarella, M. Borghi, B. Zardin, and F. Pintore, "Dynamic Modelling of an Off-Road Vehicle for the Design of a Semi-Active, Hydropneumatic Spring-Damper System," in *ASME 2015 International Mechanical Engineering Congress and Exposition*, 2015, p. V04BT04A006-V04BT04A006.
- [10] B. Zardin, M. Borghi, F. Gherardini, and N. Zanasi, "Modelling and Simulation of a Hydrostatic Steering System for Agricultural Tractors," *Energies*, vol. 11, no. 1, pp. 1–20, 2018.
- [11] N. Nervegna, *Oleodinamica e pneumatica*. Politeko, 2003.
- [12] J. Ivantysyn and M. Ivantysynova, *Hydrostatic Pumps and Motors, Principles, Designs, Performance, Modelling, Analysis, Control and Testing*, First Engl. New Delhi, India: Academic Book International, 2001.
- [13] P. Casoli, A. Anthony, and M. Rigosi, "Modeling of an Excavator System - Semi Empirical Hydraulic Pump Model," *SAE Int. J. Commer. Veh.*, vol. 4, no. 1, pp. 242–255, 2011.
- [14] D. McCloy and H. R. Martin, *Control of fluid power: analysis and design*, 2nd revise., no. Empl Id. Chichester, Sussex, England, Ellis Horwood, Ltd.; New York, Halsted Press, 1980.
- [15] J. F. Blackburn, G. Reethof, and J. L. Shearer, "Fluid Power Control." 1960.
- [16] SAE, Hydraulic Power Pump Test Procedure, "J745 (Recommended Practice)," SAE Handbook, Society of Automotive Engineers, Warrendale, 2009.
- [17] A. Benevelli, Z. Barbara, and M. Borghi, "Independent metering architectures for agricultural tractors auxiliary

- utilities,” in *The 7th FPNI PhD Symposium on Fluid Power*, 2012, vol. 1, pp. 909–928.
- [18] R. McIntosh, J. Matthews, G. Mullineux, and A. J. Medland, “Energy Dissipation of the Hydraulic Circuit of Remote Auxiliary Utilities of an Agricultural Tractor,” *Fluid Power Motion Control*, vol. 48, no. 6, p. 563, 2010.
 - [19] P. Casoli, A. Vacca, A. Anthony, and G. L. Berta, “Numerical and Experimental Analysis of the Hydraulic Circuit for the Rear Hitch Control in Agricultural Tractors,” in *7th International Fluid Power Conference*, 2010, pp. 1–13.
 - [20] OECD, “Standard Code for the Official Testing of Agricultural and Forestry Tractor Performance,” *Standards*, vol. 2, no. July, p. 91, 2012.
 - [21] O. Degrell and T. Feuerstein, “DLG-Powermix-A practical tractor test,” DLG test centre for agricultural machinery, Groß-Umstadt, Germany, pp. 1–4, 2003.